**Shallow organic soils as significant greenhouse gas source**

Von der Naturwissenschaftlichen Fakultät der

Gottfried Wilhelm Leibniz Universität Hannover

zur Erlangung des Grades

Doktorin der Naturwissenschaften (Dr. rer. nat.)

genehmigte Dissertation

von

Diplom-Geoökologin Univ.

Katharina Dominica Leiber-Sauheitl

geboren am 03.02.1982 in Bad Neustadt / Saale

2015

Referent: Prof. Dr. Gerald Kuhnt

Koreferent: Prof. Dr. Jürgen Böttcher

Koreferent: Prof. Dr. Heinz Flessa

Tag der Promotion: 16.12.2015

# Index of contents

List of tables ..... V
List of figures ..... VI
List of abbreviations ..... IX
Summary ..... XI
Zusammenfassung ..... XII
**Chapter 1: Overall introduction** ..... 1
1. Organic soils as greenhouse gas source ..... 1
1.1. Definition ..... 1
1.2. Peatland genesis and types ..... 2
1.3. Spatial distribution of organic soils ..... 3
1.4. Utilization of organic soils ..... 5
1.5. Organic soils as sink and source of greenhouse gases ..... 6
1.6. Methodological challenges in measuring GHG exchange ..... 8
1.7. Identification and quantification of GHG sources by the stable isotope technique ..... 10
1.8. International policy framework for GHG mitigation on organic soils ..... 11
1.9. Towards climate-smart management of organic soils ..... 14
2. Motivation and hypotheses ..... 16
2.1. Motivation ..... 16
2.2. Hypotheses ..... 18
3. References ..... 21
**Chapter 2: Publication no. 1** ..... 27
Abstract ..... 28
Highlights ..... 29
1. Introduction ..... 29
2. Materials and Methods ..... 31
2.1. Site description ..... 31
2.2. $R_{eco}$ measurements ..... 31
2.3. $R_{eco}$ modeling ..... 33
2.4. Statistical analyses ..... 34
3. Results ..... 36
3.1 Seasonal course of $R_{eco}$ and environmental parameters ..... 36
3.2 Temperature - soil moisture models ..... 37
3.3 Evaluation of measurement frequency - Lloyd-Taylor model with full data set ..... 37

3.4 Evaluation of measurement frequency - Lloyd-Taylor models separated by day and night ... 39
3.5 Evaluation of campaign frequency - Lloyd-Taylor models for regular campaigns ... 40
3.6 Evaluation of campaign frequency - Lloyd-Taylor models for good weather campaigns ... 41
4. Discussion ... 42
4.1 Capturing day-night $R_{eco}$ patterns is most critical ... 42
4.2 Day-to-day $R_{eco}$ patterns ... 44
4.3 Robust sampling strategies for seasonal $R_{eco}$ sums ... 45
5. Conclusions ... 46
6. References ... 48
7. Supplement ... 51
**Chapter 3: Publication no. 2** ... 54
Abstract ... 55
1. Introduction ... 55
2. Materials and methods ... 56
2.1. Study site Grosses Moor [Great Peat Bog] ... 56
2.2. Measurement of site characteristics ... 58
2.3. GHG flux measurements ... 59
2.4. $CO_2$ modeling ... 60
2.5. $CH_4$ and $N_2O$ flux calculation ... 62
2.6. Statistical analyses ... 63
3. Results ... 63
3.1. Driver variables ... 63
3.2. $CO_2$ ... 64
3.3. $CH_4$ ... 66
3.4 $N_2O$ ... 67
3.5 Annual C and GHG balance ... 67
4. Discussion ... 68
4.1. Magnitude of GHG fluxes ... 68
4.2. Precision of the annual $CO_2$ budget ... 69
4.3. $C_{org}$ effects ... 70
4.5. Vegetation effects ... 73
5. Conclusions ... 74
6. References ... 75
7. Supplement ... 78

**Chapter 4: Publication no.3** ..... 84
Abstract ..... 85
1. Introduction ..... 85
2. Materials and methods ..... 86
2.1 Experimental design ..... 86
2.2 Sheep excreta labeling ..... 87
2.3 Microcosm experiment ..... 88
2.4 Analyses ..... 89
2.5 Calculations ..... 91
2.6 Statistical analyses ..... 92
3. Results ..... 92
3.1 Total $CO_2$ and $CH_4$ fluxes ..... 92
3.2 Excreta derived $CO_2$-C emissions ..... 93
3.3 Soil derived $CO_2$-C emissions ..... 94
3.4 DOC export ..... 96
3.5 Total $N_2O$ and $NH_3$ fluxes ..... 96
3.6 Excreta derived $N_2O$ emissions ..... 96
3.7 Soil derived $N_2O$ emissions ..... 98
3.8 Extractable microbial N ..... 99
3.9 Mineral nitrogen ..... 99
3.10 DON ..... 100
4. Discussion ..... 101
4.1 Carbon losses after excreta application on peat soil ..... 101
4.2 Nitrogen losses after excreta application on peat soil ..... 102
4.3 Priming effects for C and N ..... 103
4.4 Field application of lab results ..... 104
5. Conclusions ..... 105
6. References ..... 107
7. Supplement ..... 110
**Chapter 5: Comprehensive discussion and conclusions** ..... 111
1. Summary of results ..... 111
1.1 Minimum measurement frequency for robust annual budgets of ecosystem respiration ..... 111
1.2 High $CO_2$ fluxes from histic Gleysols under grassland management ..... 111

1.3 Sheep excreta cause no positive priming effects on $CO_2$ and $N_2O$ emissions from peat soil ..... 112
2. The robustness of methods for GHG flux measurements ..... 113
3. Strong vulnerability of peat derived carbon extends to relatively low C containing soils ..... 115
4. Towards climate-smart management of grasslands on organic soils ..... 116
5. Implications and general conclusions ..... 117
6. References ..... 119
Acknowledgements ..... 120
Curriculum vitae ..... 121

# List of tables

### Chapter 2: Publication no. 1 - Supplement

**Table S2 - 1**: Model summary of generalized nonlinear least squares fit of daytime and nighttime Lloyd-Taylor parameters with “varPower” as variance structure. ..... 53

### Chapter 3: Publication no. 2

**Table 3 - 1**: Site characterization. ..... 58
**Table 3 - 2**: Biomass export from sites (June 1, 2011 to June 1, 2012; site mean value ± one standard deviation between replicate plots) and cover of sedges, grasses and mosses.. 65
**Table 3 - 3**: Annual fluxes of NEE, Reco and GPP, $CH_4$ and $N_2O$ (June 1, 2011 to June 1, 2012; annual flux ± uncertainty*). ..... 67
**Table 3 - 4**: Global warming potential for a time horizon of 100 years (GWP100) of Net C balance (NEE plus harvest), $CH_4$ and $N_2O$ and total GHG balance (annual flux ± uncertainty*; IPCC 2007). ..... 68

### Chapter 3: Publication no. 2 - Supplement

**Table S3 - 1**: Linear mixed-effects model of $R_{eco}$ vs. Water table. ..... 78

### Chapter 4: Publication no. 3

**Table 4 - 1**: Overview on experimental treatments ..... 87
**Table 4 - 2**: C and N content, $^{15}N$ and $^{13}C$ signature of faeces, urine and peat soil. Average C and N content per column. ..... 89
**Table 4 - 3**: Priming factors (PF) of soil $CO_2$ and $N_2O$ calculated according to Bol et al. (2003). Values >1 indicated positive priming, values <1 indicate negative priming. Standard deviations were calculated using Gaussian error propagation. p values were derived from two sided t-tests treatment vs. control ( = pure peat). ..... 98
**Table 4 - 4**: Extractable microbial N and $NO_3^-$, $NH_4^+$, mineral N and DON contents after 21 days. ..... 99

# List of figures

## Chapter 1: Overall introduction

**Fig. 1 - 1**: Global distribution of peatlands (= mires; Lappalainen, 1996) ..... 3
**Fig. 1 - 2**: Map of European organic soils (Montanarella et al., 2006) ..... 4
**Fig. 1 - 3**: Map of (potential) organic soils in Germany (Geological map 1:200,000; BGR, without year) ..... 5
**Fig. 1 - 4**: Amounts of GHG emissions of peat soil in dependence of drainage intensity (adapted from Drösler et al., 2008). Dark brown areas represent the water saturated part of the peat profile, light brown areas reflect aerated zone. ..... 7
**Fig. 1 - 5**: Scheme of autotrophic and heterotrophic ecosystem carbon fluxes (left). Arrows represent $CO_2$ fluxes. Equation 1 defines net ecosystem exchange (NEE) as the sum of ecosystem respiration ($R_{eco}$) and gross primary production (GPP). Equation 2: C budget is composed of NEE, $CH_4$ flux and C export. Equation 3: GHG balance completes the C budget for the $N_2O$ flux (in C equivalents). Uptake of C has a negative sign, release of C a positive sign. ..... 9
**Fig. 1 - 6**: Typical management practices on organic and wet soils (original figure from IPCC, 2014a). Letters indicate different wetland types e.g. subfigure B contains drained inland organic soils which are described in chapter 2 of the *Wetlands Supplement.* ..... 13

## Chapter 2: Publication no. 1

**Fig. 2 - 1**: Photograph of the automatic chamber system (chamber in standby position). Numbers indicate the most important components: soil frame (1), measurement chamber (2), box with control unit, data logger and $CO_2$ analyzer (3), box with vial sampling system (4). ..... 32
**Fig. 2 - 2:** Time series of (**A**) $CO_2$ flux, (**B**) soil temperature in 2 cm and (**C**) groundwater level (GWL) from June to October 2012 (original data set with gaps). ..... 37
**Fig. 2 - 3**: Evaluation of measurement frequency. (A) Dots represent the $R_{eco}$ sum of Jackknife resamples. Black dots denote $R_{eco}$ sums which consist only of nighttime data, yellow dots denote $R_{eco}$ sums which consist only of daytime data and green dots contain nighttime as well as daytime data. Dashed line represents the $R_{eco}$ sum estimate calculated with the complete data set. (B) Random uncertainty given as standard deviation (sd; circles) and bias (triangles) of different measurement frequencies. Green color for fractions and odd multiples of 0.5 days and red colors for even multiples of 0.5 days. Lines are smoothers for visualization of the trend. ..... 38
**Fig. 2 - 4**: Lloyd-Taylor fits of the full 2h data set. Data separated into night (black diamonds) and day (yellow diamonds) $CO_2$ fluxes and corresponding Lloyd-Taylor GNLS predictions for night (black line) and day (yellow line). ..... 39
**Fig. 2 - 5**: Evaluation of campaign frequency - regular campaigns. (A) Seasonal $CO_2$ Jackknife sums of resamples vs. mean campaign distance. Numbers indicate number of campaigns used for Jackknife resampling. (B) Random uncertainty (sd) and bias of seasonal $CO_2$ Jackknife sum estimates by regular campaigns. Lines are smoothers for visualization of the trend. ..... 41

**Fig. 2 - 6**: Evaluation of campaign frequency - good weather campaigns. (A) Seasonal $CO_2$ Jackknife sums of resamples vs. mean campaign distance. Numbers indicate number of campaigns used for Jackknife resampling. (B) Random uncertainty (sd) and bias of seasonal $CO_2$ Jackknife sum estimates by good weather campaigns. Lines are smoothers for visualization of the trend. ..... 42

### Chapter 2: Publication no. 1 - Supplement

**Fig. S2 - 1:** Flow scheme of the measured greenhouse gases from the chamber to $CO_2$ analyzer and to the automatic $CH_4$ and $N_2O$ sampling system. ..... 51
**Fig. S2 - 2**: Exemplary nighttime (A; 22.06.2012 02:40 am) and daytime (B; 06.07.2012 11:13 am) $CO_2$ increase during a chamber measurement in the Grosses Moor. All values left of the vertical line (first 15 seconds) were discarded. Orange lines indicate the linear fit which was estimated with all data points from 0.25 min to 5 min. Actual fits of the investigated data set were done with mass concentrations. ..... 52

### Chapter 3: Publication no. 2

**Fig. 3 - 1**: Time series of precipitation, air, and 2cm soil temperature at meteorological station..... 64
**Fig. 3 - 2**: Time series of daily $CO_2$ fluxes [g C $m^{-2}$ $d^{-1}$] at each site (June 1, 2011 - June 1, 2012). Depicted are modeled fluxes and 95% confidence band. Dashed lines indicate grazing and mulching events. ..... 66
**Fig. 3 - 3**: Annual GHG balances vs. water table level of shallow peat sites in the Grosses Moor (filled circles) and several deep peat grassland sites (open circles) in Germany (Drösler et al. 2013). ..... 69
**Fig. 3 - 4**: Violin plots of NEE emissions vs. $C_{org}$ (A; $R^2$=0.49, p= 0.121) and NEE emissions vs. water table level (B; $R^2$=0.71, p= 0.035). Violins (A, B): distribution of all simulated aggregated annual NEE sums of each site; points (B): modeled annual NEE of each site, used as basis for linear regression. ..... 71
**Fig. 3 - 5**: Ground water levels [m] vs. $R_{eco}$-$CO_2$ Flux [g C $m^{-2}$ $d^{-1}$] on the campaign dates for all six sites. Dotted vertical line: border of peat horizon; continuous line: population mean prediction from the linear mixed effects model for all sites; a fixed effect was used to distinguish water levels below the peat horizon (-0.8 to -0.3 m) and within the peat horizon (-0.3 to +0.1 m). ..... 73

### Chapter 3: Publication no. 2 - Supplement

**Fig. S3 - 1**: PAR correction for site $C_{med}$ $W_{low}$, $C_{low}$ $W_{low}$ and $C_{low}$ $W_{high}$ at a distance of 50 metres from the tree line. Dashed line = 1:1 line, continuous line = correction function $PAR = \alpha * PAR_{station}^{\beta}$. ..... 78
**Fig. S3 - 2**: Time series of water table levels at each site (June 1, 2011 to June 1, 2012)..... 79
**Fig. S3 - 3**: $R_{eco}$ flux model (A) and GPP flux model (B) of an exemplary measurement campaign (02 May 2012) showing measured data as dots and fits as lines. ..... 79
**Fig. S3 - 4: A:** Plots of measured $R_{eco}$ fluxes vs. modeled Reco fluxes of all measurement campaigns seperated by site (1 June 2011 to 1 June 2012). **B**: Plots of measured NEE

fluxes vs. modeled NEE fluxes of all measurement campaigns seperated by site (1 June 2011 to 1 June 2012). ..... 81

**Fig. S3 - 5**: Example of a flux measurement where the non-linear fit severely overestimates the flux. $N_2O$ concentrations were close to ambient and (by chance) the second to fourth concentration were almost identical and the first concentration was lower by 20 ppb (which is within typical measurement error). Robust linear fit equaled linear fit with flux = 13 µg N $m^{-2}$ $h^{-1}$, p = 0.2, AIC=-24. Shaded area depicts confidence band of the linear fit. HMR fit resulted in flux = 96 µg N $m^{-2}$ $h^{-1}$, p = 2E-5, AIC=-59. Since the HMR flux estimate is more than four times the robust linear flux estimate, we used the latter..... 82

**Fig. S3 - 6:** Annual time lines of $CH_4$ (A) and $N_2O$ (B) (mean ± standard error of the replicates; June 1, 2011 to June 1, 2012). ..... 83

## Chapter 4: Publication no. 3

**Fig. 4 - 1**: Time series of $CO_2$ fluxes since labeling of pure peat (=background; a) and different $^{15}N$ labeled treatments (b-g). Bars represent minimum and maximum values of replicates. Cumulated C fluxes of each treatment over 21 days are indicated in g C $m^{-2}$ ± standard deviation of the replicates. ..... 94

**Fig. 4 - 2**: Proportion of excreta C (a) and of soil C (b) mineralized to $CO_2$ during 3 weeks (mean ± standard deviation of the replicates; n=4)..... 95

**Fig. 4 - 3**: Mineralization kinetics for urine carbon (flux ~ c1 × exp (-k × time) with c1 = 8.73 ± 2.99 g $m^{-2}$ $d^{-1}$ and k = 1.41 ± 0.21 $d^{-1}$) derived from the $^{15}N$ urine treatment (n=4). ..... 95

**Fig. 4 - 4**: Time series of $N_2O$ fluxes since labeling of pure peat (=background; a) and different $^{15}N$ labeled treatments (b-g). Bars represent minimum and maximum values of replicates. Cumulated N fluxes of each treatment over 21 days are indicated in g N $m^{-2}$ $d^{-1}$ ± standard deviation of the replicates. ..... 97

**Fig. 4 - 5**: Proportion of excreta N (a) and soil N (b) mineralized to $N_2O$ during 3 weeks (mean ± standard deviation of the replicates; n=4)..... 98

**Fig. 4 - 6**: Source specific carbon and nitrogen release (g C or mg N $m^{-2}$) of different treatments over 21 days: (a) pure peat, (b) $^{15}N$ faeces and $^{15}N$ urine (for $CO_2$-C emissions mean value of all faeces plus urine treatments), (c) $^{15}N$ faeces and (d) $^{15}N$ urine. DOC-C and DON-N refer to emissions from total column. On top of each figure (a-d) amounts of C and N input per column are indicated. The dotted boxes represent one microcosm system. ..... 100

## Chapter 4: Publication no. 3 - Supplement

**Fig. S4 - 1**: Time series of excreta derived $CO_2$ fluxes (a-c) and excreta derived $N_2O$ fluxes (d-g) since labeling. In the figures the replicates of the same treatment are displayed. For C $^{15}N$ faeces (a, n=4), $^{15}N$ urine (b, n=4), faeces plus urine treatments (c, n=12); for N $^{15}N$ faeces (d, n=4), $^{15}N$ urine (e, n=4), $^{15}N$ faeces plus $^{15}N$ urine (f, n=4), $^{14}N$ faeces plus $^{15}N$ urine (g, n=4). ..... 110

## List of abbreviations

| | |
|---|---|
| AIC | Akaike information criterion for the intercomparison of statistical models |
| AFOLU | Agriculture, forestry and land use |
| ANOVA | Analysis of variance |
| CFE | Chloroform fumigation extraction for the determination of soil microbial biomass |
| $C_{org}$ | Organic carbon |
| DOC | Dissolved organic carbon |
| DON | Dissolved organic nitrogen |
| FAO | Food and Agriculture Organization of the United Nations |
| GC-FID/-ECD | Gas chromatograph with a flame ionization detector or a electron capture detector |
| GHG | Greenhouse gas; in this study $CO_2$, $CH_4$ and $N_2O$ |
| GPP | Gross primary production of plants |
| GWL | Groundwater level |
| GWP100 | Global Warming Potential of a greenhouse gas which refers to a time horizon of 100 years |
| HMR | Hutchinson – Mosier regression, non linear regression type |
| IPCC | Intergovernmental Panel on Climate Change |
| NEE | Net ecosystem exchange (sum of ecosystem respiration and gross primary production) |
| NIR | National Inventory Report |
| $N_{min}$ | Mineral nitrogen ($NH_4^+$, $NO_3^-$) |
| PAR | Photosynthetically active radiation in the wavelength range of 400-700 nm |
| PF | Priming factor |
| $R_{eco}$ | Ecosystem respiration (autotrophic plus heterotrophic respiration) |
| SOC | Soil organic carbon |
| SOM | Soil organic matter |
| UBA | Umweltbundesamt |

| | |
|---|---|
| UNFCCC | United Nations Framework Convention on Climate Change |
| WFPS | Water filled pore space |
| WRB | World Reference Base |

## Summary

Drained organic soils are hotspots of anthropogenic greenhouse gas (GHG) emissions. Up to now, most studies were focused on deep organic soils and peat with high organic carbon content ($C_{org}$). Shallow organic soils (e.g. histic Gleysols) formed after peat extraction or mixing of peat with mineral soil for melioration are sparsely investigated concerning their GHG emission potential. The aim of this work is to close this knowledge gap, including the investigation of requirements for methods to quantify GHG fluxes and identifying drivers of GHG fluxes and management effects.

The minimum measurement frequency for robust annual budgets of ecosystem respiration ($R_{eco}$) was determined within this thesis by analyzing a continuous seasonal $R_{eco}$ data set measured by an automatic chamber system. The $R_{eco}$ measurement approach based on campaigns of diurnal $CO_2$ fluxes proved to be suitable for determining robust $R_{eco}$ sums. In contrast, $R_{eco}$ models based on pure daytime or nighttime measurements were substantially biased. Therefore, $R_{eco}$ measurements should be started before sunrise lasting until the late afternoon. $CO_2$ campaigns during sunny, dry weather produced more accurate and precise $R_{eco}$ models and should be preferred to a strict interval based measurement pattern. Thus, a measurement frequency of three weeks is sufficient for the calculation of robust annual carbon budgets for histic Gleysols under grassland.

Furthermore, it was investigated if shallow, nutrient-poor histic Gleysols under grassland release as high GHG emissions as deep peat soils. This was done by manual chamber measurements for six sites which had a shallow histic horizon (0.3 m) or were mixed with mineral soil ($C_{org}$ from 9 to 52%). The net GHG balance, corrected for C export by harvest, was around 4 t $CO_2$-C-eq $ha^{-1}$ $yr^{-1}$ on soils with peat layer and little drainage. The net GHG balance reached 7-9 t $CO_2$-C-eq $ha^{-1}$ $yr^{-1}$ on soils with sand mixed into the peat layer and deeper drainage. These results show the linear increase of GHG emissions of shallow organic soils (mainly $CO_2$) with drainage depth. Emissions did not level off when the water table fell below the peat level. Thus, grasslands on histic Gleysols emit as high GHG amounts as grasslands on Histosols. Peat mixed with mineral subsoil and $C_{org}$ concentration around 10% emits as much GHG as unmixed peat soil (> 30% $C_{org}$).

In addition, the effect of sheep excreta on GHG emissions from a strongly degraded peat soil was investigated in a microcosm experiment. Since sheep excreta contain labile organic substances, they have a strong potential for positive priming in peat soil. $^{15}N$ and $^{13}C$ stable isotopes were used to partition sources of $CO_2$ and $N_2O$. Sheep excreta enhanced $CO_2$ emissions proportionally to the amount of C added. In contrast, $N_2O$ and $CH_4$ emissions were not affected by excreta addition. Sheep excreta caused no or small negative priming on peat decomposition and led to a source shift of the nitrogen released as $N_2O$ from peat to labile N forms in excreta. However, no mechanism was found that would suggest a risk of increased peat mineralization by sheep excreta.

The results of this PhD thesis indicate that shallow organic soils release as high GHG emission as deep peat soils. Therefore, they have to be considered in the national GHG inventory reports. GHG mitigation on shallow organic soils can be realized by climate-smart management e.g. pastures with a controlled water management or rewetting measures.

**Keywords**: organic soils, peatland, greenhouse gas emission

# Zusammenfassung

Dränierte organische Böden sind anthropogene Hotspots für die Emissionen von Treibhausgasen (THG). Bislang haben sich die meisten diesbezüglichen Studien auf tiefgründige Torfböden oder Torfe mit hohen Gehalten an organischem Kohlenstoff ($C_{org}$) konzentriert. Im Gegensatz hierzu sind histic Gleysole durch flachgründige Torfhorizonte charakterisiert, die nach Torfabbau oder einer Durchmischung von Torf mit Mineralboden zu Meliorationszwecken entstanden sind, und deren THG-Potential wenig untersucht ist. Das Ziel dieser Arbeit besteht darin, diese Wissenslücke zu schließen, indem die Voraussetzungen für Methoden zur Quantifizierung von THG–Flüssen untersucht werden, sowie deren Steuergrößen und der Einfluss von Bewirtschaftungseffekten auf THG–Flüsse untersucht werden.

Die minimale Messfrequenz zur Bestimmung robuster Jahresbilanzen der Ökosystematmung ($R_{eco}$) wurde in dieser Dissertation durch Analyse eines kontinuierlichen saisonalen $R_{eco}$–Datensatzes ermittelt, der mit einem automatischen Haubensystem erfasst wurde. Der $R_{eco}$–Messansatz, basierend auf Kampagnen mit über den gesamten Messtag verteilten Haubenmessungen, erwies sich als geeignet zur Ermittlung von robusten $R_{eco}$-Summen. Im Gegensatz hierzu wiesen $R_{eco}$–Modelle, die auf reinen Tages- oder Nachtmessungen basierten, eine systematische Abweichung auf. Daher sollten $R_{eco}$–Messungen immer vor Sonnenaufgang beginnen und bis in den späten Nachmittag verteilt sein. $CO_2$-Kampagnen bei sonnigem, trockenem Wetter lieferten $R_{eco}$–Modelle mit geringerem systematischen und zufälligen Fehler und sollten rein abstandsbasierten Messterminen vorgezogen werden. Ein Messabstand von drei Wochen ist daher ausreichend für die Bestimmung einer robusten jährlichen Kohlenstoffbilanz auf histic Gleysols unter Grünlandnutzung.

Diese Dissertation untersucht, ob flachgründige, nährstoffarme histic Gleysols (0.3 m) unter Grünlandnutzung ebenso hohe THG- Emissionen freisetzen wie tiefgründige Torfböden. Dies wurde mittels manuellen Haubenmessungen für sechs Standorte ermittelt, die entweder einen histic Horizont oder Durchmischung mit dem mineralischen Boden ($C_{org}$ von 9 bis 52%) aufwiesen. Die um den C-Export durch Ernte korrigierte netto THG-Bilanz betrug ca. 4 t $CO_2$-C-Äqu. $ha^{-1}$ $a^{-1}$ auf Standorten mit einem Torfhorizont und geringer Entwässerung. Die netto THG-Bilanz erreichte ca. 7-9 t $CO_2$-C-Äqu. $ha^{-1}$ $a^{-1}$ auf Standorten mit Sandbeimischung im Torfhorizont und starker Entwässerung. Diese Ergebnisse zeigen den linearen Anstieg der THG-Emissionen von flach- zu tiefgründiger Drainage. Die Emissionen gingen nicht zurück als der Grundwasserstand unterhalb des Torfhorizontes fiel. Somit emittiert Grünland auf drainierten histic Gleysols ebenso hohe THG-Mengen wie Grünland auf tiefgründigen Histosols. Organische Böden mit sandigen Einmischungen in den Torf und $C_{org}$ Konzentrationen um 10% emittieren ebenso hohe THGs wie unvermischter Torf (> 30% $C_{org}$).

Zudem wurde der Effekt von Schafexkrementen auf die THG-Emissionen aus einem stark degradierten Torfboden in einem Mikrokosmenexperiment untersucht. Da Schafexkremente labile organische Substanzen enthalten, besitzen sie ein starkes Potential für positives Priming in Torfboden. $^{15}N$ und $^{13}C$ Stabilisotope wurden zu Quellendifferenzierung von $CO_2$ und $N_2O$ eingesetzt. Die Zugabe von Schafexkrementen erhöhte die gesamten $CO_2$-Emissionen proportional zur zugegebenen C-Menge, jedoch wurde unter den aeroben Experimentbedingungen kein Effekt auf die

$CH_4$-Emissionen beobachtet. Durch die Zugabe der Schafexkremente wurden die $N_2O$-Emissionen des inkubierten Bodens nicht erhöht. Es wurden keine oder geringe negative Priming Effekte auf torfbürtiges $CO_2$-C und $N_2O$-N beobachtet. Bei Stickstoff trat eine Verschiebung der $N_2O$-Quelle von Torf-N zu labilen N-Verbindungen aus den Exkrementen auf. Es wurde allerdings kein Mechanismus identifiziert, der auf das Risiko einer verstärkten Torfmineralisation durch Schafexkremente hinweist.

Die Ergebnisse dieser Dissertation zeigen, dass flachgründige organische Böden ebenso hohe THG Emissionen freisetzen wie tiefgründige Torfböden. Daher müssen sie in den nationalen THG Inventarberichten berücksichtigt werden. THG-Minderung auf flachgründigen organischen Böden kann durch klimaschützendes Management wie z.B. Beweidung bei kontrolliertem Wassermanagement oder Wiedervernässungsmaßnahmen umgesetzt werden.

**Schlagworte**: organische Böden, Moor, Treibhausgasemission

# Chapter 1: Overall introduction

## 1. Organic soils as greenhouse gas source

Organic soils are relevant potential greenhouse gas (GHG) sources on a global and European scale and in Germany (Lappalainen, 1996; Joosten and Clarke, 2002; Drösler et al., 2008) since they store large amounts of organic carbon. Undisturbed organic soils are water saturated and contain one third of the world's soil carbon stored as peat (Joosten and Clarke, 2002), equivalent to 450 Pg carbon (Gorham, 1991). However, most organic soils are drained for land use and subsequently peat is mineralized and organic soils turn from a sink into a source of GHGs, mostly $CO_2$ and $N_2O$. Therefore, drained organic soils represent hotspots of the anthropogenic contribution to climate change. However, adapted management of these soils poses the chance of mitigation of GHG emissions. This chapter sets the scientific background for GHG fluxes from organic soils and of management impacts on GHG fluxes. It highlights important scientific knowledge gaps, which gave the motivation for this PhD thesis.

### 1.1. Definition

Organic soils comprise all soils with a peat layer, however with a wider scope than the soil definition of Histosols (WRB, 2008). In pedological classification systems, definitions of organic soils vary strongly. Therefore, the following section overviews the most important pedological classification systems.

In the manual of soil mapping (AG Boden, 2005), soils with more than 30 mass percent organic substance within the organic horizon are classified as peat soils ("Moore") which comprise a separate soil section. These horizons consist of remains of peat forming plants and were formed under conditions of water excess. The organic horizon located on the surface requires a minimum depth of 30 cm to be classified as peat soil.

The international soil classification system of the world reference base (WRB, 2008) affiliates peat soils to the reference soil group "Histosol" which comprises soils with thick organic layers with a minimum thickness of 40 cm.

The IPCC definition of organic soils was generalized from the WRB (2008) and classifies by duration of water saturation, percentage of organic carbon (≥ 12 % $C_{org}$) and thickness (≥ 10 cm) of the diagnostic horizon. As a result, this also includes shallower and more degraded peat soils compared to other classification systems (IPCC, 2006).

The IPCC definition was transferred into the German classification system by Roßkopf et al. (2015) as follows: at least 12-18% $C_{org}$ per dry mass and a thickness of ≥ 10 cm for the upper organic horizon were used as selection criteria of organic soils for a German map of organic soils. Therefore, they include besides deep, carbon rich fens and bogs also shallow, low carbon non-peat organic soils ("Anmoor") in their classification.

Currently, most studies focus on peat soils, which meet the definition of Histosols (WRB, 2008) or "Moorböden" (AG Boden, 2005).

Many peat soils in Europe have been subjected to peat extraction in the past and the remaining peat cannot be classified easily, as it often contains disturbed layers, is partly too shallow to meet the definition of peat soils or has been mixed with external or the underlying mineral material. These disturbed remainders of peat soils at the edge between "Moorböden" and mineral soils have rarely been studied so far. Due to their neglected potential as significant carbon source, they are the focus of this work.

## 1.2. Peatland genesis and types

Natural peatlands are characterized by (partly) peat forming plants at the surface, an aerobic soil layer where plant litter is mineralized (= acrotelm) and large accumulations of dead plant material in the underlying water logged, anaerobic layer (= catotelm). Due to reduced mineralization under anaerobic conditions, incompletely decomposed plant material accumulates in undisturbed peatlands (Meier-Uhlherr et al., 2011), continuously raising the peat surface.

According to the prevailing plant species and hydrological conditions, peat layers indicate different peatland types which can be classified as bogs or fens (Göttlich, 1990). Bogs are rainwater fed and nutrient poor. The typical plant species are *Sphagnum* mosses. Fens on the other hand are ground-water fed, often nutrient rich with higher plant diversity, e.g. sedges, reed, willow and birch are typical for fen sites. Various intermediate stages exist between these two extremes. Besides this classification system which is coarse but universally applied, peatlands can also be grouped into more specific classes according to hydrological and ecological peatland types (Succow and Joosten, 2001; Meier-Uhlherr et al., 2011).

In this work, focus is set on a study area in a former bog-fen complex which is degraded due to drainage and peat extraction.

### 1.3. Spatial distribution of organic soils

Organic soils cover substantial parts of the land surface on a global and European scale and in Germany. Organic soils are found worldwide in zones with appropriate hydrological and climatic conditions for the formation of organic layers. In the boreal region, the occurrence of permafrost and in the tropics high precipitation result in impeded water drainage, waterlogging soil conditions and peat formation. In the temperate region, bogs and fens are formed if annual precipitation is higher than evapotranspiration or if permanent high groundwater levels influence soil conditions, respectively (Göttlich, 1990). Globally organic soils cover around 400 million ha of the land surface area including peatlands with > 30 cm thick peat layers (Lappalainen, 1996; Joosten and Clarke, 2002; Fig. 1-1).

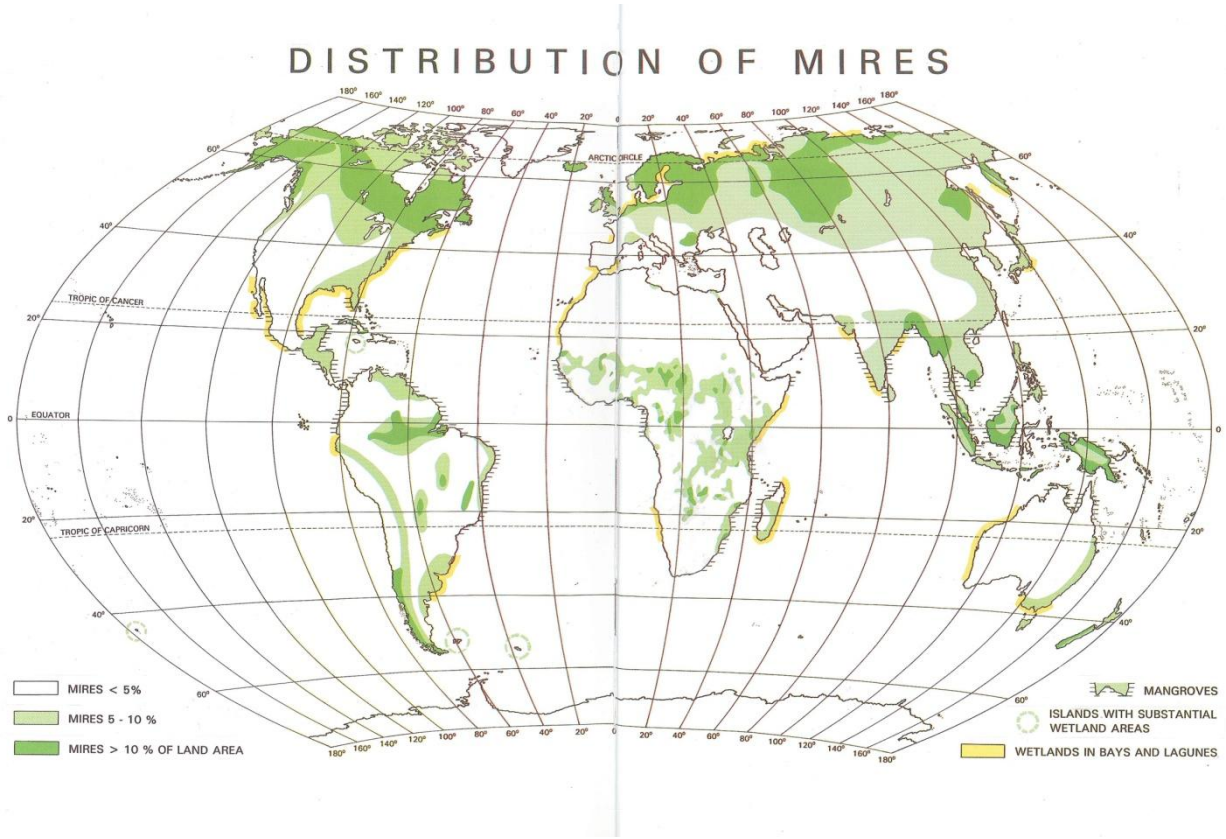


**Fig. 1 - 1**: Global distribution of peatlands (= mires; Lappalainen, 1996)

In Europe, the area of organic soils declines from North to South with increasing temperatures and from West to East with decreasing precipitation (excluding peatlands in mountain ranges; Montanarella et al. 2006; see Fig. 1-2). European organic soils with an organic carbon content of more than 20% comprise an area of around 368,000 km² which equals 7.6% of the land area of Europe (Montanarella et al., 2006).

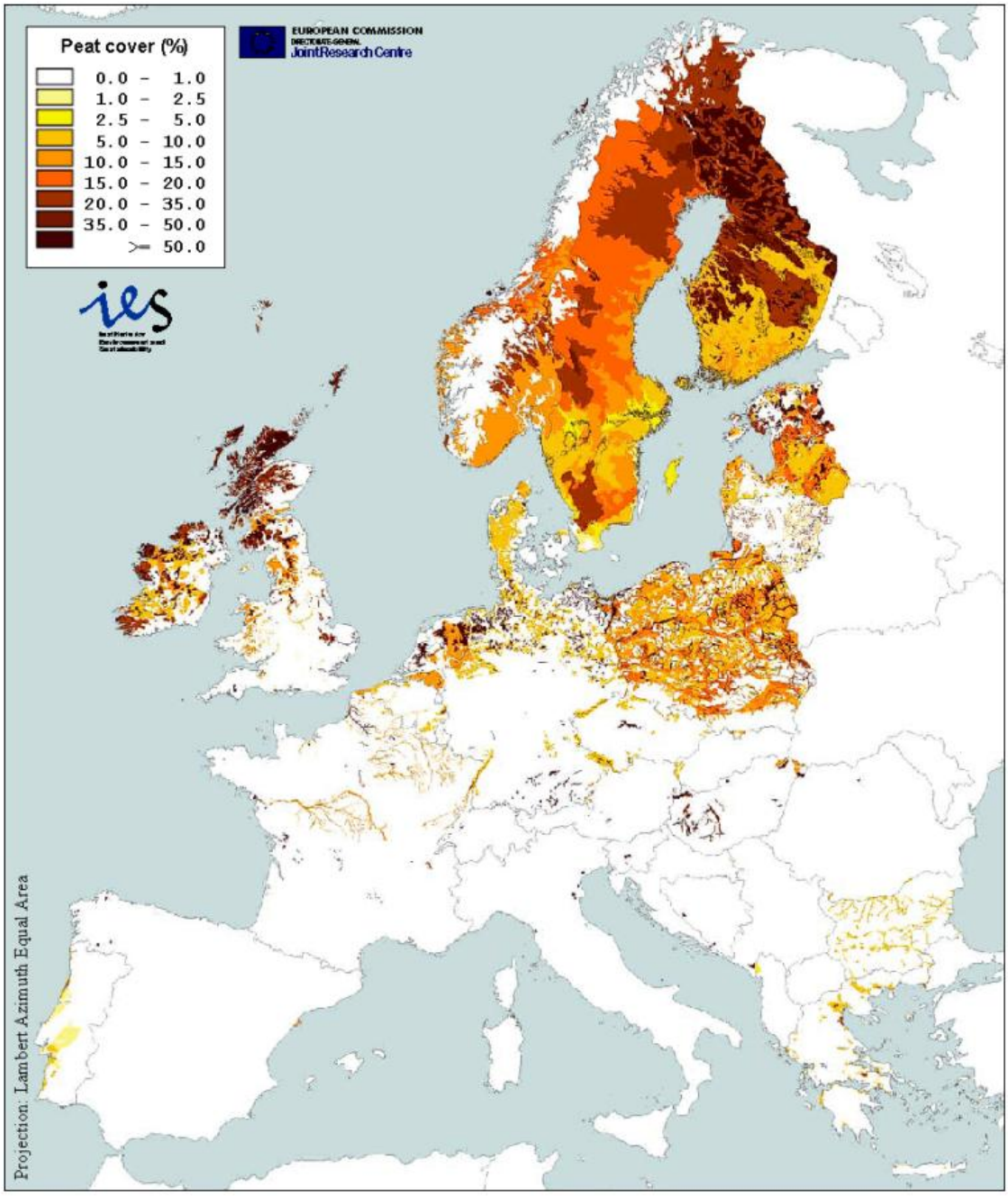


**Fig. 1 - 2**: Map of European organic soils (Montanarella et al., 2006)

In Germany, bog formation is mainly found in the northwestern lowlands, low mountain ranges and Alpine foothills due to high precipitation whereas the northeast and riverine lowlands in the South are dominated by fens in river valleys and depressions driven by geogenic and topographic conditions (Roßkopf et al., 2015; see also Fig. 1-3). According to a new study by Rosskopf et al. (2015) organic soils cover 15,682 $km^2$of Germany which amounts to 4.4% of the total area.

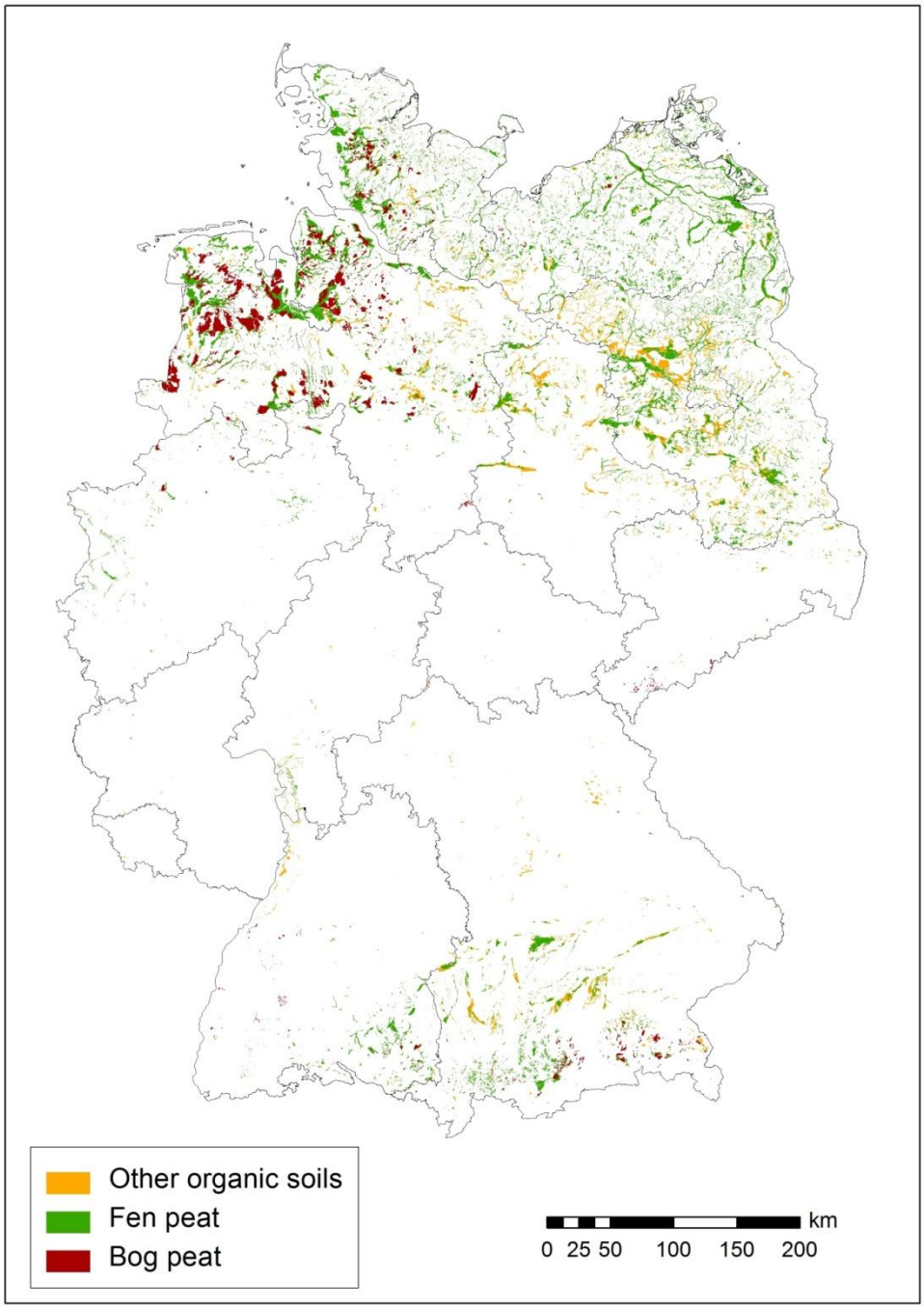


**Fig. 1 - 3**: Map of (potential) organic soils in Germany (Geological map 1:200,000; BGR, without year).

### 1.4. Utilization of organic soils

In this chapter, anthropogenic management practices of organic soils on a global scale and with a special focus on temperate regions are discussed. Worldwide the percentage of natural peatlands is declining due to drainage for peat extraction, agriculture, forestry or settlements.

Timber production in boreal regions, fodder production and grazing in temperate regions and palm-oil plantations in the tropics as well as peat extraction for horticultural use or energy production are the main land use types on peat soils worldwide (Joosten and Clarke, 2002).

According to Drösler et al. (2008) half of the peatlands in Europe are subject to various sorts of land use. The dominant land use on peat soils in the boreal region is forestry (Drösler et al., 2008), whereas in the temperate zone grasslands of varying management intensity predominate (Schrier-Uijl et al., 2010). In Germany, 53% of organic soils are managed as grasslands (UBA, 2014).

All land use types are typically coupled with drainage resulting in aeration of the peat body, subsidence and chemical and microbial peat mineralization. As a consequence, GHG emissions of peat soils increase and substantial amounts of $CO_2$ are released.

Since more than a decade, the protection of peatlands as part of the Habitats Directive (European Economic Community, 1992) has been aiming at the conservation or restoration of peatlands as habitat for plants and animals. Rewetting of peatlands or the extensification of farming practices, e.g. extensive grassland utilization with extensive sheep grazing, are two potential activities in nature protection areas in Germany. As a new objective, peatland protection also aims at the reduction of greenhouse gas emissions for climate protection (Drösler et al., 2012) which is implemented e.g. in the program for peatland protection of Mecklenburg - West Pomerania (Ziebarth et al., 2009).

However, the influence of nature conservation practices like sheep grazing on the GHG emission potential of shallow peat soils has not been evaluated so far.

## 1.5. Organic soils as sink and source of greenhouse gases

Natural peatlands, which accumulated their carbon stocks over several millennia, represent one of the largest terrestrial carbon sinks. First global estimates of carbon accumulation in boreal and subarctic peatlands resulted in a current accumulation rate for organic material of 0.5 mm $yr^{-1}$ equivalent to 0.3 t C $ha^{-1}$ $yr^{-1}$ (Gorham, 1991). The long term sink function of several centuries amounts to 0.1 - 3 t C $ha^{-1}$ $yr^{-1}$ in boreal regions (Joosten and Clarke, 2002 and citation therein). Therefore, one-third of the global soil carbon store is found in peatlands (Joosten and Clarke, 2002).

Due to the high carbon concentration in peat soils, disturbed peatlands act as huge carbon and nitrogen sources (Smith and Conen, 2004). Besides carbon dioxide ($CO_2$), two other main greenhouse gases, nitrous oxide ($N_2O$) and methane ($CH_4$), are released from organic soils (Fig. 1-4). In order to compare the greenhouse effect of different GHGs, the Global Warming Potential was created which refers to a time horizon of 100 years (GWP100). In this concept, $CO_2$ has a GWP100 of 1 (= reference base), $N_2O$ of 298 kg $CO_2$ $kg^{-1}$ $N_2O$ and $CH_4$ of 25 kg $CO_2$ $kg^{-1}$ $CH_4$ (Forster, 2007). Drained organic soils

have been identified as major source of GHGs induced by peat mineralization and peat fires (Drösler et al., 2008 for Europe; Page et al., 2011 for tropics; IPCC, 2014a for global contribution). In Germany, the majority of the 1.5 million ha peatlands are drained and subject to subsidence and peat degradation (Roßkopf et al., 2015).

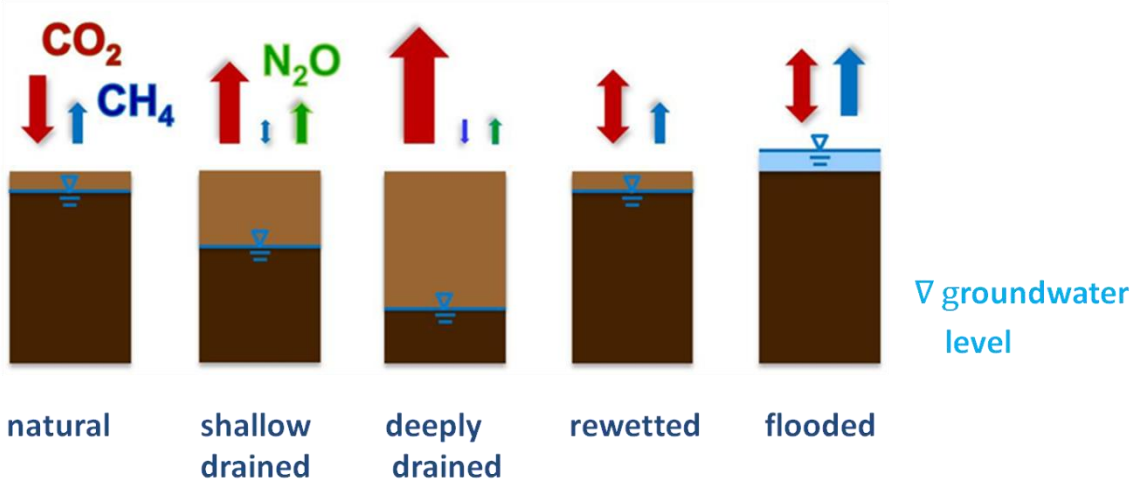


**Fig. 1 - 4**: Amounts of GHG emissions of peat soil in dependence of drainage intensity (adapted from Drösler et al., 2008). Dark brown areas represent the water saturated part of the peat profile, light brown areas reflect aerated zone.

A series of physical and chemical processes is induced by drainage of organic soils. First, drainage of peat soils lowers the groundwater table within the peat body. By this, the large percentage of water filled pore space of 80 to 97 vol.% of natural peatlands is drained, initiating peat texture changes (Göttlich, 1990). Accordingly, the subsidence of the soil surface results in a compaction of the peat material. An increase of the bulk density from a minimum of 0.1 g $cm^{-3}$ in natural peat soils (moss peat) to the range of mineral soils with up to 1-2 g $cm^{-3}$ are the consequence (Kasimir-Klemedtsson et al., 1997). Furthermore, aeration of the peat material stimulates aerobic mineralization of the soil organic matter which mainly increases $CO_2$ emissions.

Besides the loss of soil organic carbon in the form of $CO_2$, mineralization of fibrous peat to homogeneous degraded peat profoundly changes peat properties. Water retention capacity is reduced due to changes in pore size distribution. Subsidence and compaction result in a reduction of large pores and an increase of small ones. Moreover, with increasing degree of peat decomposition water permeability of peat soil is reduced (Göttlich, 1990). Additionally, with lowering water content and exceeding of a certain threshold, peat can also become hydrophobic (Berglund and Persson, 1996) which impedes rewetting of organic soils.

Drainage also affects water quality since filtration effectivity is dependent on hydrogen ion activity and the degree of peat decomposition (Göttlich, 1990). There are a number of processes leading to

peat loss after draining: Physical loss of substances occurs as a result of ground or surface water erosion or chemical loss due to leaching.

Especially in the tropics and boreal zones, the threat of peat loss due to large peat fires exists. Deflation of peat is especially important on peat extraction sites during dry seasons. If peat soils are drained, wet and moist habitats for certain well adapted plants and animals are lost, which results in a loss of biodiversity.

Drainage exposes the peat layer to oxic conditions and the general biogeochemical mechanism of the resulting peat degradation is known and linked to main driving parameters. However, a general quantitative relation to drivers of peat degradation, such as temperature, moisture, and nutrient status (IPCC, 2014a, Wetlands Supplement) is lacking.

## 1.6. Methodological challenges in measuring GHG exchange

GHG emissions from organic soils have a comparatively short research history, in which most studies were conducted in the boreal region (e.g. Frolking et al., 1998; Alm et al., 2007a) focusing on natural and forest ecosystems (e.g. Jungkunst et al., 2008; Lai et al., 2012). Moreover, most studies have looked at one or two GHGs only (e.g. Flessa et al., 1998; Marinier et al., 2004; Regina et al., 2004).

Studies with a full GHG budget on grassland in the temperate zone have been restricted to few sites, which were either intensively managed (Schrier-Uijl et al., 2010) or rewetted (Hendriks et al., 2007) and studies were mainly located in the Netherlands (Hendriks et al., 2007; Jacobs et al., 2007; Veenendaal et al., 2007; Schrier-Uijl et al., 2014). Though extensively managed grasslands are quite frequent, they have not been studied in depth so far.

Most studies used manual chamber techniques for measuring experimental plots in weekly to monthly frequency. There has been a long debate about robustness of the calculation of GHG fluxes, the necessary measurement frequency of GHG fluxes and the coverage of environmental conditions in summer and winter for robust annual GHG budgets (Alm et al., 1999; Aurela et al., 2002; Bubier et al., 2002; Huth et al., 2012).

Also the temporal positioning of measurement campaigns before and after management events (harvest, soil cultivation or fertilization) or meteorological events (e.g. precipitation) is crucial for further calculation of annual GHG balances. Since between campaigns interpolation is needed which can be linear in the case of $N_2O$ and $CH_4$ or complex function based models (e.g. Lloyd and Taylor, 1994 for $R_{eco}$; Falge et al., 2001 for NEE) in the case of $CO_2$, positioning of campaigns has a direct impact on annual GHG budgets (e.g. Beetz et al., 2013; Hoffmann et al., 2015).

Observed $CO_2$ fluxes are composites of vegetation and soil fluxes. What matters for understanding the processes of peat degradation and mineralization, however, is the contribution of peat to the $CO_2$ flux. For this purpose, flux partitioning into soil and plant derived fluxes is necessary. This can be achieved by several methods.

First, the budget approach was often used to determine soil derived C fluxes e.g. for the European carbon balance (Schulze et al., 2009; Schulze et al., 2010) or for the GHG balance in agricultural peatlands (Schrier-Uijl et al., 2014). Determination of soil derived carbon fluxes by measuring net ecosystem carbon exchange (NEE; Fig. 1-5) with transparent chambers requires a correction for above ground biomass, carbon export by harvest and carbon import by fertilization (IPCC, 2014a-Annex 2A.1). The precision of this method thus depends on precise data for each of these terms.

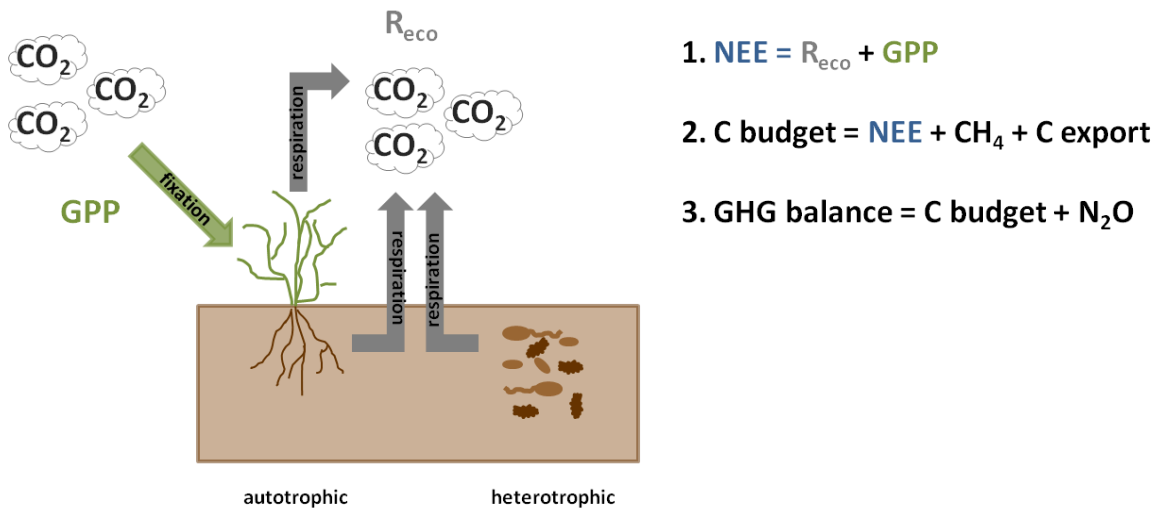


**Fig. 1 - 5**: Scheme of autotrophic and heterotrophic ecosystem carbon fluxes (left). Arrows represent $CO_2$ fluxes. Equation 1 defines net ecosystem exchange (NEE) as the sum of ecosystem respiration ($R_{eco}$) and gross primary production (GPP). Equation 2: C budget is composed of NEE, $CH_4$ flux and C export. Equation 3: GHG balance completes the C budget for the $N_2O$ flux (in C equivalents). Uptake of C has a negative sign, release of C a positive sign.

Other approaches for separation of soil and plant derived $CO_2$ sources are trenching of roots or bare soil measurements which are frequently used in peatland forests (Alm et al., 2007b; Makiranta et al., 2008; Jauhiainen et al., 2012; Ojanen et al., 2012) but also in agricultural systems (Biasi et al., 2012). Disadvantages of these techniques are the major disruption of the natural ecosystem as well as different microbial activity in trenched and untrenched plant-soil systems due to loss of root exudates which in turn results in different soil organic matter (SOM) decomposition rates (Kuzyakov, 2006).

As an alternative method, isotope techniques which do not disturb the plant-soil system can be applied to quantify the contribution of single $CO_2$ sources to the total $CO_2$ flux. As an example, moderately expensive measurements of natural abundance of the isotope $^{13}C$ can be used if the signal difference between peat and vegetation is large enough (see section 1.7.).

### 1.7. Identification and quantification of GHG sources by the stable isotope technique

Besides other applications in soil science like reconstruction of historic vegetation changes in natural systems or quantification of soil organic matter turnover (Balesdent et al., 1993; Boutton et al., 1998), the stable isotope tracer technique can be used to quantify the contribution of two different carbon or nitrogen sources to a joint pool in labeling experiments (Hart and Myrold, 1996; Kuzyakov, 2006). This is because if two sources with different isotope composition form a third pool, the resulting isotopic composition of this pool is a mixture of the isotope signals of the two sources. If the isotopic composition of the two sources and the mixed pool are known, the quantitative contribution of the two sources to the resulting pool can be calculated. The higher the difference in isotopic composition between the two source pools, the higher the accuracy of the calculated contributions to the mixed pool. In situations where the difference between the source pools is very small or not significant, one pool is usually enriched in the heavy isotope by the addition of naturally or artificially enriched label. If e.g. the contribution of old SOM versus fresh C input, e.g. excreta in extensive grasslands, to soil $CO_2$ formation is to be quantified, the addition of $^{13}C$ enriched fresh C would lead to a change of the isotopic C composition of $CO_2$ being proportional to the contribution of fresh C input to the $CO_2$ production.

Source identification or quantification by utilization of natural abundance differences of two isotopes (for $^{12}C/^{13}C$ see Balesdent and Mariotti, 1996; for $^{14}N/^{15}N$ see Hoegberg, 1997) or by artificial enrichment of one isotope in relation to the other (e.g. $^{14}N$ and $^{15}N$; Hart and Myrold, 1996) are two methods of applying stable isotopes in pedological studies.

In this context, short-term changes in SOM decomposition induced by easily available C or N sources (e.g. glucose, rhizodeposits or sheep excreta), the so called priming effect, can also be investigated by the stable isotope technique (Kuzyakov et al., 2000). The addition of easily available substrate can either cause a positive priming effect, i.e. more soil carbon or nitrogen is released in comparison to an untreated control, or a negative priming effect, i.e. less soil C or N is emitted in comparison to an untreated control.

The natural abundance of $^{13}C$ in C3 and C4 plants is in the range of -26 to -28 δ‰ and -12 to -14 δ‰, respectively (Tieszen, 1991) , due to different fractionation during photosynthesis. Main processes of isotope discrimination during photosynthesis are diffusion of $CO_2$, incorporation of $CO_2$ by phosphoenolpyruvate (C4-plants) or ribulose bisphosphate carboxylase (C3 plants) as well as plant

respiration (O'Leary, 1981). During decomposition of plant litter or any other C input and soil forming processes, the original isotopic signal is only slightly changed by enrichment of the heavier isotope $^{13}C$ in SOM. As a result, depletion in the product gases, e.g. $CO_2$, is small and $\delta\,^{13}C$ of $CO_2$ still reflects the signal of the plant source. Thus, when adding C4 derived C to a C3 influenced soil, any changes in the isotopic composition of produced $CO_2$ can be attributed to the mineralization of fresh C. In this way, the contribution of fresh plant litter or excreta derived C to newly formed $CO_2$ can be calculated.

In contrast, the use of natural differences in isotopic composition for source identification or quantification in the case of N is more difficult. There are two reasons for this: first, the natural difference in the $^{15}N$ content of plant material usually is much lower than for $^{13}C$, i.e. the resulting difference in any product pool will be smaller, thus lowering the precision of calculated source contribution. Second, a number of degradation processes like nitrification or denitrification can form $N_2O$ (Yoneyama, 1996), but show different fractionation factors that are higher than the existing difference in source signatures. In this case, the resulting isotopic signature of $N_2O$ is determined by both, the source (fresh or old organic matter) and the chemical formation process making source identification and calculation of source contribution difficult. In these cases it is essential to level out the influence of any chemical fractionation by 1) comparing $^{15}N$ changes of e.g. $N_2O$ in a naturally enriched treatment with those in an unlabelled one or 2) using highly enriched N sources that exceed any isotope shifts caused by fractionation effects (Baggs, 2008).

Tracing $CO_2$ and $N_2O$ sources in animal production systems by using stable isotopes is necessary to identify GHG mitigation options (Clough et al., 2013). The GHG emission potential of peat soils used as pastures should be minimized with respect to global warming. The effect of sheep excreta on the GHG emissions of peat, dividing the total $CO_2$ and $N_2O$ fluxes into peat or excreta derived $CO_2$-C or $N_2O$-N fluxes has, however, not been studied up to now. As shown above, the use of stable isotope techniques offers the possibility to quantify the importance of this management effect on the GHG potential of organic soils. Thus, these techniques form the basic requirement to identify the potential of management practices for GHG mitigation.

## 1.8. International policy framework for GHG mitigation on organic soils

The existence of global warming, which has been induced by anthropogenic activities, has been recognized on an international level. Efforts for its restriction resulted in the formation of the United Nations Framework Convention on Climate Change (United Nations, 1992) and the Kyoto protocol (United Nations, 1998), which aimed at the reduction of GHG emissions of industrial countries of average 5.2% compared to 1990 in the first commitment period (2008-2012). All countries who

signed the Kyoto protocol committed themselves to report national GHG emissions and subsequently follow the guidelines for national GHG inventories edited by the intergovernmental panel on climate change (IPCC).

In the *Revised 1996 IPCC Guidelines for National Greenhouse Gas Inventories* first standards for reporting of $N_2O$ emissions from agriculture and grassland were introduced (IPCC, 1997). In the following *2003 IPCC Good Practice Guidance for Land Use, Land-Use Change and Forestry* first emission factors for $CO_2$ from grassland were indicated (IPCC, 2003). In the *2006 IPCC Guidelines for National Greenhouse Gas Inventories (2006 IPCC Guidelines)* standards for monitoring and reporting GHG emissions on a national scale were updated and amended (IPCC, 2006). With the *2013 Revised Supplementary Methods and Good Practice Guidance arising from the Kyoto Protocol*, the IPCC guidelines for national greenhouse gas inventories were comprehensive and nearly complete (IPCC, 2014b).

*The 2013 Supplement to the 2006 IPCC Guidelines for National Greenhouse Gas Inventories: Wetlands (Wetlands Supplement)* provided updated methods for estimating anthropogenic emissions and reduction of greenhouse gas emissions from additional wetland types and drained soils (IPCC, 2014a). The *Wetlands Supplement* described for the first time comprehensively all land use categories, climate regions and GHGs with emissions factors for organic soils (for a short overview see Fig. 1-6).

As mentioned earlier, the IPCC definition of peat soils is broader than the international one of Histosols (WRB, 2008) or “Moore” in the soil survey manual (AG Boden, 2005). It assumes that also shallow peat soils and strongly degraded ones react like real peat soils concerning GHG fluxes (IPCC, 2006). Most countries ignore soils with a lower organic carbon content in the “organic soil” classification for their national GHG inventory, treating the soils with intermediate carbon content or shallow peat horizons as mineral soils. In contrast, in the Danish GHG inventory it is assumed that soils with an organic C content ranging between typical mineral soils ($C_{org}$ concentration < 6%) and peat ($C_{org}$ concentration > 12%) emit half as much GHGs as organic soils (Nielsen et al., 2012). Yet, the basis for this assumption is rather unclear.

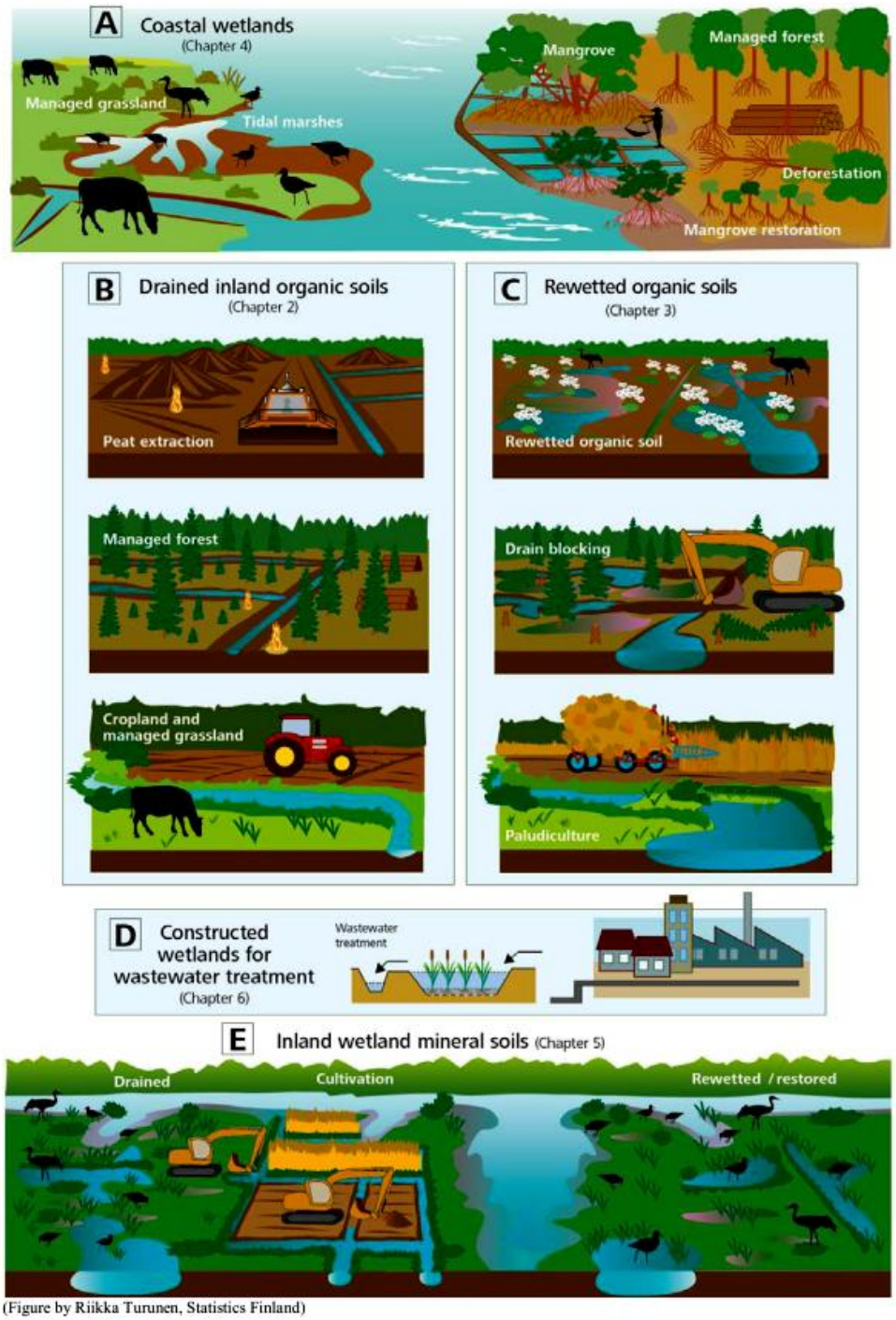


**Fig. 1 - 6**: Typical management practices on organic and wet soils (original figure from IPCC, 2014a). Letters indicate different wetland types e.g. subfigure B contains drained inland organic soils which are described in chapter 2 of the *Wetlands Supplement.*

A large proportion of organic soils (2.9 million ha) in Germany is classified as non-peat organic soils (Roßkopf et al., 2015) which also include soils that are subject to successional soil development with ongoing peat degradation and soil mixing due to land management practices. Due to their wide distribution in Germany, the emission potential of these shallow organic soils should be considered.

Besides a recently published study by Eickenscheidt et al. (2015), nearly no published GHG budgets of shallow organic soil exist in Germany up to now. Eickenscheidt et al. (2015) showed that mainly land use rather than $C_{org}$ content control the amount of GHG emissions of intensively managed organic soils.

Thus, the development of methods e.g. regarding the measurement frequency of GHG and data acquisition on shallow organic soils is of high importance in order to improve the data base on shallow organic soils in the German GHG inventory. These GHG data from shallow organic soils, typically under anthropogenic use, can then be used to identify a so far neglected GHG source and climate-smart management strategies for organic soils.

## 1.9. Towards climate-smart management of organic soils

Agriculture causes 14% of global GHG emissions contributing significantly to global climate change (FAO, 2013a, b). Immediate consequences of this climate change e.g. an increased occurrence of precipitation and temperature extremes (for Europe Seneviratne et al., 2006; global IPCC, 2007) have a direct influence on agricultural yields. This is of particular importance in developing countries where food security is already at risk. However, agriculture on the other hand also has the potential to contribute to climate protection in the form of climate-smart agriculture e.g. on peatlands.
According to FAO 2013 climate-smart agriculture is "an agriculture that sustainably increases *productivity*, strengthens the resilience to climate change (*adaptation*) and reduces / removes greenhouse gases (*mitigation*) while enhancing the achievement of national food security and development goals" (FAO, 2010).

Intensively used peatlands could adopt climate-smart agriculture practices in several ways. Rewetting of peatlands poses a mitigation option for GHG emissions. In most cases this is a nature protection activity which implicates an abandonment of intensive agriculture or forestry activities (Vasander et al., 2003; Höper et al., 2008). Rewetting can be challenging if peat cannot be rewetted due to changes in soil structure during decomposition, the water demand cannot be met or if high $CH_4$ emissions occur in the course of flooding. Also, a competitive intensive agricultural use for bioenergy crops constitutes an obstacle for rewetting measures.

During the last years there has been a debate about wet grassland management in order to re-establish agricultural use to some extent. Paludiculture – the cultivation of crops adapted to wet soil conditions (e.g. reed canary grass or peat moss) - has been proposed as one option (Joosten et al., 2012). Several studies on this topic showed the relevance for wet peatland cultivation as GHG mitigation option (Guenther et al., 2015; Karki et al., 2015; Pouliot et al., 2015). In peatland areas

where rewetting is not possible or only to a relatively low extent, management by mowing or grazing is needed to prevent succession of woody plants in order to preserve open land species. Therefore, an extensification of agricultural utilization is a primary GHG mitigation aim.

Due to the fact that climate change cannot be reversed but only attenuated, agricultural adaptation strategies are required. Keeping organic soils in a wet state could reduce the impact of drought spells which will become more frequent (Turral et al., 2011). Since grassland yields are strongly related to water availability (Olesen et al., 2011), wet organic soils are more resilient to dry weather conditions. In a current project “climate-smart agriculture on organic soils” (CAOS), coordinated by the Thünen Institute, attempts to enhance and test climate-smart management practices on European organic soils are made which includes the reduction of GHG emissions. Controlled drainage and active water management are tested as climate-smart management strategies in grasslands (Van den Akker et al., 2012; Deru et al., 2014) and first results indicate that the use of submerged drains can reduce $CO_2$ emission from organic soils with at least 50% (Van den Akker et al., 2012).

# 2. Motivation and hypotheses

## 2.1. Motivation

Climate change caused by anthropogenic greenhouse gas emissions poses an unavoidable challenge in different areas of life. The loss of carbon in degraded peatlands due to mineralization significantly contributes to global warming (Limpens et al., 2008). In Germany, 88% of all GHG emissions derive from the energy sector and 7.5% from agriculture, forestry and land use (AFOLU; UBA, 2014). 50 % of the emissions from the AFOLU sector are derived from peatlands, although these comprise only 4.4%-5% of the land surface area of Germany (UBA, 2009; Roßkopf et al., 2015). Therefore, mitigation options for the reduction of GHG emissions like peatland restoration or at least extensification of peatland management must be taken into account as they only affect a small land surface area but have a high effect on total fluxes of this sector. Shallow organic soils are often located on the border between protected peatlands and surrounding intensively cultivated fields. They are still subject to a relatively high intensity of anthropogenic utilization, which implies the ongoing degradation of soil organic carbon. Therefore, shallow organic soils need to be evaluated in terms of their GHG emission and saving potential, which is the scope of this work.

Although the need for determination of GHG emissions is commonly clear, the representative measurement of GHG emissions, especially $CO_2$, from soils on heterogeneous sites is a frequently discussed issue. Eddy covariance towers are able to measure net ecosystem exchange (NEE) continuously over large areas, but they are restricted to homogeneous vegetation coverage. Automated chamber measurements provide continuous high resolution data from heterogeneous vegetated areas, but with smaller spatial resolution due to high costs. In contrast, manual chamber measurements are operated as campaigns with a lower sampling frequency, but lower cost intensity and higher spatial resolution (Subke et al., 2009). Therefore, the utilization of manual chambers were most applicable in the study area of this thesis. Due to the high carbon emission potential of organic soils and the high temporal dynamics of carbon fluxes (e.g. Beetz et al., 2013; Beyer et al., 2015), measurement frequency can have a significant impact on calculated $CO_2$ balances. Campaign frequency is often defined according to plant growth stage and management events, though no clear numbers on the influence of this on the calculated $CO_2$ balance are available. Evaluating the robustness of $CO_2$ balances determined with different measurement frequencies on shallow organic soils is therefore part of this PhD thesis.

The organic soils remaining after peat cutting, are at the transition between “peat soils” and “non-peat soils”. They are characterized by shallow peat horizons which are partly mixed with mineral subsoil. Therefore, they possess a higher bulk density, a lower carbon content and a different moisture regime compared to undisturbed organic soils. Due to more frequent dry conditions in

these soils, peat degradation proceeds until no peat is left or a new equilibrium carbon content is reached which is accompanied by ongoing GHG emissions. However, the precise effects of water content, groundwater table and SOC contents on the extent of GHG emissions in these drained soils are still widely unknown. The investigation of these effects on GHG emissions and their implementation into models used for calculation of annual GHG balances is another focus of this work.

Grassland on organic soils is the most important land-use form for these soils in the temperate climate zone (Drösler et al., 2008). Sustainable grassland management in drained or semi-natural peatlands is often combined with nature protection aims. Frequently, sheep grazing is conducted on extensively managed grasslands on organic soils which poses an important source of income for local farmers (Germer, 2006; ANL 2015). Up to now there is no detailed information on whether the concentrated easily degradable carbon and nutrients in excreta could stimulate peat degradation by priming. The clarification of this topic is another aim of this PhD thesis.

A peatland with strong small-scale gradients was selected as study area allowing a systematic study of these drivers of GHGs within a small area. The Grosses Moor near Gifhorn is located at the driest end of bog formation in North Germany (fen-bog transition peat). It is a former ombrotrophic peat bog which was altered by peat drainage and peat cutting during the 19$^{th}$ and 20$^{th}$ century. Nowadays the Grosses Moor is influenced by groundwater. The study area is characterized by small peat shoulders and depressions with different water table levels and an irregular anthropogenic mixing of peat layer and mineral soil. It is managed as extensive grassland with sheep grazing one to three times a year (for more detailed information see Chapter 3).

The mentioned main topics of this PhD thesis are to be studied by means of field and laboratory experiments. Continuous automated $CO_2$ measurements were exemplary conducted in the field in order to evaluate the best practice measurement frequency and procedure on grassland on shallow organic soils. Campaign based GHG measurements of several field sites were conducted to quantify $CO_2$, $N_2O$ and $CH_4$ emissions of extensive grassland on shallow organic soils along groundwater table and carbon gradients. In order to avoid damages on the field sites and of the equipment by animals, measurement sites were fenced and plots were cut according to grazing frequency. Since the influence of sheep excreta on the GHG emissions and potential priming effects were not determined in the field, a laboratory experiment under stable temperature and moisture conditions was set up using undisturbed peat soil columns of the same field site.

## 2.2. Hypotheses

This PhD thesis aims at providing research results on three major topics in connection with GHG emissions from shallow organic soils:

First, the influence of measurement frequency and interpolation procedure on $CO_2$ emissions, with the focus on ecosystem respiration ($R_{eco}$), was investigated on an exemplary field data set.

Second, the influence of groundwater table depth and organic carbon content on GHG emissions was analyzed based on one year of field campaign data.

Third, the risk of enhanced peat mineralization by priming due to extensive sheep grazing on shallow organic soils was quantified by a laboratory microcosm experiment using source partitioning of carbon and nitrogen.

In the following sections each of these three topics is substantiated in detail by corresponding hypotheses.

### *2.2.1. Influence of measurement frequency on calculated $CO_2$ emission budgets*

Manual chamber measurements with campaign-based approaches are commonly used for the determination of annual $R_{eco}$ and NEE sums (Beetz et al., 2013; Beyer et al., 2015; Eickenscheidt et al., 2015; Hoffmann et al., 2015). The inter-campaign distance is often dependent on management and plant phenology. If, however, short-term fluctuations in groundwater table significantly affect soil respiration at time scales of days, campaign-based $R_{eco}$ measurements on organic soils have a considerable risk of temporal misrepresentation. Therefore, inter-campaign uncertainty is likely to be larger than the intra-campaign uncertainty. In addition, differences between daytime and nighttime $R_{eco}$ parameterization were already observed on mineral and organic soils (Falge et al., 2003; Mielke et al., 2005; Juszczak et al., 2012).

Hypotheses of study 1:

(A) Temperature – soil moisture response functions explain more of the $R_{eco}$ variability than purely temperature driven models.

(B) Flux measurements must capture day-night patterns, but not necessarily day-to-day variations for robust seasonal $R_{eco}$ estimates.

(C) Monthly measurement campaigns covering representative diurnal temperature ranges produce robust seasonal $R_{eco}$ estimates with small additional systematic and random uncertainty compared to continuous measurements.

### *2.2.2. Influence of groundwater table depth and organic carbon content on GHG emissions*

GHG emissions increase with increasing drainage depth in deep peat soils (Silvola et al., 1996; Schrier-Uijl et al., 2010; Berglund and Berglund, 2011). Organic soils released more GHG emissions than mineral soils (Freibauer, 2003), mainly due to higher organic carbon content. However, it is still unknown if the correlation between GHG emissions and groundwater table depth and $C_{org}$ is also valid for shallow organic soils, e.g. histic Gleysols. Most studies focus on deep peat soils, which meet the definition of Histosols (WRB, 2008). However, the IPCC definition of organic soils also includes shallow organic soils with a lower $C_{org}$ content (IPCC, 2006). Improvement of the data basis for GHG emission reporting on organic soils and testing the validity of GHG inventory assumptions for organic soils is done in this part of the PhD thesis.

Hypotheses of study 2:

(D) GHG emissions (mainly $CO_2$) of histic Gleysols increase linearly with drainage depth in the peat layer and level off when the water table falls below the peat layer.

(E) Peat mixed with mineral subsoil and resulting lower $C_{org}$ concentration emits lower amounts of GHG than unmixed peaty soil with a high $C_{org}$ concentration.

### *2.2.3. Influence of management on GHG emissions*

Intensively managed organic soils emit high amounts of GHG gases due to deep drainage, fertilizer input and soil cultivation (Beetz et al., 2013; IPCC, 2014a and citations therein; Eickenscheidt et al., 2015). In order to reduce GHG emissions and for nature protection purposes, organic soils are often transferred to a more extensive or no utilization state. Extensive grassland management with sheep grazing is commonly used (Germer, 2006). Up to now few information is available on the influence of easily degradable material like sheep excreta on GHG emissions of shallow organic soils. In former laboratory studies peat emitted large amounts of GHGs if high-energy carbohydrates and lignin (Reiche et al., 2010) or fresh organic material (Hahn-Schoefl et al., 2011) were applied to the peat soil. Since also on mineral soils positive priming of sheep excreta was observed (Ma et al., 2013), sheep grazing on shallow organic soils poses the risk of increased peat carbon loss. For clarification, a laboratory experiment with undisturbed soil columns was set up in the context of this PhD thesis and sheep grazing as GHG mitigation option was evaluated.

Hypotheses of study 3:

(F) Sheep excreta increase emissions of $CO_2$, $CH_4$ and $N_2O$ from peat soil.

(G) Sheep excreta induce a positive carbon and nitrogen priming in peat soil triggering $CO_2$ and $N_2O$ release from the peat.

In the subsequent chapters all hypotheses are elucidated in detail on the basis of three manuscripts. Applied material and methods for each study are listed in the respective chapter. Accepted manuscripts were adapted to the format of this PhD thesis without changing the content of the original papers.

## 3. References


AG Boden, 2005. Bodenkundliche Kartieranleitung (German soil mapping guide) - KA5. Bundesanstalt für Geowissenschaften und Rohstoffe in Zusammenarbeit mit den Staatlichen Geologischen Diensten, Hannover. 438 pp.

Alm, J., Saarnio, S., Nykanen, H., Silvola, J., Martikainen, P. J., 1999. Winter $CO_2$, $CH_4$ and $N_2O$ fluxes on some natural and drained boreal peatlands. Biogeochemistry 44, 163-186.

Alm, J., Shurpali, N. J., Minkkinen, K., Aro, L., Hytonen, J., Laurila, T., Lohila, A., Maljanen, M., Martikainen, P. J., Makiranta, P., Penttila, T., Saarnio, S., Silvan, N., Tuittila, E.-S., Laine, J., 2007a. Emission factors and their uncertainty for the exchange of $CO_2$, $CH_4$ and $N_2O$ in Finnish managed peatlands. Boreal Environment Research 12, 191-209.

Alm, J., Shurpali, N. J., Tuittila, E.-S., Laurila, T., Maljanen, M., Saarnio, S., Minkkinen, K., 2007b. Methods for determining emission factors for the use of peat and peatlands - flux measurements and modelling. Boreal Environment Research 12, 85-100.

ANL, 2015. Forschungsbereich Beweidung im Naturschutz. Bayerische Akademie für Naturschutz und Landschaftspflege, Laufen. http://www.anl.bayern.de/forschung/beweidung/index.htm. 07.09.2015

Aurela, M., Laurila, T., Tuovinen, J. P., 2002. Annual $CO_2$ balance of a subarctic fen in northern Europe: Importance of the wintertime efflux. Journal of Geophysical Research-Atmospheres 107, 4607.

Baggs, E. M., 2008. A review of stable isotope techniques for $N_2O$ source partitioning in soils: recent progress, remaining challenges and future considerations. Rapid Communications in Mass Spectrometry 22, 1664-1672.

Balesdent, J., Girardin, C., Mariotti, A., 1993. Site-related $\delta^{13}C$ of tree leaves and soil organic matter in a temperate forest. Ecology 74, 1713-1721.

Balesdent, J., Mariotti, A., 1996. Measurement of soil organic matter turnover using $^{13}C$ natural abundance, In: Boutton, T.W., Yamasaki, S. (Eds.), Mass spectrometry of soils. Marcel Dekker Inc., New York, Basel, Hongkong, 83-112.

Beetz, S., Liebersbach, H., Glatzel, S., Jurasinski, G., Buczko, U., Hoeper, H., 2013. Effects of land use intensity on the full greenhouse gas balance in an Atlantic peat bog. Biogeosciences 10, 1067-1082.

Berglund, K., Persson, L., 1996. Water repellence of cultivated organic soils. Acta Agriculturae Scandinavica Section B-Soil and Plant Science 46, 145-152.

Berglund, O. , Berglund, K., 2011. Influence of water table level and soil properties on emissions of greenhouse gases from cultivated peat soil. Soil Biology & Biochemistry 43, 923-931.

Beyer, C., Liebersbach, H., Hoeper, H., 2015. Multiyear greenhouse gas flux measurements on a temperate fen soil used for cropland or grassland. Journal of Plant Nutrition and Soil Science 178, 99-111.

BGR, without year. Geologische Übersichtskarte 1:200.000. Bundesanstalt für Geowissenschaften und Rohstoffe, Hannover.

Biasi, C., Pitkamaki, A. S., Tavi, N. M., Koponen, H. T., Martikainen, P. J., 2012. An isotope approach based on $^{13}C$ pulse-chase labelling vs. the root trenching method to separate heterotrophic and autotrophic respiration in cultivated peatlands. Boreal Environment Research 17, 184-192.

Boutton, T. W., Archer, S. R., Midwood, A. J., Zitzer, S. F., Bol, R., 1998. $\delta^{13}C$ values of soil organic carbon and their use in documenting vegetation change in a subtropical savanna ecosystem. Geoderma 82, 5-41.

Bubier, J., Crill, P., Mosedale, A., 2002. Net ecosystem CO2 exchange measured by autochambers during the snow-covered season at a temperate peatland. Hydrological Processes 16, 3667-3682.

Clough, T. J., Mueller, C., Laughlin, R. J., 2013. Using stable isotopes to follow excreta N dynamics and $N_2O$ emissions in animal production systems. Animal 7, 418-426.

Deru, J., Lenssinck, F., Hoving, I., van den Akker, J.J.H., Bloem, J., van Eekeren, N., 2014. Effect of submerged drains in peat meadows on soil quality and ecosystem services. Netherlands, 36 pp.

Drösler, M., Augustin, J., Bergmann, L., Förster, C., Fuchs, D., Hermann, J.-M., Kantelhardt, J., Kapfer, A., Krüger, G., Schaller, L., Sommer, M., Schweiger, M., Steffenhagen, P., Tiemeyer, B., Wehrhan, M., 2012. Beitrag ausgewählter Schutzgebiete zum Klimaschutz und dessen monetäre Bewertung. BfN-Skripten 328, Bonn, 163 pp.

Drösler, M., Freibauer, A., Christensen, T. R., Friborg, T. , 2008. Observations and status of peatland greenhouse gas emissions in Europe, In: Dolman, A.J., Freibauer, A., Valentini, R. (Ed.), The continental-scale greenhouse gas balance of Europe. Springer, New York, 243-261.

Eickenscheidt, T., Heinichen, J., Drösler, M., 2015. The greenhouse gas balance of a drained fen peatland is mainly controlled by land-use rather than soil organic carbon content. Biogeosciences 12, 5161-5184.

European Economic Community, 1992. Habitats Directive (Council Directive 92/43/EEC on the Conservation of natural habitats and of wild fauna and flora). 44 pp.

Falge, E., Baldocchi, D., Olson, R., Anthoni, P., Aubinet, M., Bernhofer, C., Burba, G., Ceulemans, R., Clement, R., Dolman, H., Granier, A., Gross, P., Grunwald, T., Hollinger, D., Jensen, N. O., Katul, G., Keronen, P., Kowalski, A., Lai, C. T., Law, B. E., Meyers, T., Moncrieff, H., Moors, E., Munger, J. W., Pilegaard, K., Rannik, U., Rebmann, C., Suyker, A., Tenhunen, J., Tu, K., Verma, S., Vesala, T., Wilson, K., Wofsy, S., 2001. Gap filling strategies for defensible annual sums of net ecosystem exchange. Agricultural and Forest Meteorology 107, 43-69.

Falge, E., Tenhunen, J., Aubinet, M., Bernhofer, C., Clement, R., Granier, A. , Kowalski, A., Moors, E., Pilegaard, K., Rannik, Ü., Rebmann, C., 2003. A Model-Based Study of Carbon Fluxes at Ten European Forest Sites, In: R.Valentini (Ed.), Fluxes in Carbon, Water and Energy of European Forests. Springer, Berlin Heidelberg, 151-177.

FAO, 2010. “Climate-Smart” Agriculture - Policies, Practices and Financing for Food Security, Adaptation and Mitigation. Rome, Italy, 49 pp.

FAO, 2013a. Climate-smart agriculture - Sourcebook. Rome, Italy, 570 pp.

FAO, 2013b. Climate-smart agriculture - Infographic. Rome, Italy, 2 pp.

Flessa, H., Wild, U., Klemisch, M., Pfadenhauer, J., 1998. Nitrous oxide and methane fluxes from organic soils under agriculture. European Journal of Soil Science 49, 327-335.

Forster, P., V. Ramaswamy, P. Artaxo, T. Berntsen, R. Betts, D.W. Fahey, J. Haywood, J. Lean, D.C. Lowe, G. Myhre, J. Nganga, R. Prinn, G. Raga, M. Schulz and R. Van Dorland, 2007. Changes in Atmospheric Constituents and in Radiative Forcing., In: Solomon, S., D. Qin, M. Manning, Z. Chen, M. Marquis, K.B. Averyt, M.Tignor and H.L. Miller (Ed.), Climate Change 2007: The Physical Science Basis. Contribution of Working Group I to the Fourth Assessment Report of the Intergovernmental Panel on Climate Change. Cambridge University Press, Cambridge, United Kingdom and New York, NY, USA, 131-234.

Freibauer, A., 2003. Regionalised inventory of biogenic greenhouse gas emissions from European agriculture. European Journal of Agronomy 19, 135-160.

Frolking, S. E., Bubier, J. L., Moore, T. R., Ball, T., Bellisario, L. M., Bhardwaj, A., Carroll, P., Crill, P. M., Lafleur, P. M., McCaughey, J. H., Roulet, N. T., Suyker, A. E., Verma, S. B., Waddington, J. M., Whiting, G. J., 1998. Relationship between ecosystem productivity and photosynthetically active radiation for northern peatlands. Global Biogeochemical Cycles 12, 115-126.

Germer, P., 2006. Regeneration des Großes Torfmoores - LIFE-Natur-Projekt (Regeneration of the Großes Torfmoor - LIFE-Nature-Project). NUA-Heft 23, 80-84.

Gorham, E., 1991. Northern peatlands - role in the carbon-cycle and probable responses to climatic warming. Ecological Applications 1, 182-195.

Göttlich, K., 1990. Moor- und Torfkunde. E. Schweizerbart'sche Verlagsbuchhandlung (Nägele und Obermiller), Stuttgart, 529 pp.

Guenther, A., Huth, V., Jurasinski, G., Glatzel, S., 2015. The effect of biomass harvesting on greenhouse gas emissions from a rewetted temperate fen. Global Change Biology Bioenergy 7, 1092-1106.

Hahn-Schoefl, M., Zak, D., Minke, M., Gelbrecht, J., Augustin, J., Freibauer, A., 2011. Organic sediment formed during inundation of a degraded fen grassland emits large fluxes of $CH_4$ and $CO_2$. Biogeosciences 8, 1539-1550.

Hart, S.C., Myrold, D.D., 1996. $^{15}N$ tracer studies of soil nitrogen transformations, In: Boutton, T.W., Yamasaki, S. (Eds.), Mass spectrometry of soils. Marcel Dekker Inc., New York, Basel, Hongkong, 225-246.

Hendriks, D. M. D., van Huissteden, J., Dolman, A. J., van der Molen, M. K., 2007. The full greenhouse gas balance of an abandoned peat meadow. Biogeosciences 4, 411-424.

Hoegberg, P., 1997. $^{15}N$ natural abundance in soil-plant systems - Tansley Review No. 95. New Phytologist 137, 179-203.

Hoffmann, M., Jurisch, N., Borraz, E. A., Hagemann, U., Droesler, M., Sommer, M., Augustin, J., 2015. Automated modeling of ecosystem $CO_2$ fluxes based on periodic closed chamber measurements: A standardized conceptual and practical approach. Agricultural and Forest Meteorology 200, 30-45.

Höper, H., Augustin, J., Cagampan, J. P., Drösler, M., Lundin, L., Moors, E., Vasander, H., Waddington, J. M., Wilson, D., 2008. Restoration of peatlands and greenhouse gas balance, In: Strack, M. (Ed.), Peatlands and climate change. Intnernational Peat Society, Finland, 182-210.

Huth, V., Jurasinski, G., Glatzel, S., 2012. Winter emissions of carbon dioxide, methane and nitrous oxide from a minerotrophic fen under nature conservation management in north-east Germany. Mires and Peat 10, 1-13.

IPCC, 1997. Revised 1996 IPCC Guidelines for National Greenhouse Gas Inventories - Reporting Instructions (Volume 1) Annex 3. 9 pp.

IPCC, 2003. Good Practice Guidance for Land Use, Land-Use Change and Forestry. 590 pp.

IPCC, 2006. Guidelines for National Greenhouse Gas Inventories.Chapter 3: Consistent Representation of Lands. 42 pp.

IPCC, 2007. Summary for Policymakers. In: Solomon, S., Qin, D., Manning, M., Chen, Z., Marquis, M., Averyt, K. B., Tignor, M., Miller, H. L. (Eds.), Climate Change 2007: The Physical Science Basis. Contribution of Working Group I to the Fourth Assessment Report of the Intergovernmental Panel on Climate Change. Cambridge, UK and New York, NY, USA., 18 pp.

IPCC, 2014a. 2013 Supplement to the 2006 IPCC Guidelines for National Greenhouse Gas Inventories: Wetlands. Switzerland, 354 pp.

IPCC, 2014b. Revised Supplementary Methods and Good Practice Guidance arising from the Kyoto Protocol. Switzerland, 268 pp.

Jacobs, C. M. J., Jacobs, A. F. G., Bosveld, F. C., Hendriks, D. M. D., Hensen, A., Kroon, P. S., Moors, E. J., Nol, L., Schrier-Uijl, A., Veenendaal, E. M., 2007. Variability of annual $CO_2$ exchange from Dutch grasslands. Biogeosciences 4, 803-816.

Jauhiainen, J., Hooijer, A., Page, S. E., 2012. Carbon dioxide emissions from an Acacia plantation on peatland in Sumatra, Indonesia. Biogeosciences 9, 617-630.

Joosten, H., Clarke, D., 2002. Wise use of mires and peatlands - background and principles including a framework for decision-making. International Mire Conservation Group and International Peat Society, Saarijärvi, 304 pp.

Joosten, H., Tapio-Biström, M.-L., Tol, S., (eds.), 2012. Peatlands - guidance for climate change mitigation through conservation, rehabilitation and sustainable use. Mitigation of climate change in agriculture series 5, Rome, 114 pp.

Jungkunst, H. F., Flessa, H., Scherber, C., Fiedler, S., 2008. Groundwater level controls $CO_2$, $N_2O$ and $CH_4$ fluxes of three different hydromorphic soil types of a temperate forest ecosystem. Soil Biology & Biochemistry 40, 2047–2054.

Juszczak, R., Acosta, M., Olejnik, J., 2012. Comparison of Daytime and Nighttime Ecosystem Respiration Measured by the Closed Chamber Technique on a Temperate Mire in Poland. Polish Journal of Environmental Studies 21, 643-658.

Karki, S., Elsgaard, L., Laerke, P. E., 2015. Effect of reed canary grass cultivation on greenhouse gas emission from peat soil at controlled rewetting. Biogeosciences 12, 595-606.

Kasimir-Klemedtsson, A., Klemedtsson, L., Berglund, K., Martikainen, P., Silvola, J., Oenema, O., 1997. Greenhouse gas emissions from farmed organic soils: a review. Soil Use and Management 13, 245-250.

Kuzyakov, Y., 2006. Sources of $CO_2$ efflux from soil and review of partitioning methods. Soil Biology & Biochemistry 38, 425-448.

Kuzyakov, Y., Friedel, J. K., Stahr, K., 2000. Review of mechanisms and quantification of priming effects. Soil Biology & Biochemistry 32, 1485-1498.

Lai, D. Y. F., Roulet, N. T., Humphreys, E. R., Moore, T. R., Dalva, M., 2012. The effect of atmospheric turbulence and chamber deployment period on autochamber $CO_2$ and $CH_4$ flux measurements in an ombrotrophic peatland. Biogeosciences 9, 3305-3322.

Lappalainen, E., 1996. Global Peat Resources. International Peat Society, Jyskä, Finland, 161 pp.

Limpens, J., Berendse, F., Blodau, C., Canadell, J. G., Freeman, C., Holden, J., Roulet, N., Rydin, H., Schaepman-Strub, G., 2008. Peatlands and the carbon cycle: from local processes to global implications - a synthesis. Biogeosciences 5, 1475-1491.

Lloyd, J., Taylor, J. A., 1994. On the temperature dependence of soil respiration. Functional Ecology 8, 315-323.

Ma, X., Ambus, P., Wang, S., Wang, Y., Wang, C., 2013. Priming of Soil Carbon Decomposition in Two Inner Mongolia Grassland Soils following Sheep Dung Addition: A Study Using $^{13}C$ Natural Abundance Approach. Plos One 8, 1-9.

Makiranta, P., Minkkinen, K., Hytonen, J., Laine, J., 2008. Factors causing temporal and spatial variation in heterotrophic and rhizospheric components of soil respiration in afforested organic soil croplands in Finland. Soil Biology & Biochemistry 40, 1592-1600.

Marinier, M., Glatzel, S., Moore, T. R., 2004. The role of cotton-grass (Eriophorum vaginatum) in the exchange of $CO_2$ and $CH_4$ at two restored peatlands, eastern Canada. Ecoscience 11, 141-149.

Meier-Uhlherr, R, Schulz, C., Luthardt, V., 2011. Steckbriefe Moorsubstrate. HNE Eberswalde (Eds.), Berlin, 154 pp.

Mielke, M. S., de Almeida, A. A. F., Gomes, F. P., 2005. Photosynthetic traits of five neotropical rainforest tree species: Interactions between light response curves and leaf-to-air vapour pressure deficit. Brazilian Archives of Biology and Technology 48, 815-824.

Montanarella, L., Jones, R. J. A., Hiederer, R., 2006. The distribution of peatland in Europe. Mires and Peat 1, 1-11.

Nielsen, O.-K., Mikkelsen, M.H., Hoffmann, L., Gyldenkærne, S., Winther,, M., Nielsen, M., Fauser, P., Thomsen, M., Plejdrup, M.S., Albrektsen, R., Hjelgaard,, K., Bruun, H.G., Johannsen, V.K., Nord-Larsen, T., Bastrup-Birk, A., Vesterdal, L.,, Møller, I.S., Rasmussen, E., Arfaoui, K., Baunbæk, L. & Hansen, M.G., 2012. Denmark's National Inventory Report 2012. Emission Inventories 1990-2010 - Submitted under the United Nations Framework Convention on Climate Change and the Kyoto Protocol. 1168 pp.

O'Leary, M. H., 1981. Carbon isotope fractionation in plants. Phytochemistry 20, 553-567.

Ojanen, P., Minkkinen, K., Lohila, A., Badorek, T., Penttila, T., 2012. Chamber measured soil respiration: A useful tool for estimating the carbon balance of peatland forest soils? Forest Ecology and Management 277, 132-140.

Olesen, J. E., Trnka, M., Kersebaum, K. C., Skjelvag, A. O., Seguin, B., Peltonen-Sainio, P., Rossi, F., Kozyra, J., Micale, F., 2011. Impacts and adaptation of European crop production systems to climate change. European Journal of Agronomy 34, 96-112.

Page, S. E., Rieley, J. O., Banks, C. J., 2011. Global and regional importance of the tropical peatland carbon pool. Global Change Biology 17, 798-818.

Pouliot, R., Hugron, S., Rochefort, L., 2015. Sphagnum farming: A long-term study on producing peat moss biomass sustainably. Ecological Engineering 74, 135-147.

Regina, K., Syvasalo, E., Hannukkala, A., Esala, M., 2004. Fluxes of $N_2O$ from farmed peat soils in Finland. European Journal of Soil Science 55, 591-599.

Reiche, M., Gleixner, G., Kuesel, K., 2010. Effect of peat quality on microbial greenhouse gas formation in an acidic fen. Biogeosciences 7, 187-198.

Roßkopf, N., Fell, H., Zeitz, J., 2015. Organic soils in Germany, their distribution and carbon stocks. Catena 133, 157-170.

Schrier-Uijl, A. P., Kroon, P. S., Hendriks, D. M. D., Hensen, A., Van Huissteden, J., Berendse, F., Veenendaal, E. M., 2014. Agricultural peatlands: towards a greenhouse gas sink - a synthesis of a Dutch landscape study. Biogeosciences 11, 4559-4576.

Schrier-Uijl, A. P., Kroon, P. S., Hensen, A., Leffelaar, P. A., Berendse, F., Veenendaal, E. M., 2010. Comparison of chamber and eddy covariance-based $CO_2$ and $CH_4$ emission estimates in a heterogeneous grass ecosystem on peat. Agricultural and Forest Meteorology 150, 825-831.

Schulze, E. D., Ciais, P., Luyssaert, S., Schrumpf, M., Janssens, I. A., Thiruchittampalam, B., Theloke, J., Saurat, M., Bringezu, S., Lelieveld, J., Lohila, A., Rebmann, C., Jung, M., Bastviken, D., Abril, G., Grassi, G., Leip, A., Freibauer, A., Kutsch, W., Don, A., Nieschulze, J., Boerner, A., Gash, J. H., Dolman, A. J., 2010. The European carbon balance. Part 4: integration of carbon and other trace-gas fluxes. Global Change Biology 16, 1451-1469.

Schulze, E. D., Luyssaert, S., Ciais, P., Freibauer, A., Janssens, I. A., Soussana, J. F., Smith, P., Grace, J., Levin, I., Thiruchittampalam, B., Heimann, M., Dolman, A. J., Valentini, R., Bousquet, P., Peylin, P., Peters, W., Roedenbeck, C., Etiope, G., Vuichard, N., Wattenbach, M., Nabuurs, G. J., Poussi, Z., Nieschulze, J., Gash, J. H., CarboEurope, Team, 2009. Importance of methane and nitrous oxide for Europe's terrestrial greenhouse-gas balance. Nature Geoscience 2, 842-850.

Seneviratne, S. I., Luthi, D., Litschi, M., Schar, C., 2006. Land-atmosphere coupling and climate change in Europe. Nature 443, 205-209.

Silvola, J., Alm, J., Ahlholm, U., Nykanen, H., Martikainen, P. J., 1996. CO2 fluxes from peat in boreal mires under varying temperature and moisture conditions. Journal of Ecology 84, 219-228.

Smith, K. A., Conen, F., 2004. Impacts of land management on fluxes of trace greenhouse gases. Soil Use and Management 20, 255-263.

Subke, J.-A., Heinemeyer, A., Reichstein, M., 2009. Experimental design: scaling up in time and space, and its statistical considerations., In: Kutsch, W., Bahn, M., Heinemeyer, A. (Eds.), Soil carbon dynamics: an integrated methodology. Cambridge University Press, Cambridge, UK, 34-48.

Succow, M., Joosten, H. , 2001. Landschaftsökologische Moorkunde. E. Schweizerbart'sche Verlagsbuchhandlung (Nägele und Obermiller), Stuttgart, 622 pp.

Tieszen, L. L., 1991. Natural Variations in the carbon isotope values of plants: implications for archaeology, ecology and paleoecology. Journal of Archaeological Science 18, 227-248.

Turral, H., Burke, J., Faurès, J. M., 2011. Climate change, water and food security. FAO Water Report No. 36, Rome, 18 pp.

UBA, 2009. Nationaler Inventarbericht zum Deutschen Treibhausgasinventar 1990 - 2007. Berichterstattung unter der Klimarahmenkonvention der Vereinten Nationen 2009. Dessau, Germany, 572 pp.

UBA, 2014. National Inventory Report for the German Greenhouse Gas Inventory 1990 – 2012. Submission under the United Nations Framework Convention on Climate Change and the Kyoto Protocol 2014. Dessau, Germany, 956 pp.

United Nations, 1992. United Nations Framework Convention on Climate Change (UNFCCC). New York, USA. 25 pp.

United Nations, 1998. Kyoto protocol to the United Nations framework convention of climate change. 21 pp.

Van den Akker, J.J.H., Hendriks, R.F.A., Pleijter, M., 2012. $CO_2$ emissions of peat soils in agricultural use: calculation and prevention. Agrociencia 16, 43-50.

Vasander, H., Tuittila, E. S., Lode, E., Lundin, L., Ilomets, M., Sallantaus, T., Heikkilä, R., Pitkänen, M. L., Laine, J., 2003. Status and restoration of peatlands in northern Europe. Wetlands Ecology and Management 11, 51-63.

Veenendaal, E. M., Kolle, O., Leffelaar, P. A., Schrier-Uijl, A. P., Van Huissteden, J., Van Walsem, J., Moeller, F., Berendse, F., 2007. $CO_2$ exchange and carbon balance in two grassland sites on eutrophic drained peat soils. Biogeosciences 4, 1027-1040.

WRB, 2008. World Reference Base for Soil Resources 2006. Ein Rahmen für internationale Klassifikation, Korrelation und Kommunikation., Deutsche Ausgabe ed. Bundesanstalt für Geowissenschaften und Rohstoffe, Hannover, 148 pp.

Yoneyama, T., 1996. Characterization of natural $^{15}N$ abundance of soils, In: Boutton, T.W., Yamasaki, S. (Eds.), Mass spectrometry of soils. Marcel Dekker Inc., New York, Basel, Hongkong, 205-224.

Ziebarth, M., Lenschow, U., Permien, T., 2009. Konzept zum Schutz und zur Nutzung der Moore - Fortschreibung des Konzeptes zur Bestandssicherung und zur Entwicklung der Moore in Mecklenburg-Vorpommern (Moorschutzkonzept) Ministerium für Landwirtschaft, Umwelt und Verbraucherschutz Mecklenburg-Vorpommern, Schwerin, 109 pp.

# Chapter 2: Publication no. 1

## Minimum measurement frequency for robust annual budgets of ecosystem respiration

**Authors:**

K. Leiber-Sauheitl[1,2], R. Fuß[1], D. Lempio[1], B. Tiemeyer[1], M. Bechtold[1], A. Freibauer[1]

[1] Thünen Institute of Climate-Smart Agriculture, Bundesallee 50, 38116 Braunschweig, Germany
[2] corresponding author: Phone +49 (0) 531 596 2669, E-mail: katharina.leiber@ti.bund.de

**Status of publication:**

To be published

**Own contributions:**

- data analyses
- model development
- graphical presentation
- preparation of the manuscript

**Contributions by coauthors:**

- R. Fuß: support during statistical analyses, contribution to the manuscript
- D. Lempio: maintenance of autochamber, contribution to the manuscript
- M. Bechtold: data processing of groundwater and soil moisture data, contribution to the manuscript
- B. Tiemeyer: contribution to the manuscript
- A. Freibauer: contribution to the manuscript

## Abstract

Ecosystem $CO_2$ respiration ($R_{eco}$) is the carbon loss component of the net $CO_2$ ecosystem exchange (NEE) in ecosystems. It is commonly assessed based on manual campaign-wise chamber measurements, which are performed every few weeks. Annual values are derived from measured $CO_2$ fluxes and continuous measurements of temperature using temperature response models such as the Lloyd-Taylor function. Measurement frequency and specific campaign dates are set based on ecosystem phenology, weather or groundwater dynamics, and management events.

In order to assess the impact of measurement frequency on accuracy (bias) and precision (random uncertainty) of seasonal $R_{eco}$ sums, an automated chamber system with an opaque chamber was installed on extensively managed grassland located on a drained histic Gleysol. $CO_2$ fluxes were continuously measured six to twelve times per day during 4.5 months in the vegetation period.

The Lloyd-Taylor temperature response function explained 70% of the $R_{eco}$ variance. None of the other tested response functions using temperature, temperature and soil moisture, and temperature and groundwater table performed significantly better. In contrast to studies on mineral soils, we did not detect any direct influence of soil moisture on $R_{eco}$.

The seasonal $R_{eco}$ sum by the Lloyd-Taylor temperature response function proved to be very robust. Little short-term variability in response function parameters was observed, even when environmental conditions substantially changed (e.g. before/after strong rain). $R_{eco}$ sums were significantly biased by up to 30% when only daytime or nighttime measurements were used. A purely day- or nighttime based sampling strategy would therefore also introduce a strong bias in NEE partitioning into GPP and $R_{eco}$. Moving from continuous measurements to campaign-based, i.e., measurements every few weeks, led to a surprisingly small loss of accuracy (by 5%) and a certain loss of precision (by 5-20%), which is in the same order of magnitude as the spatial variability. It is most critical for seasonal $R_{eco}$ sums to capture the difference in day- and nighttime temperature response of $R_{eco}$ while in comparison measurement frequency is much less critical. The following minimum standards for campaign-wise $R_{eco}$ measurements are proposed: An effective campaign for robust $R_{eco}$ estimates should cover the period from before sunrise until the late afternoon. A campaign frequency of every three weeks can be recommended as minimum for extensive grasslands on organic soils. This minimum standard is close to common measurement practice.

## Highlights

- $R_{eco}$ measurements based on campaigns of diurnal $CO_2$ fluxes are suitable for determining robust annual $R_{eco}$ sums.
- $R_{eco}$ models based on pure daytime or nighttime measurements are substantially biased.
- A measurement frequency of three weeks is sufficient for histic Gleysols under grassland.
- $CO_2$ campaigns during sunny, dry weather produce more accurate and precise $R_{eco}$ models than fixed campaign intervals.

## 1. Introduction

The net ecosystem exchange of $CO_2$ (NEE) describes the carbon balance of an ecosystem resulting from the two opposing ecophysiological processes of photosynthesis (gross primary production, GPP) and ecosystem respiration ($R_{eco}$). Ecosystem respiration sums up the $CO_2$ losses from autotrophic and heterotrophic processes in plants and soils. While NEE can be measured in a straightforward way by eddy covariance (FLUXNET project e.g. Baldocchi et al., 1996; Running et al., 1999; ICOS project, www.icos-infrastructure.eu) or chambers (e.g. Alm et al., 1997; Burrows et al., 2005), the partitioning of NEE into GPP and $R_{eco}$ remains a methodological challenge as it requires the combination of various types of measurements or estimates (e.g. Reichstein et al., 2005; Reichstein et al., 2012). At nighttime, when GPP is zero, NEE equals $R_{eco}$. At daytime, however, $R_{eco}$ must be separated from GPP by measurements in darkness, which is directly only possible with chamber-based approaches using opaque chambers. Chambers are also the method of choice in studies with factorial design, of small-scale heterogeneity, and whenever the conditions for micrometeorological measurements are not met. Therefore, most studies in ecosystems on organic soils outside forests have deployed chambers for NEE and $R_{eco}$ measurements (Alm et al., 1997; Maljanen et al., 2007; Beyer et al., 2015).

Large automatic chamber systems recording $R_{eco}$ provide continuous high resolution data, but are cost intensive and pose challenges at more remote sites, e.g. with regard to power supply and maintenance. Therefore, manual chamber measurements with campaign-based approaches are commonly used for the determination of annual $R_{eco}$ and NEE sums (Alm et al., 1997; Drösler, 2005; Schrier-Uijl et al., 2010; Beetz et al., 2013; Eickenscheidt et al., 2015) where inter-campaign distance is chosen according to management practice and plant phenology. The good weather campaign approach has most frequently been applied when using manual chambers (Beetz et al., 2013; Eickenscheidt et al., 2015; Hoffmann et al., 2015).

Uncertainties in chamber measurements have often been discussed regarding their spatial representativeness of the footprint of eddy covariance measurements due to their small spatial

coverage and consequent risk of spatial bias (von Arnold et al., 2005; e.g. for overview: Reichstein et al., 2012). The uncertainty in the temporal patterns introduced by interpolation and modeling between the measurement campaigns, however, has rarely systematically and comprehensively been quantified (challenge mentioned in Reichstein et al., 2012). Leiber-Sauheitl et al. (2014) and Hoffmann et al. (2015) propagate the intra-campaign uncertainty into the annual $R_{eco}$ sum, but cannot account for the inter-campaign uncertainty caused by the potential temporal misrepresentation of the campaigns, which is likely larger than the intra-campaign uncertainty. Cross-validation strategies have been used to assess the inter-campaign uncertainty (e.g. Beetz et al., 2013; Hoffmann et al., 2015), but due to the low number of campaigns and the large distance of campaigns these cannot be expected to provide a good estimate of this uncertainty.

In the case of mineral soils, temporal sampling strategies were studied for forests (Savage and Davidson, 2003; Savage et al., 2008) and agricultural sites (Parkin and Kaspar, 2004). However, only few studies have been carried out on organic soils, where $R_{eco}$ can easily be one or two orders of magnitude larger than on mineral soils, in particular when peat is degrading under drained conditions (e.g. for grasslands see IPCC, 2006, Chapter 6). Significantly higher nighttime than daytime $R_{eco}$ fluxes have been observed in many ecosystems and are assumed to be related to light inhibition of plant respiration (Falge et al., 2003; Mielke et al., 2005). Juszczak et al. (2012) considered higher nighttime than daytime $R_{eco}$ fluxes in a temperate peatland as artifacts of chamber measurements during low atmospheric turbulence. Consequently, these measurement artifacts due to atmospheric layering were discarded by them.

Soil respiration (heterotrophic plus autotrophic) accounted for half of $R_{eco}$ in a boreal forest on organic soils (Kurbatova et al., 2013) and may be even more important on drained organic soils. Soil respiration dynamics were driven by temperature and groundwater table, which were strongly seasonally co-correlated (Kurbatova et al., 2013). If, however, short-term fluctuations in groundwater table significantly affect soil respiration at time scales of days, campaign-based $R_{eco}$ measurements on organic soils have a considerable risk of temporal misrepresentation.

This study aims to quantify bias (systematic uncertainty, accuracy) and random uncertainty (standard deviation, precision) in seasonal $R_{eco}$ estimates introduced by the temporal sampling strategy and interpolation model. We use a continuous two hour data set of $R_{eco}$ measurements by an automatic chamber in an extensive grassland ecosystem on a shallow drained histic Gleysol (WRB, 2008) to investigate the following hypotheses:

1. Temperature - soil moisture response functions explain more of the $R_{eco}$ variability than purely temperature driven models.

2. Flux measurements must capture day-night patterns, but not necessarily day-to-day variations for robust seasonal $R_{eco}$ estimates.
3. Monthly measurement campaigns covering representative diurnal temperature ranges produce robust seasonal $R_{eco}$ estimates with small additional systematic and random uncertainty compared to continuous measurements.

Synthetic temporal sampling strategies were generated using leave-N-out Jackknife resampling strategies (Efron and Gong, 1983), testing measurement frequency, daytime versus nighttime measurements, regular intervals versus diurnal measurement campaigns, and regular versus good weather campaigns. The site represents a situation with high and highly variable $R_{eco}$ fluxes and a strong contribution of soil respiration from the degrading peat, which is considered particularly challenging for $R_{eco}$ modeling.

## 2. Materials and Methods

### 2.1. Site description

Measurements were performed on a histic Gleysol (WRB, 2008) under extensive grassland management in the Grosses Moor (Gifhorn, Germany). The site is characterized by a soil organic carbon content of 11.3% in the top 30 cm. Between June and October 2012 groundwater level fluctuated between -0.11 and -0.59 m (mean: -0.33 m). The site is a mesotrophic grassland (dominant species: *Agrostis stolonifera* L., *Poa pratensis* L.) and coincides with "$C_{low}$ $W_{29}$" described in detail in Leiber-Sauheitl et al. (2014) in which manual chamber data measured from June 2011 to June 2012 were presented.

### 2.2. $R_{eco}$ measurements

#### *2.2.1 Automatic chamber system*

In May 2012, an automatic chamber system was installed next to manual chamber plots at site "$C_{low}W_{29}$" from Leiber-Sauheitl et al. (2014). The automatic chamber system (Fig. 2-1 and S2-1) consists of a direction rack with a soil frame of aluminum, a measurement chamber, a motor unit with a cable winch for lifting and lowering the chamber, a control unit, a data logger and a $CO_2$ analyzer. Two solar panels (two 80 W modules) were used as power supply. The chamber can also sample $CH_4$ and $N_2O$ via a vial system (Fig. S2-1) for subsequent measurement on a gas chromatograph in the laboratory. Here we only present $CO_2$ data.


**Fig. 2 - 1**: Photograph of the automatic chamber system (chamber in standby position). Numbers indicate the most important components: soil frame (1), measurement chamber (2), box with control unit, data logger and $CO_2$ analyzer (3), box with vial sampling system (4).

The automatic chamber system was equipped with a non-transparent chamber with the length of the lateral edge of 0.78 m and 0.50 m height. A fan for homogenous air mixing, a temperature sensor, a vent tube and an air suction hose were installed inside the chamber similarly to Drösler (2005). Between two measurements, the chamber is lifted and automatically moved to the side in northern direction in order to minimize effects of shading, rain and wind exclusion.

The chamber air is transported through a tubing system to a control box including a valve block and the infrared gas analyzer (LI-820, LI-COR, USA). A downstream membrane pump (0.8 L $min^{-1}$) transports the chamber air through a silica water absorption unit and back into the chamber, in order to avoid condensed water in tubes and valves (Fig. S2-1).

Photosynthetically active radiation (PAR), precipitation and wind speed were continuously recorded every 0.5 hours at a meteorological station at the field site.

Groundwater levels were recorded every 15 min by groundwater data loggers (Mini-Diver, Schlumberger Water Services, Delft, The Netherlands) at the "$C_{low}W_{29}$" site. Water level data were smoothed by a running median over five values for outlier elimination and, subsequently, aggregated to hourly values.

### *2.2.2 Flux measurements and flux calculation*

In order to cover the diurnal cycle of ecosystem respiration $CO_2$ flux, sampling frequency was set to two hours. Chamber closure time was eight minutes, during which $CO_2$ concentration was measured

every second. Data from the first five minutes of each flux measurement were used for $CO_2$ flux calculation. The first 15 seconds were removed from the data in order to exclude possible disturbances directly after chamber closure. Flux rates were calculated using linear regression in R (R version 3.2.0; R core team, 2015). Linearity of single fluxes was checked by plotting and analyzing graphs, $R^2$ values and standard error. 99% of $R^2$ values were > 0.9 and all $R^2$ values were larger than 0.7. Corresponding to this, 99% of all standard errors were smaller than 5 mg $CO_2$-C $m^{-2}$ $h^{-1}$ and all standard error were smaller than 10.9 mg $m^{-2}$ $h^{-1}$.

Continuous data of 4.5 months during the vegetation period (19th June to 31st October 2012) were used for statistical analyses. Occasional gaps due to discarded flux values or system breakdown of up to one week (Fig. 2-2A) were cut out, thereby creating a pseudo-continuous data set.

## 2.3. $R_{eco}$ modeling

### *2.3.1 Temperature dependent Lloyd-Taylor model*

A temperature-dependent ecosystem respiration ($R_{eco}$) flux model as suggested by Lloyd and Taylor (1994) was fitted to the data:

$$R_{eco} = R_{ref} \times \exp\left[E_0 \times \left(1/(T_{ref} - T_0) - 1/(T - T_0)\right)\right] \quad \text{Equ. (1)}$$

$R_{ref}$ respiration at the reference temperature (mg $CO_2$–C $m^{-2}$ $h^{-1}$)

$E_0$ an activation-like parameter (K)

$T_{ref}$ reference temperature: 283.15 (K)

$T_0$ temperature constant for the start of biological processes: 227.13 (K).

Air temperature was measured directly at the automatic chamber and soil temperatures in 2, 5 and 10 cm depth were measured at the nearby manual chamber plots. According to Leiber-Sauheitl et al. (2014), soil temperature in 2 cm depth can be considered to be representative for plant and soil respiration at this site and was thus used for further analyses.

### *2.3.2 Temperature and soil moisture dependent models*

Several published temperature (Savage and Davidson, 2001; Flanagan and Johnson, 2005; Wagle and Kakani, 2014) and temperature-soil moisture models (Savage and Davidson, 2001 with modifications for groundwater level and air filled pore space) were tested. In addition, generalized additive models (Guisan et al., 2002) with soil moisture or groundwater level as additional variables were set up.

Soil moisture time series of the site were generated for the unsaturated soil profile by 1-D hydrological modeling (Hydrus-1D, Šimůnek et al., 2013). Therefore, soil hydraulic parameters were

determined in the laboratory for undisturbed peat samples of the site. The parameterized soil hydraulic model was driven by measured meteorological and water level data.

## 2.4. Statistical analyses

### *2.4.1 Jackknife-like resampling*

A leave-N-out resampling method, e.g. as employed by the Jackknife method (Efron and Gong, 1983), was used to evaluate the $CO_2$ flux data set. N consecutive data points of the original data set were removed, resulting in N + 1 resamples, and seasonal $R_{eco}$ values were estimated as before with the full data set. In contrast to the original Jackknife the focus of the analyses was set on the influence of diminishing sampling frequency of a time series as described in 2.4.2 and not on estimating uncertainty of a model fit to data without auto-correlation.

Precision and bias were calculated similarly to Efron and Stein (1981). The random uncertainty (≙ precision; σ) was calculated as the square root of the summed-up differences between the seasonal $R_{eco}$ sums calculated from Jackknife resamples and the mean of all $A_i$ values:

$$\sigma = \sqrt{\frac{1}{n} \times \sum_{i=1}^{n} (A_i - A_*)^2} \qquad \text{Equ. (2)}$$

$n$ number of Jackknife resamples

$A_i$ seasonal $R_{eco}$ sums calculated from Jackknife resamples

$A_*$ mean of all $A_i$ values

The bias (≙ accuracy; B) was calculated as the difference between the mean of all Jackknife random estimates and the original random estimate:

$$B = \left(A_* - \hat{A}\right) \qquad \text{Equ. (3)}$$

$\hat{A}$ original estimate

### *2.4.2 Resampling strategies*

Various strategies were used for resampling from the time series data set:

(i) Measurement frequency in regular intervals

(1) Reference data set: The complete 2h data set from June to October 2012 is considered as the reference data set.

(2) Evaluation of measurement frequency: Resample data sets were generated from the original measurement frequency of every two hours for measurement frequencies of every 4h, 6h,

8h, 12h, 24h, 36h, 72h and 168h (1 week). $CO_2$ fluxes at PAR values < 0.5 µmol $m^{-2}$ $s^{-1}$ were defined as nighttime values.

(ii) Measurement campaigns

(3) Measurement campaigns in regular intervals: Measurement campaigns were created by pooling the measurements obtained during two day time periods. This resulted in 59 campaigns covering almost continuously the observation period of 134 days. Two consecutive days were pooled to include enough variability in $CO_2$ fluxes and temperature for fitting the model. Resample campaign data sets were generated from the original 59 campaigns by increasing the interval between campaigns from every two, every four, to every 27 days, which is equivalent to a minimum of 5 campaigns in 4.5 months.

(4) Good weather campaigns: campaigns were defined by weather conditions. In this approach one day of data was pooled per campaign which was selected by the following criteria. A precipitation sum of zero millimeters between 4 a.m. and 8 p.m. as well as PAR maxima of 1500 µmol $m^{-2}$ $s^{-1}$ in June, July and August, of 1300 µmol $m^{-2}$ $s^{-1}$ in September and of 800 µmol $m^{-2}$ $s^{-1}$ in October were used as campaign selection criteria. This resulted in 23 good weather campaigns. Resample campaign data sets were generated from the original 23 campaigns by selecting every second, third, fourth … good weather campaign.

### *2.4.3 Determination of cumulated seasonal $R_{eco}$ estimates*

For measurements in regular intervals, the Lloyd-Taylor fitting parameters $R_{ref}$ and $E_0$ and the daily mean $R_{eco}$ for the whole period were calculated for each resample. Lloyd-Taylor fits with negative estimates of the $E_0$ parameter were discarded from further analysis. Half-hourly $R_{eco}$ values for the whole study period of 134 days (4.5 months) were predicted for all (original and resample) data sets based on the Lloyd-Taylor function with temperature in 2 cm soil depth as the driver variable (see 2.3.1). Thereafter, they were summed up to derive seasonal $R_{eco}$ sums. Mean values of all cumulated $R_{eco}$ sums of one measurement frequency type were calculated as well as minimum and maximum values, precision and bias.

In order to estimate the seasonal $R_{eco}$ sums for measurement campaigns in regular intervals as well as good weather campaigns, the original start and end campaigns were always included in the resamples. In both, resample sets with regular campaigns and with good weather campaigns one $R_{eco}$ function was set up per campaign which created one parameter set. Lloyd-Taylor fits with negative estimates of the $E_0$ parameter were again discarded from further analysis. $R_{eco}$ fluxes between two measurement campaigns were derived by predicting from Lloyd-Taylor fits of the previous and the

subsequent campaign and by calculating a distance weighted mean of both predictions (Leiber-Sauheitl et al., 2014). Finally, cumulated $R_{eco}$ sums were calculated.

### *2.4.4 Significance tests*

In order to the test the significance of differences between different parameter sets of $R_{ref}$ and $E_0$, generalized nonlinear least squares (GNLS) models were applied in R (nlme Package, Version 3.1-120, Pinheiro and Bates, 2000). The following variance structure ("varPower") was used since high $CO_2$ fluxes exhibited a larger variance than low $CO_2$ fluxes:

$\sigma_i^2 = \left|\hat{R}_{eco,i}\right|^{2t}$, where $\hat{R}_{eco,i}$ are fitted values and t is a model parameter Equ. (4)

## 3. Results

### 3.1 Seasonal course of $R_{eco}$ and environmental parameters

During the measurement period from June to October 2012, $R_{eco}$ fluxes exhibited clear seasonal patterns (Fig. 2-2A; original fluxes with gaps are shown). During June, July and August $R_{eco}$ fluxes and amplitudes tended to be higher in comparison to the $R_{eco}$ fluxes in September and October. A similar trend was observed for soil temperature in 2 cm depth (Fig. 2-2B). Groundwater levels were lower during the summer months than in autumn (Fig. 2-2C). Few larger rain events in July and October caused a short-term increase in groundwater levels.

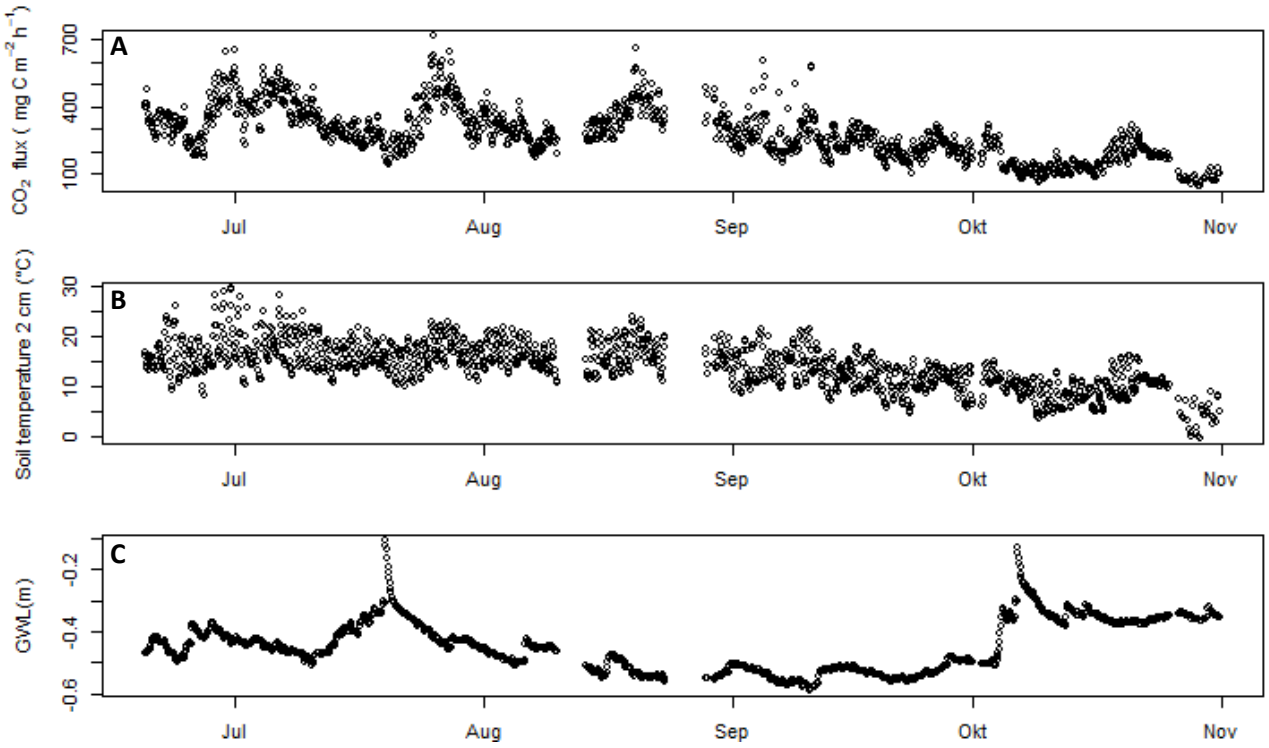


**Fig. 2 - 2:** Time series of (**A**) $CO_2$ flux, (**B**) soil temperature in 2 cm and (**C**) groundwater level (GWL) from June to October 2012 (original data set with gaps).

### 3.2 Temperature - soil moisture models

Neither any of the temperature - soil moisture models nor the generalized additive model achieved a significant improvement in model performance compared to purely temperature driven models. Around 70 percent of the variance was explained by all models (data not shown). Temperature had a strong temporal covariance to groundwater level and soil moisture over daily and seasonal time scales at our site, e.g. rain coincided with cooler temperatures. Maximum observed daily variation in groundwater table was +0.2 m, which coincided with a temperature change of -5°C. The temperature response of $R_{eco}$ thus could not be distinguished from the soil respiration response to water table or soil moisture at our site at any interval.

### 3.3 Evaluation of measurement frequency - Lloyd-Taylor model with full data set

The Lloyd-Taylor function of the full (=reference) data set (June-October) resulted in a cumulated ecosystem respiration of 8.94 Mg C $ha^{-1}$ 134 $d^{-1}$ (Fig. 2-3A). Resample data sets of cumulated $R_{eco}$ sums with decreasing measurement frequency, i.e. increasing measurement interval of up to seven days, exhibited small deviations from the reference for all odd multiples of 0.5 days (Fig. 2-3A). In contrast, the cumulated $R_{eco}$ sums derived from even multiples of 0.5 days deviated much more (Fig.

2-3A) with a systematic pattern. $R_{eco}$ sums above the reference were derived from nighttime $R_{eco}$ measurements whereas the $R_{eco}$ sums below the reference were derived from daytime $R_{eco}$ measurements (Fig. 2-3A).

Even multiples of 0.5 days exhibited a nearly constant high random uncertainty of 1.6 Mg C $ha^{-1}$ 134 $d^{-1}$ (18% of reference $R_{eco}$ sum). Odd multiples or fractions of 0.5 days exhibited lower random uncertainty which increased with decreasing measurement frequency from 2 to 12 hours from 0 to 0.3 Mg C $ha^{-1}$ 134 $d^{-1}$ (3% of reference $R_{eco}$ sum). At a measurement frequency of 6.5 days, random uncertainty was 0.5 Mg C $ha^{-1}$ 134 $d^{-1}$ (6% of reference $R_{eco}$ sum)

The bias also differed widely between 0.4 Mg C $ha^{-1}$ 134 $d^{-1}$ (4% of reference $R_{eco}$ sum) and 0.05 Mg C $ha^{-1}$ 134 $d^{-1}$ (0.6% of reference $R_{eco}$ sum) for even multiples and fractions or odd multiples of 0.5 days cumulated $R_{eco}$ sums, respectively. However, bias of both even and odd multiples of 0.5 days remained constant with decreasing measurement frequency (Fig. 2-3B).

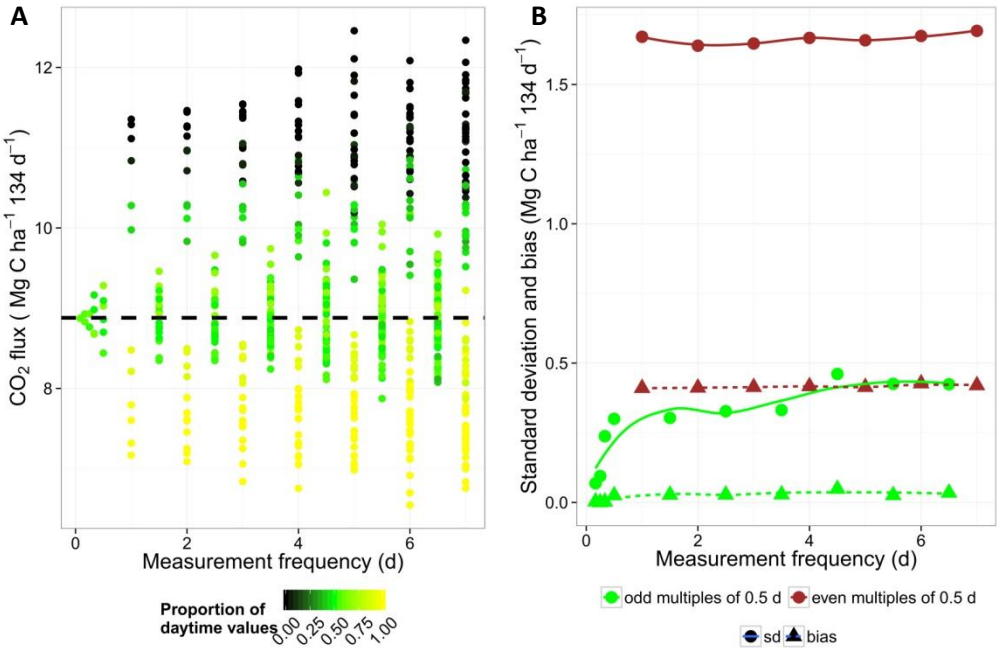


**Fig. 2 - 3**: Evaluation of measurement frequency. (A) Dots represent the $R_{eco}$ sum of Jackknife resamples. Black dots denote $R_{eco}$ sums which consist only of nighttime data, yellow dots denote $R_{eco}$ sums which consist only of daytime data and green dots contain nighttime as well as daytime data. Dashed line represents the $R_{eco}$ sum estimate calculated with the complete data set. (B) Random uncertainty given as standard deviation (sd; circles) and bias (triangles) of different measurement frequencies. Green color for fractions and odd multiples of 0.5 days and red colors for even multiples of 0.5 days. Lines are smoothers for visualization of the trend.

### 3.4 Evaluation of measurement frequency - Lloyd-Taylor models separated by day and night

Determination of $R_{eco}$ parameters $R_{ref}$ and $E_0$ using only day or night $CO_2$ fluxes resulted in a difference of the cumulated $R_{eco}$ sum of 3 Mg C $ha^{-1}$ 134 $d^{-1}$ (30 % of the total flux).

Lloyd-Taylor fitting parameters $R_{ref}$ and $E_0$ were significantly different between daytime and nighttime as tested by generalized nonlinear least squares fits (see also Table S2-1). Reference respiration ($R_{ref}$) and activation energy ($E_0$) were significantly higher during night (Fig. 2-4, Table 2-1). The temperature range of all daytime fluxes was larger than for nighttime fluxes (Fig. 2-4). During nighttime, most fluxes were in the temperature range between 5 and 15 °C whereas during daytime the range was 10 to 25 °C (Fig. 2-4).

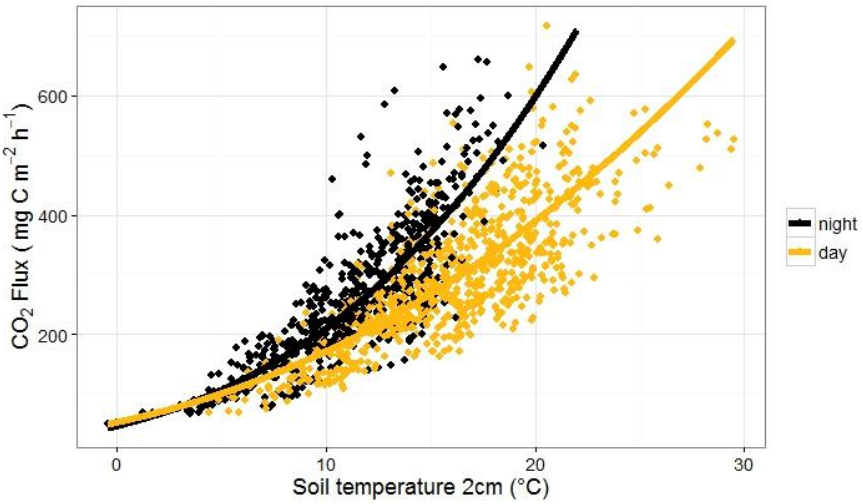


**Fig. 2 - 4**: Lloyd-Taylor fits of the full 2h data set. Data separated into night (black diamonds) and day (yellow diamonds) $CO_2$ fluxes and corresponding Lloyd-Taylor GNLS predictions for night (black line) and day (yellow line).

**Table 2 - 1**: Lloyd-Taylor fitting parameters $R_{ref}$ (in mg C $m^{-2}$ $h^{-1}$) and $E_0$ (in K) as well as variance structure of different subsets of the total 2h data set ± standard error

| Time of day | $R_{ref}$ | $E_0$ | Variance structure |
|---|---|---|---|
| Night | 211.3 ± 1.99 | 385.4 ± 7.97 | varPower |
| Day | 172.5 ± 2.4 | 302.3 ± 7.22 | varPower |
| Day and night | 195.58 ± 1.77 | 286.62 ± 5.50 | varPower |
| Day and night* | 210.06 ± 2.62 | 235.00 ± 5.99 | none |

*Parameter set for the calculation of seasonal $R_{eco}$ sums (=reference)

Including the variance structure significantly improved the models and impacted parameter estimates (Table 2-1). However, since it is not common to include a variance structure for fitting the Lloyd-Taylor function, we only did so for this statistical evaluation and used fits without variance structure otherwise.

Consequently, the cumulated $R_{eco}$ sum over the whole measurement period with daytime $R_{eco}$ parameters (8.30 Mg C $ha^{-1}$ 134 $d^{-1}$) was lower than the reference whereas the cumulated $R_{eco}$ sum with nighttime $R_{eco}$ parameters was much higher than the reference (11.39 Mg C $ha^{-1}$ 134 $d^{-1}$, 27% above reference).

The results clearly indicate that it is more important to capture the diurnal pattern with daytime and nighttime measurements than to increase measurement frequency. At odd multiples of 0.5 days, all $R_{eco}$ sums of Jackknife resamples are in the range of 37.5% - 78.3% proportion of daytime values in which no severe bias occurred. In contrast, at even multiples of 0.5 days $R_{eco}$ sums of Jackknife resamples with only nighttime or only daytime values created the largest bias. As a consequence a smaller bias is produced with fewer nighttime than daytime measurements.

### 3.5 Evaluation of campaign frequency - Lloyd-Taylor models for regular campaigns

The total measurement period (June-October) was systematically divided into campaigns. Model fits of 89% of the campaigns were successful, which resulted in 59 campaigns and in a cumulated $R_{eco}$ sum of 8.94 Mg C $ha^{-1}$ 134 $d^{-1}$. Extending intervals between regular campaigns up to three weeks clearly increased the deviation from the original cumulated $R_{eco}$ sum significantly. The difference between the minimum and maximum cumulated $R_{eco}$ sum estimate were 3 Mg C $ha^{-1}$ 134 $d^{-1}$ (7 campaigns) at a mean campaign distance of 18 days. With decreasing campaign frequency the range of cumulated $R_{eco}$ sum resamples increased from 1 Mg C $ha^{-1}$ 134 $d^{-1}$ for weekly campaigns to 2 Mg C $ha^{-1}$ 134 $d^{-1}$ for bi-weekly campaigns and up to up to 3 Mg C $ha^{-1}$ 134 $d^{-1}$ for a campaign every three weeks (Fig. 2-5A and B).

The random uncertainty increased with decreasing campaign frequency to 0.8 Mg C $ha^{-1}$ 134 $d^{-1}$ (9% of reference; Fig. 2-5B). Due to the stable mean cumulated $R_{eco}$ sums with increasing inter-campaign length, the bias of the cumulated C flux was small and scattered in the range of ±0.5 Mg C $ha^{-1}$ 134 $d^{-1}$ (6% of reference) up to an inter-campaign distance of three weeks (Fig. 2-5B).

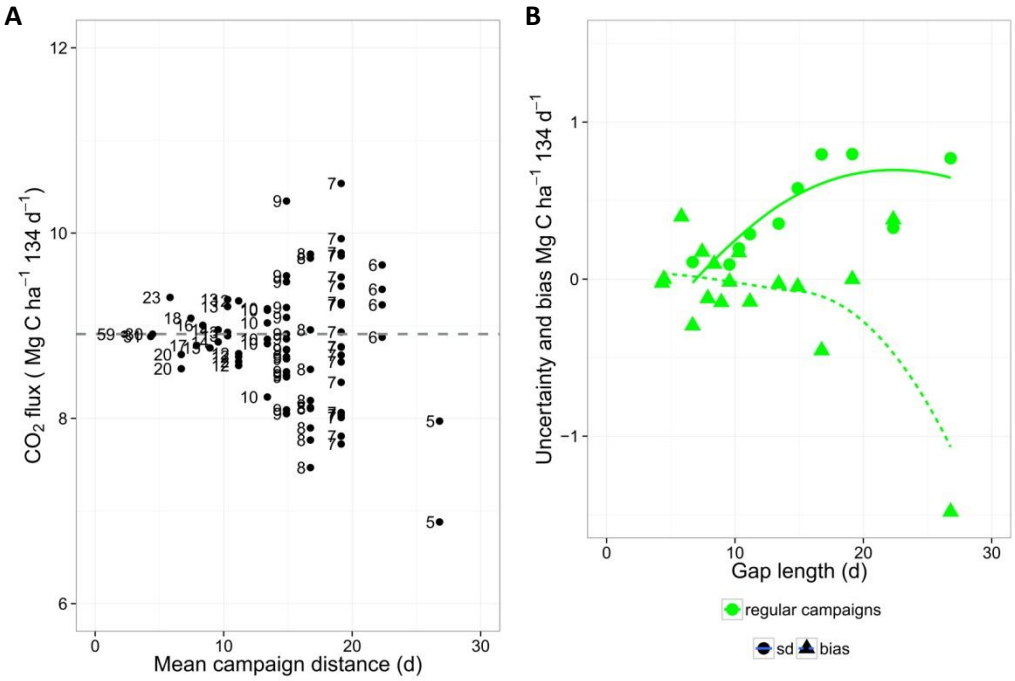


**Fig. 2 - 5**: Evaluation of campaign frequency - regular campaigns. (A) Seasonal $CO_2$ Jackknife sums of resamples vs. mean campaign distance. Numbers indicate number of campaigns used for Jackknife resampling. (B) Random uncertainty (sd) and bias of seasonal $CO_2$ Jackknife sum estimates by regular campaigns. Lines are smoothers for visualization of the trend.

### 3.6 Evaluation of campaign frequency - Lloyd-Taylor models for good weather campaigns

During June to October 2012, 27 days were suitable as measurement campaigns following the criteria defined as good weather. Model fits to 85% of the good weather campaigns were successful, which resulted in 23 campaign days. Inter-campaign distance varied since the selection criteria were weather dependent. The cumulated $R_{eco}$ sum over the measurement period with all 23 campaigns resulted in C emissions of 8.51 Mg C $ha^{-1}$ 131 $d^{-1}$ (Fig. 2-6A). Since the Lloyd-Taylor fit of the first campaign was not successful, the total measurement period of the good weather campaigns was three days shorter than for the other approaches. The range of $R_{eco}$ sum resamples increased with increasing inter-campaign distance and decreasing number of campaigns in the measurement period. Using every sixth campaign for the calculation of cumulated $R_{eco}$ sums, which was equivalent to 4 to 6 campaigns in 131 days, the range of the seasonal $R_{eco}$ estimates based on the resamples was 2 Mg C $ha^{-1}$ 131 $d^{-1}$. For every 11$^{th}$ campaign (three up to five measurement campaigns) cumulated $R_{eco}$ sums varied up to 2.5 Mg C $ha^{-1}$ 131 $d^{-1}$.

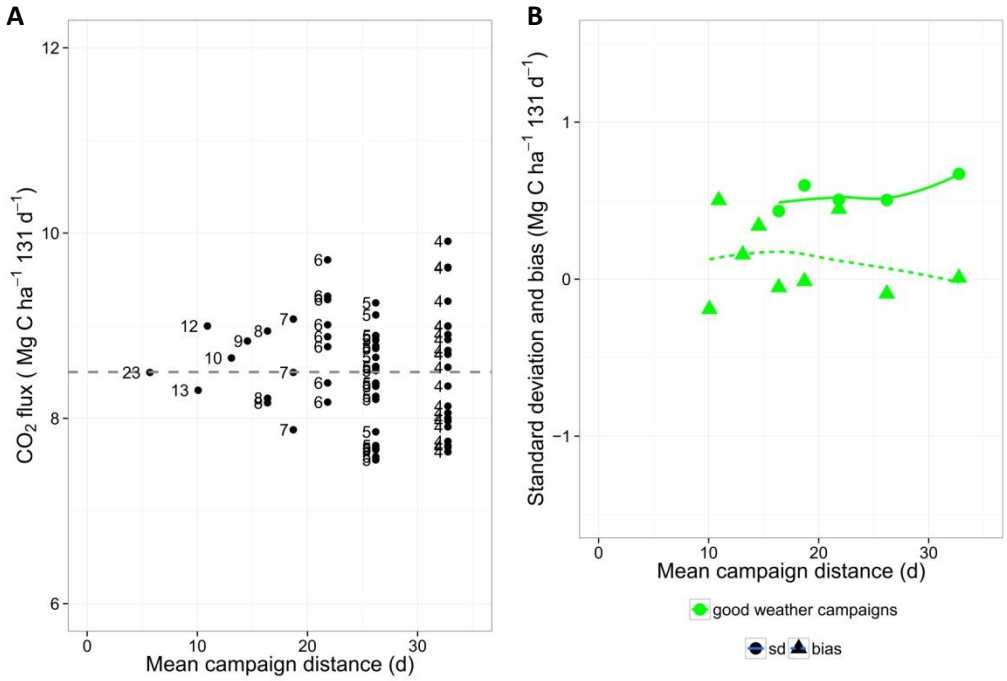


**Fig. 2 - 6**: Evaluation of campaign frequency - good weather campaigns. (A) Seasonal $CO_2$ Jackknife sums of resamples vs. mean campaign distance. Numbers indicate number of campaigns used for Jackknife resampling. (B) Random uncertainty (sd) and bias of seasonal $CO_2$ Jackknife sum estimates by good weather campaigns. Lines are smoothers for visualization of the trend.

The random uncertainty of the cumulated $R_{eco}$ sums of the good weather campaigns slightly increased with decreasing campaign numbers in the resamples up to 0.6 Mg C $ha^{-1}$ 131 $d^{-1}$ (7% of reference; Fig. 2-6B). The corresponding bias irregularly fluctuated from 0 to 0.5 Mg C $ha^{-1}$ 131 $d^{-1}$ showing a slightly decreasing trend with increasing inter-campaign length (6% of reference; Fig. 2-6B).

# 4. Discussion

## 4.1 Capturing day-night $R_{eco}$ patterns is most critical

Calibrating a model only with daytime or only with nighttime measurements produced a substantial bias in seasonal $R_{eco}$ of 3 Mg C $ha^{-1}$ 134$d^{-1}$ (30%), even when measured at high frequency. This agrees with and even exceeds previous studies (Falge et al., 2003; Schneider et al., 2009; Juszczak et al., 2012; Lai et al., 2012; Koskinen et al., 2014). Difference between night- and daytime Lloyd-Taylor-parameters and derived cumulated $R_{eco}$ sums for the whole measurement period can be caused by two effects.

First, higher $CO_2$ effluxes have been reported to occur during nighttime due to down-regulation of leaf respiration during day (Farquhar and Von Caemmerer, 1982) and thus could be a correct flux

estimate. For example, Falge et al. (2002) reported higher nighttime $R_{eco}$ fluxes in several forest, grassland and crop sites measured by eddy covariance technique. They attributed this to down-regulation of leaf respiration.

Second, $R_{eco}$ fluxes can be systematically overestimated due to low turbulence conditions during nighttime (Schneider et al., 2009; Lai et al., 2012), i.e. $R_{eco}$ fluxes could be biased flux estimates. Such conditions create a stable layered distribution of $CO_2$ concentrations with very high concentrations close to the soil surface. These result in low concentration gradients between soil air and atmosphere. If a chamber is deployed, turbulence will be created, in particular if the chamber is equipped with a fan. The layered concentration profile is then dissolved and very high concentration gradients are created, resulting in high fluxes. This can often be recognized by a strongly non-linear increase of concentration inside the chamber during deployment which was not found at our site (see Supplement Fig. S2-2A and B). Due to possible disturbance at chamber deployment, the first 15 seconds of each flux measurement were removed. For the remaining time, robust linear fluxes were calculated.

This mechanism has been reported in several studies, in particular at natural peatland sites, where it can be stronger due to high air-filled soil porosity. Juszczak et al. (2012) measured $CO_2$ with manual opaque chambers in a temperate mire ecosystem. If they used all nighttime $R_{eco}$ fluxes, nighttime fluxes were 15 % higher than daytime fluxes. Restricting the data set to nighttime fluxes measured under stable atmospheric conditions, the difference between nighttime and daytime was even higher (26%). Schneider et al. (2009) measured $R_{eco}$ with manual chambers in a boreal mire complex and Lai et al. (2012) in an ombrotrophic peatland with an automatic chamber system and reported the same. Automated chamber measurements on a porous peat in two forest stands with thin understory vegetation resulted also in an overestimation of nighttime fluxes due to a strong $CO_2$ gradient from the soil to the atmosphere (Koskinen et al., 2014) induced by stable layered atmospheric conditions with very high $CO_2$ concentrations close to the soil surface.

At our site, wind speed tended to be lower during nighttime than during daytime, with a mean nighttime and daytime wind speed 0.72 m $s^{-1}$ ± 0.77 m $s^{-1}$ and 2.21 m $s^{-1}$ ± 1.11 m $s^{-1}$, respectively. However, low wind speed also occurred to a smaller extent during daytime. Therefore, we consider down regulation of leaf respiration responsible for the difference between day and nighttime cumulated $R_{eco}$ sums.

The substantial systematic difference in $CO_2$ fluxes and the $CO_2$ response to temperature are well described ecophysiological features, which have to be carefully considered in the temporal sampling strategy. In fact, both daytime and nighttime $CO_2$ fluxes need to be adequately considered. Measurement protocols for campaign-based chamber measurements therefore measure the full

diurnal cycle starting in the coldest dark phase before sunrise until the late afternoon (Alm et al., 1997; Drösler, 2005; Beetz et al., 2013; Leiber-Sauheitl et al., 2014; Beyer et al., 2015; Eickenscheidt et al., 2015; Pohl et al., 2015). This procedure produces a smaller bias (maximum 6% deviation from reference) compared to only nighttime or only daytime measurements, but a larger one compared to an equal number of nighttime and daytime measurements.

Simplified approaches measuring NEE and $R_{eco}$ by chambers during daytime with shading (Elsgaard et al., 2012; Goerres et al., 2014) likely estimate a substantially biased partitioning of seasonal and annual NEE.

Gap-filling in eddy covariance measurements faces similar challenges for NEE partitioning as eddy covariance only measures nighttime $R_{eco}$. At the same time, nighttime $R_{eco}$ fluxes measured with this methodology under low turbulence conditions also have to be discarded. Recent gap-filling methodologies have suggested solutions like the comparison of multiple methods on one site to reduce the bias in NEE partitioning, but a robust NEE partitioning must rely on combined daytime and nighttime $R_{eco}$ measurements (Reichstein et al., 2012) and thus on chamber measurements.

### 4.2 Day-to-day $R_{eco}$ patterns

Despite substantial short-term variability in groundwater level and soil moisture of the unsaturated zone, seasonal $R_{eco}$ was adequately modeled with a univariate temperature response function for our grassland site on drained organic soils. This can be attributed to covariance (Pearson's correlation coefficient = -0.25; $p < 0.001$) between groundwater table increase after precipitation and temperature decrease, which both reduce soil respiration. This finding agrees with a result of Kurbatova et al. (2013) from a Russian boreal forest on shallow peat soil. Indeed, we found little day-to-day-variation in the $R_{eco}$ response to temperature (data not shown), supported by only a small bias and by the fact that bias and precision were relatively independent of measurement frequency for intervals of > 1 d. The two studies suggest that the unmodified Lloyd-Taylor function can work well for interpolating $R_{eco}$ measurements in ecosystems on organic soils.

Parkin and Kaspar (2004) recommended sampling every three days on mineral agricultural soils to capture the influence of rain events on emissions. Soil respiration estimates sampled every 20 days were within + 60% and – 40% of the actual cumulated flux measured on mineral soil (Parkin and Kaspar, 2004). In contrast, on the investigated histic Gleysol, precipitation events did not significantly influence ecosystem respiration (data not shown) which allows a sampling frequency of more than three days.

Savage's and Davidson's (2003) weekly sampling schedule was sufficient to capture the most important variation of seasonal soil $CO_2$ efflux (June to August) measured by manual chambers with

numerous (n=12; once per week) and spatially well distributed collars. High temporal resolution of flux recording (n=3; hourly) was used to measure and model rapidly changing water contents and temperature of soil respiration in a forest (Savage and Davidson, 2003). Since the prediction of $R_{eco}$ fluxes at our site could not be significantly improved by adding parameters such as soil moisture or groundwater level, the interpolation of $CO_2$ flux measurements at the intervals of several weeks on basis of soil temperature data can be considered adequate for the calculation of cumulated $R_{eco}$ fluxes. This may be different for sites with a weaker covariance between soil temperature and hydrological variables.

### 4.3 Robust sampling strategies for seasonal $R_{eco}$ sums

The primary concern of sampling strategies for $R_{eco}$ measurements is to accurately capture diurnal $R_{eco}$ patterns. Results of our resampling approach indicate that reasonable timing of $R_{eco}$ measurements over the course of the day is more important than the measurement frequency. On average, diurnal misrepresentation and intervals of 3 weeks both led to a maximal difference of Jackknife resample estimates of 3 Mg C $ha^{-1}$ 134 $d^{-1}$ (30%). The maximal difference of Jackknife resample estimates of diurnal misrepresentation was 3 Mg C $ha^{-1}$ 134 $d^{-1}$ as well, but only 1.5 Mg C $ha^{-1}$ 134 $d^{-1}$ (17%) for long intervals in regular observations, and at best 1 Mg C $ha^{-1}$ 131 $d^{-1}$ (12%) for good weather campaigns.

Parkin and Kaspar (2004) also used the Jackknife technique for investigating sampling frequency effects on cumulative $CO_2$ fluxes of hourly autochamber data. Sampling every three days resulted in a difference between Jackknife sums of ± 20% of the expected value which is similar to the average of our findings. In their study, the variance increased from daily up to a 12 day measurement interval and remained constant when the measurement interval was increased up to 20 days. Franzluebbers et al. (2002) recommended a 10 day sampling interval of soil respiration or $R_{eco}$ on the basis of time lag analyses in order to cover changing environmental conditions in a tallgrass prairie. Savage et al (2008) suggested a bi-weekly sampling frequency, which achieved a good estimation of seasonal soil respiration values in two forest sites, i.e. a more than 90% probability of an estimate within 10% of the best estimate based on autochamber data. In our study, little difference between 1-, 2- and 3-weekly inter-campaign distances were observed, suggesting that 3 weeks are robust for extensive grassland on shallow drained organic soil.

The extrapolation of $R_{eco}$ parameters into temperature ranges or seasons beyond the observation range introduce systematic as well as random uncertainty (Hoffmann et al., 2015). Good weather campaigns covered the interpolated temperature ranges in 98% of the time, while the regular

campaigns only achieved a coverage of 93% - 99% because some of the campaigns were cloudy and rainy in case of 14 day gaps.

In order to avoid severe bias, it is important to measure daytime and nighttime $CO_2$ fluxes. If due to practical considerations complete night measurements are not possible, at least the coldest period of night before sunrise should be covered. Additionally, campaigns during good weather should be preferred to regular campaigns since a large temperature range favors good Lloyd-Taylor fits. Before determining campaign frequency, short term effects of soil moisture or groundwater level on $R_{eco}$ fluxes have to be checked. If these occur, a high temporal frequency of sampling should be applied to capture e.g. precipitation events (Savage and Davidson, 2003).

Since precision and bias of 2h data sets were in the same dimension as for the campaign based approaches, the often applied campaign based calculation of annual $R_{eco}$ sums can be considered adequate for recording GHG emissions on organic soils. Therefore, an inter-campaign distance of two to three weeks can be considered adequate for receiving a robust cumulated $R_{eco}$ sum of the vegetation period of a grassland on organic soils, providing that nighttime and daytime are both represented. This measurement scheme was applied in several studies (Beetz et al., 2013; Beyer et al., 2015; Eickenscheidt et al., 2015), which had a similar or slightly larger campaign distance of up to 4 weeks during vegetation period. A maximum error of $R_{eco}$ of up to 30% can be expected if daytime and nighttime measurements are not considered as proposed above.

## 5. Conclusions

By using synthetic resample data sets from continuous $R_{eco}$ measurements by automatic chambers we proved that the manual campaign-wise measurements of $R_{eco}$ are robust if minimum standards are met. A good weather (maximum diurnal PAR and temperature gradients) orientated measurement pattern should be preferred to a strict interval based measurement pattern. Good weather campaigns covering the diurnal cycle, in particular the day-night pattern are suitable to set up a robust $R_{eco}$ model and calculate cumulated $R_{eco}$ sums with high accuracy and adequate precision. Maximum deviation from the mean cumulated $R_{eco}$ flux occurred if only day or night values were used for $R_{eco}$ modeling. Therefore, $R_{eco}$ measurement should be distributed from early in the morning (before sunrise) until the late afternoon which produces a smaller bias than using only daytime measurements for the calculation of the cumulated $R_{eco}$ sum. A minimum measurement frequency of every three weeks can be recommended for extensive grasslands on organic soils.

## Acknowledgement

We acknowledge the Thünen Institute of Climate-Smart Agriculture and the joint research project “Organic soils” for funding. We thank S. Belting for her expertise on plant taxonomy and identification as well as K. Gilke and A. Oehns-Rittgerodt for laboratory assistance.

## 6. References

Alm, J., Talanov, A., Saarnio, S., Silvola, J., Ikkonen, E., Aaltonen, H., Nykanen, H., Martikainen, P. J., 1997. Reconstruction of the carbon balance for microsites in a boreal oligotrophic pine fen, Finland. Oecologia 110, 423-431.

Baldocchi, D., Valentini, R., Running, S., Oechel, W., Dahlman, R., 1996. Strategies for measuring and modelling carbon dioxide and water vapour fluxes over terrestrial ecosystems. Global Change Biology 2, 159-168.

Beetz, S., Liebersbach, H., Glatzel, S., Jurasinski, G., Buczko, U., Hoeper, H., 2013. Effects of land use intensity on the full greenhouse gas balance in an Atlantic peat bog. Biogeosciences 10, 1067-1082.

Beyer, C., Liebersbach, H., Hoeper, H., 2015. Multiyear greenhouse gas flux measurements on a temperate fen soil used for cropland or grassland. Journal of Plant Nutrition and Soil Science 178, 99-111.

Burrows, E. H., Bubier, J. L., Mosedale, A., Cobb, G. W., Crill, P. M., 2005. Net ecosystem exchange of carbon dioxide in a temperate poor fen: a comparison of automated and manual chamber techniques. Biogeochemistry 76, 21-45.

Drösler, M., 2005. Trace gas exchange and climatic relevance of bog ecosystems, Southern Germany. Dissertation, TUM München.

Efron, B., Gong, G., 1983. A leisurely look at the bootstrap, the jackknife, and cross-validation. American Statistician 37, 36-48.

Efron, B., Stein, C., 1981. The Jackknife estimate of variance. The Annals of Statistics 9, 586-596.

Eickenscheidt, T., Heinichen, J., Drösler, M., 2015. The greenhouse gas balance of a drained fen peatland is mainly controlled by land-use rather than soil organic carbon content. Biogeosciences 12, 5161-5184.

Elsgaard, L., Gorres, C.-M., Hoffmann, C. C., Blicher-Mathiesen, G., Schelde, K., Petersen, S. O., 2012. Net ecosystem exchange of $CO_2$ and carbon balance for eight temperate organic soils under agricultural management. Agriculture Ecosystems & Environment 162, 52-67.

Falge, E., Baldocchi, D., Tenhunen, J., Aubinet, M., Bakwin, P., Berbigier, P., Bernhofer, C., Burba, G., Clement, R., Davis, K. J., Elbers, J. A., Goldstein, A. H., Grelle, A., Granier, A., Guomundsson, J., Hollinger, D., Kowalski, A. S., Katul, G., Law, B. E., Malhi, Y., Meyers, T., Monson, R. K., Munger, J. W., Oechel, W., Paw, K. T., Pilegaard, K., Rannik, U., Rebmann, C., Suyker, A., Valentini, R., Wilson, K., Wofsy, S., 2002. Seasonality of ecosystem respiration and gross primary production as derived from FLUXNET measurements. Agricultural and Forest Meteorology 113, 53-74.

Falge, E., Tenhunen, J., Aubinet, M., Bernhofer, C., Clement, R., Granier, A. , Kowalski, A., Moors, E., Pilegaard, K., Rannik, Ü., Rebmann, C., 2003. A Model-Based Study of Carbon Fluxes at Ten European Forest Sites, In: R.Valentini (Ed.), Fluxes in Carbon, Water and Energy of European Forests. Springer, Berlin Heidelberg, 151-177.

Farquhar, G.D., Von Caemmerer, S., 1982. Modelling of photosynthetic response to environmental conditions, In: Lange O.L., Nobel P.S., Osmond C.B., H., Z. (Eds.), Encyclopedia of plant physiology, vol. 12B. Springer, Berlin Heidelberg New York, 549–587

Flanagan, L. B., Johnson, B. G., 2005. Interacting effects of temperature, soil moisture and plant biomass production on ecosystem respiration in a northern temperate grassland. Agricultural and Forest Meteorology 130, 237-253.

Franzluebbers, K., Franzluebbers, A. J., Jawson, M. D., 2002. Environmental controls on soil and whole-ecosystem respiration from a tallgrass prairie. Soil Science Society of America Journal 66, 254-262.

Goerres, C. M., Kutzbach, L., Elsgaard, L., 2014. Comparative modeling of annual $CO_2$ flux of temperate peat soils under permanent grassland management. Agriculture Ecosystems & Environment 186, 64-76.

Guisan, A., Edwards, T. C., Hastie, T., 2002. Generalized linear and generalized additive models in studies of species distributions: setting the scene. Ecological Modelling 157, 89-100.

Hoffmann, M., Jurisch, N., Borraz, E. A., Hagemann, U., Droesler, M., Sommer, M., Augustin, J., 2015. Automated modeling of ecosystem $CO_2$ fluxes based on periodic closed chamber measurements: A standardized conceptual and practical approach. Agricultural and Forest Meteorology 200, 30-45.

IPCC, 2006. Guidelines for National Greenhouse Gas Inventories.Chapter 6:Grasslands. 49 pp.

Juszczak, R., Acosta, M., Olejnik, J., 2012. Comparison of Daytime and Nighttime Ecosystem Respiration Measured by the Closed Chamber Technique on a Temperate Mire in Poland. Polish Journal of Environmental Studies 21, 643-658.

Koskinen, M., Minkkinen, K., Ojanen, P., Kamarainen, M., Laurila, T., Lohila, A., 2014. Measurements of $CO_2$ exchange with an automated chamber system throughout the year: challenges in measuring night-time respiration on porous peat soil. Biogeosciences 11, 347-363.

Kurbatova, J., Tatarinov, F., Molchanov, A., Varlagin, A., Avilov, V., Kozlov, D., Ivanov, D., Valentini, R., 2013. Partitioning of ecosystem respiration in a paludified shallow-peat spruce forest in the southern taiga of European Russia. Environmental Research Letters 8, 1-9.

Lai, D. Y. F., Roulet, N. T., Humphreys, E. R., Moore, T. R., Dalva, M., 2012. The effect of atmospheric turbulence and chamber deployment period on autochamber $CO_2$ and $CH_4$ flux measurements in an ombrotrophic peatland. Biogeosciences 9, 3305-3322.

Leiber-Sauheitl, K., Fuß, R., Voigt, C., Freibauer, A., 2014. High $CO_2$ fluxes from grassland on histic Gleysol along soil carbon and drainage gradients. Biogeosciences 11, 749-761.

Lloyd, J., Taylor, J. A., 1994. On the temperature dependence of soil respiration. Functional Ecology 8, 315-323.

Maljanen, M., Hytonen, J., Makiranta, P., Alm, J., Minkkinen, K., Laine, J., Martikainen, P. J., 2007. Greenhouse gas emissions from cultivated and abandoned organic croplands in Finland. Boreal Environment Research 12, 133-140.

Mielke, M. S., de Almeida, A. A. F., Gomes, F. P., 2005. Photosynthetic traits of five neotropical rainforest tree species: Interactions between light response curves and leaf-to-air vapour pressure deficit. Brazilian Archives of Biology and Technology 48, 815-824.

Parkin, T. B., Kaspar, T. C., 2004. Temporal variability of soil carbon dioxide flux: Effect of sampling frequency on cumulative carbon loss estimation. Soil Science Society of America Journal 68, 1234-1241.

Pinheiro, J., Bates, D., 2000. Mixed-Effects Models in S and S-PLUS. Springer, New York, 537 pp.

Pohl, M., Hoffmann, M., Hagemann, U., Giebels, M., Albiac Borraz, E., Sommer, M., Augustin, J., 2015. Dynamic C and N stocks – key factors controlling the C gas exchange of maize in heterogenous peatland. Biogeosciences 12, 2737-2752.

R Core Team, 2015. R: A language and environment for statistical computing. R Foundation for Statistical Computing., Vienna, Austria. Version 3.2.0, available at: http://www.R-project.org/

Reichstein, M., Falge, E., Baldocchi, D., Papale, D., Aubinet, M., Berbigier, P., Bernhofer, C., Buchmann, N., Gilmanov, T., Granier, A., Grunwald, T., Havrankova, K., Ilvesniemi, H., Janous, D., Knohl, A., Laurila, T., Lohila, A., Loustau, D., Matteucci, G., Meyers, T., Miglietta, F., Ourcival, J. M., Pumpanen, J., Rambal, S., Rotenberg, E., Sanz, M., Tenhunen, J., Seufert, G., Vaccari, F., Vesala, T., Yakir, D., Valentini, R., 2005. On the separation of net ecosystem exchange into assimilation and ecosystem respiration: review and improved algorithm. Global Change Biology 11, 1424-1439.

Reichstein, M., Stoy, P. C., Desai, A. R., Lasslop, G., Richardson, A. D., 2012. Partitioning of net fluxes., In: Aubinet, M., Vesala, T., Papale, D. (Eds.), Eddy Covariance. Springer Netherlands, 263-289.

Running, S. W., Baldocchi, D. D., Turner, D. P., Gower, S. T., Bakwin, P. S., Hibbard, K. A., 1999. A global terrestrial monitoring network integrating tower fluxes, flask sampling, ecosystem modeling and EOS satellite data. Remote Sensing of Environment 70, 108-127.

Savage, K., Davidson, E. A., Richardson, A. D., 2008. A conceptual and practical approach to data quality and analysis procedures for high-frequency soil respiration measurements. Functional Ecology 22, 1000-1007.

Savage, K. E., Davidson, E. A., 2001. Interannual variation of soil respiration in two New England forests. Global Biogeochemical Cycles 15, 337-350.

Savage, K. E., Davidson, E. A., 2003. A comparison of manual and automated systems for soil $CO_2$ flux measurements: trade-offs between spatial and temporal resolution. Journal of Experimental Botany 54, 891-899.

Schneider, J., Kutzbach, L., Schulz, S., Wilmking, M., 2009. Overestimation of $CO_2$ respiration fluxes by the closed chamber method in low-turbulence nighttime conditions. Journal of Geophysical Research-Biogeosciences 114, 1-10.

Schrier-Uijl, A. P., Kroon, P. S., Hensen, A., Leffelaar, P. A., Berendse, F., Veenendaal, E. M., 2010. Comparison of chamber and eddy covariance-based $CO_2$ and $CH_4$ emission estimates in a heterogeneous grass ecosystem on peat. Agricultural and Forest Meteorology 150, 825-831.

Šimůnek, J., Šejna, M., Saito, H., Sakai, M., van Genuchten, M.T, 2013. The HYDRUS-1D Software Package for Simulating the One-Dimensional Movement of Water, Heat, and Multiple Solutes in Variably-Saturated Media. Department of Environmental Sciences, University of California Riverside, California, 307 pp.

von Arnold, K., Nilsson, M., Hanell, B., Weslien, P., Klemedtsson, L., 2005. Fluxes of $CO_2$, $CH_4$ and $N_2O$ from drained organic soils in deciduous forests. Soil Biology & Biochemistry 37, 1059-1071.

Wagle, P., Kakani, V. G., 2014. Confounding Effects of Soil Moisture on the Relationship Between Ecosystem Respiration and Soil Temperature in Switchgrass. Bioenergy Research 7, 789-798.

WRB, 2008. World Reference Base for Soil Resources 2006. Ein Rahmen für internationale Klassifikation, Korrelation und Kommunikation., Deutsche Ausgabe ed. Bundesanstalt für Geowissenschaften und Rohstoffe, Hannover, 148 pp.

# 7. Supplement

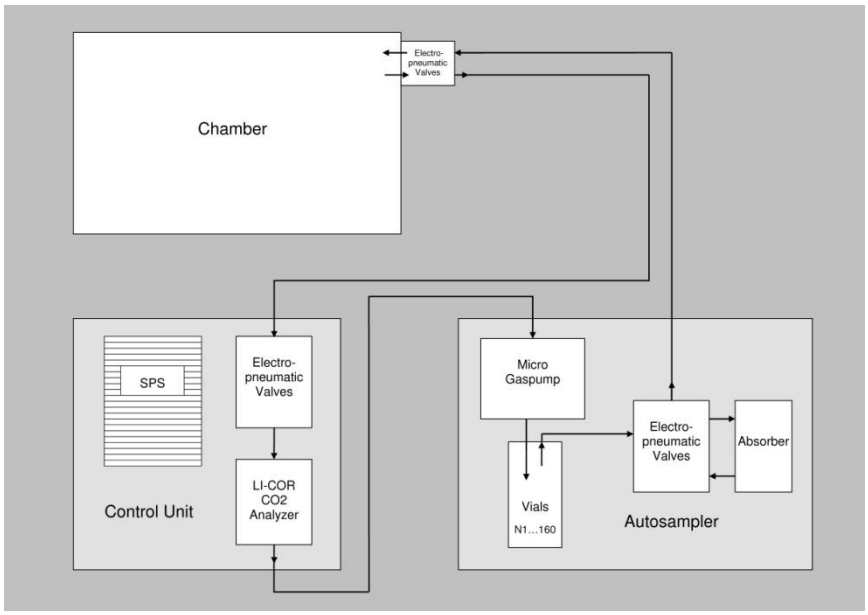


**Fig. S2 - 1:** Flow scheme of the measured greenhouse gases from the chamber to $CO_2$ analyzer and to the automatic $CH_4$ and $N_2O$ sampling system.

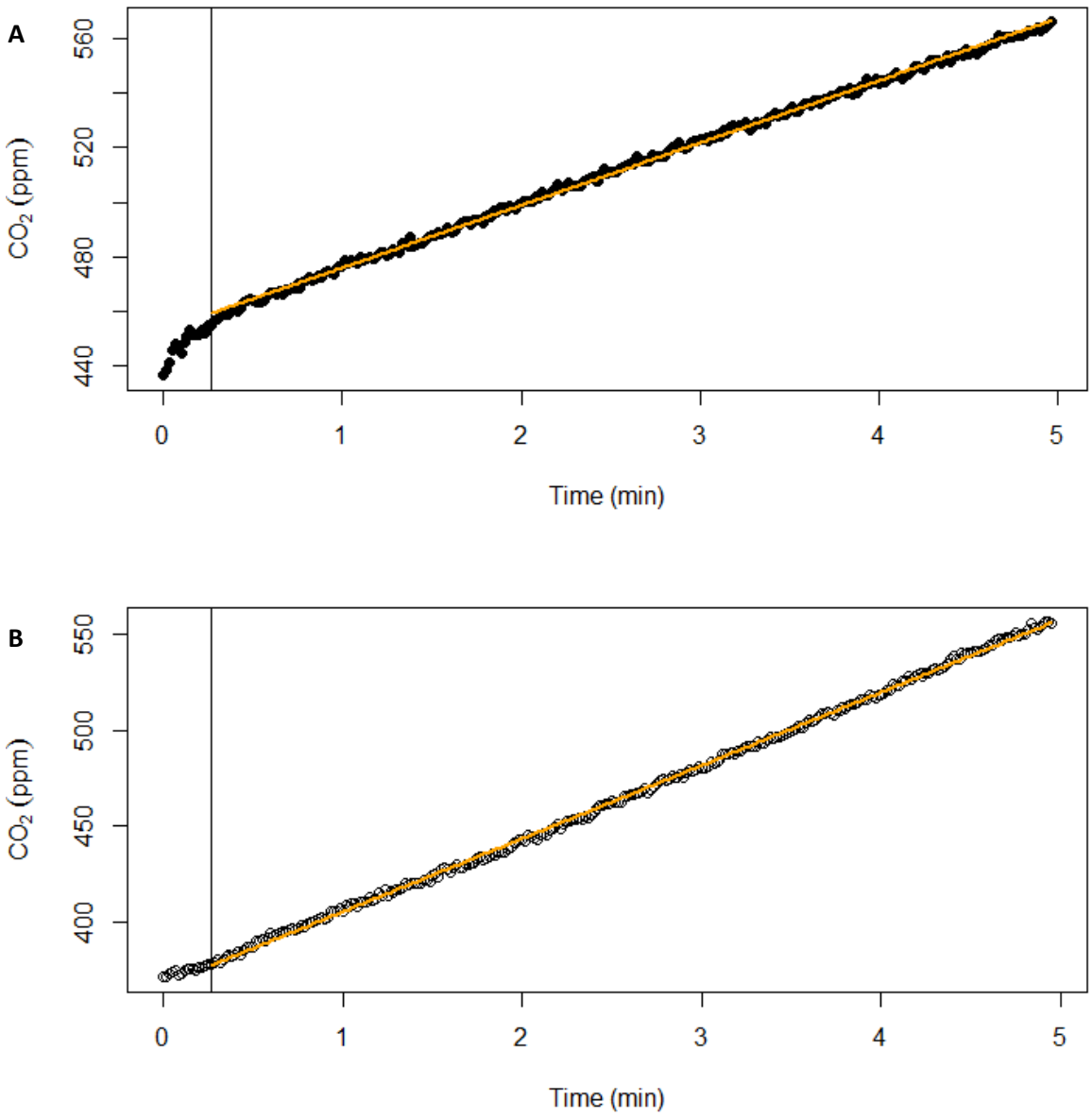


**Fig. S2 - 2**: Exemplary nighttime (A; 22.06.2012 02:40 am) and daytime (B; 06.07.2012 11:13 am) $CO_2$ increase during a chamber measurement in the Grosses Moor. All values left of the vertical line (first 15 seconds) were discarded. Orange lines indicate the linear fit which was estimated with all data points from 0.25 min to 5 min. Actual fits of the investigated data set were done with mass concentrations.

**Table S2 - 1**: Model summary of generalized nonlinear least squares fit of daytime and nighttime Lloyd-Taylor parameters with "varPower" as variance structure.

```
Generalized nonlinear least squares fit
  Model: p_Fluss ~ SSLloydTaylor(TB2a, Rref, e0)
  Data: recotest_pooled
    AIC   BIC logLik
  15889 15921  -7939

Variance function:
 Structure: Power of variance covariate
 Formula: ~fitted(.)
 Parameter estimates:
power
 1.06

Coefficients:
                  Value Std.Error t-value p-value
Rref.(Intercept)    211      1.99   106.2       0
Rref.dayTRUE        -39      3.11   -12.5       0
e0.(Intercept)      385      7.97    48.4       0
e0.dayTRUE          -83     10.76    -7.7       0

 Correlation:
               Rr.(I) R.TRUE e0.(I)
Rref.dayTRUE   -0.639
e0.(Intercept) -0.228  0.146
e0.dayTRUE      0.169 -0.526 -0.741

Standardized residuals:
   Min     Q1    Med     Q3    Max
-2.212 -0.704 -0.099  0.583  4.729

Residual standard error: 0.169
Degrees of freedom: 1438 total; 1434 residual
```

# Chapter 3: Publication no. 2

## High $CO_2$ fluxes from grassland on histic Gleysol along soil carbon and drainage gradients

**Authors:**
K. Leiber-Sauheitl[1], R. Fuß[1,*], C. Voigt[1,2,*], A. Freibauer[1,*]

[1] Thünen Institute of Climate-Smart Agriculture, Bundesallee 50, 38116 Braunschweig, Germany
[2] Department of Environmental Science, University of Eastern Finland, PO Box 1627, 70211 Kuopio, Finland

**Status of publication:**
published in Biogeosciences 11, 749–761, 2014

**Own contributions:**

- field work
- data collection
- data analyses
- application and modification of R model to all data sets
- preparation of the manuscript

**Contributions by coauthors:**

- R. Fuß: programming the model in R, contribution to the manuscript
- C. Voigt: support in the field, comments to improve the manuscript
- A. Freibauer: experimental design, contribution to the manuscript

## Abstract

Drained organic soils are anthropogenic emission hotspots of greenhouse gases (GHGs). Most studies have focused on deep peat soils and on peats with high organic carbon content. In contrast, histic Gleysols are characterized by shallow peat layers, which are left over from peat cutting activities or by peat mixed with mineral soil. It is unknown whether they emit less GHGs than deep Histosols when drained. We present the annual carbon and GHG balance of grasslands for six sites on nutrient-poor histic Gleysols with a shallow (30 cm) histic horizon or mixed with mineral soil in Northern Germany (soil organic carbon concentration ($C_{org}$) from 9 to 52 %).

The net GHG balance, corrected for carbon export by harvest, was around 4 t $CO_2$-C-eq. $ha^{-1}$ $yr^{-1}$ on soils with peat layer and little drainage (mean annual water table <20 cm below surface). The net GHG balance reached 7-9 t $CO_2$-C-eq. $ha^{-1}$ $yr^{-1}$ on soils with sand mixed into the peat layer and water tables between 14 cm and 39 cm below surface. GHG emissions from drained histic Gleysols (i) were as high as those from deep Histosols, (ii) increase linearly from shallow to deeper drainage, (iii) but are not affected by $C_{org}$ content of the histic horizon. Ecosystem respiration ($R_{eco}$) was linearly correlated with water table level even if it was below the histic horizon. The $R_{eco}$/GPP ratio was 1.5 at all sites, so that we ruled out a major influence of the inter-site variability in vegetation composition on annual net ecosystem exchange (NEE).

The IPCC definition of organic soils includes shallow histic topsoil, unlike most national and international definitions of Histosols. Our study confirms that this broader definition is appropriate considering anthropogenic GHG emissions from drained organic soils. Countries currently apply soil maps in national GHG inventories which are likely not to include histic Gleysols. The land area with GHG emission hotspots due to drainage is likely to be much higher than anticipated.

Deeply drained histic Gleysols are GHG hotspots which have so far been neglected or underestimated. Peat mixing with sand does not mitigate GHG emissions. Our study implies that rewetting organic soils, including histic Gleysols, has a much higher relevance for GHG mitigation strategies than currently recognized.

## 1. Introduction

Organic soils constitute three percent of the land area of the temperate zone in Europe (Kottek et al., 2006; Montanarella et al., 2006). A large fraction of them has been drained for forestry, agriculture, and peat extraction. In Germany, organic soils make up approximately five percent of the land area, about 1.7 million ha (Richter, 1998; UBA, 2012) and drainage for agricultural purposes or industrial peat extraction was conducted on nearly all of these soils (UBA, 2012). During cultivation of organic soils, degradation of soil organic substances causes emission of high amounts of $CO_2$ and often $N_2O$

as well as subsidence of the peat layers (Smith and Conen, 2004). As a result, only shallow peat soils remain at many former peatland areas and many peatlands even have completely disappeared (e.g. 61% over 30 years in Denmark, Nielsen et al., 2012). Such loss of peatland areas as carbon storage significantly contributes to global warming (Limpens et al., 2008).

The dominant land use on peat soils of the European boreal zone is forestry (Drösler et al., 2008), whereas in the temperate zone grassland of varying management intensity predominates (Schrier-Uijl et al., 2010). In laboratory studies, $CO_2$ emissions from drained peat scale almost linearly with the depth of the aerated soil above the water table (Dinsmore et al., 2009). Peat quality is an important issue concerning $CO_2$ emissions (Reiche et al., 2010). Due to Blodau (2002) the amount of easily degradable carbon is positively correlated with $CO_2$, $CH_4$ and $N_2O$ fluxes. Moreover, mixing peat with mineral subsoil can either result in C loss by mobilization of $C_{org}$ due to increase of aerated surfaces or result in a reduction of C emissions by $C_{org}$ stabilization on mineral surfaces (Mikutta et al., 2006; Marschner et al., 2008) and/or by $C_{org}$ dilution by mineral soil material (Don et al., 2013).

Most studies focus on peat soils, which meet the definition of Histosols. Histosols are defined to feature high carbon contents (20 to 30%) and an organic horizon larger than 40 cm (WRB, 2008). The IPCC definition of peat soils is broader and assumes that also shallow peat soils (≥ 10 cm) and strongly degraded ones (≥ 12% $C_{org}$) behave like real peat soils concerning GHG fluxes (IPCC, 2006). Most countries ignore soils with a lower organic carbon content in the national GHG inventory and often focus on deep organic soils. In contrast, in the Danish GHG inventory it is assumed that soils intermediate to typical mineral soils ($C_{org}$ concentration < 6%) and peat ($C_{org}$ concentration > 12%) emit half as much GHG as organic soils (Nielsen et al., 2012). However, according to this report no measurements were conducted on these soils.

To fill this data gap and to test the validity of GHG inventory assumptions, we focus on the most common land-use type in temperate climates (grassland) and measure GHGs along drainage and carbon gradients on a heavily degraded organic soil, which meets the IPCC definition of “organic soil”. We test two hypotheses: Firstly, GHG emissions (mainly $CO_2$) of histic Gleysols increase linearly with drainage depth in the peat layer and level off when the water table falls below the peat layer. Secondly, peat mixed with mineral subsoil and resulting lower $C_{org}$ concentration emits lower amounts of GHG than unmixed peaty soil with a high $C_{org}$ concentration.

## 2. Materials and methods

### 2.1. Study site Grosses Moor [Great Peat Bog]

The Grosses Moor [Great Peat Bog] (Gifhorn, Germany, [52° 34' 54.22" N, 10° 39' 46.43" E]) is a bog-fen peat complex of 6000 hectares situated close to the eastern climatic boundary for bog formation.

It is located within a former moraine plain from the Saale ice age and the meltwater of the Warthe stage initiated bog formation (Overbeck, 1952). The original ombrotrophic peat bog was altered by peat drainage and peat cutting during the 19$^{th}$ century. As a result, nowadays the Grosses Moor is influenced by groundwater. Mean annual temperature was 8.5 °C and mean annual precipitation was 663 mm in the time period 2008-2011. Mineral substrates below the peat are sandy terraces and partly Pleistocene clay layers. Formerly up to six meter deep peat layers were altered by peat cutting and deep plough cultivation, which created strong small-scale heterogeneity. The original bog vegetation has been nearly completely destroyed. Typical vegetation now consists of large cultivated areas, grasslands, and forests of pine and birch as well as purple moor-grass (*Molinia caerulea*), soft rush (*Juncus effusus*) and Erica heath in peat harvest areas. About 2700 hectares were turned into restoration areas in 1984. About 2720 hectares of abandoned peat cut areas are used as extensive grassland.

The study area is managed as extensive grassland. Sheep graze one to three times a year. Mulching is conducted in autumn. No fertilizer is applied.

The study area is characterized by small peat shoulders and depressions with different water table levels and an irregular anthropogenic mixing of peat layer and mineral soil. Although the entire study area is classified as grassland, the vegetation also shows a gradient from grass dominance to moss dominance.

The small-scale heterogeneity of the study area was surveyed to select sites with diverging soil organic carbon (SOC) concentration in topsoil, C stocks, and water table levels. According to a survey report and own preliminary investigations, two transects (each 310 m) were established at 100 m distance to each other in the area of the field where peat cutting and sand mixing from ploughing into strata beneath the peat layer occurred. Every ten meters sampling was carried out by auger until the sandy layer was reached. Auger samples were divided in 0-0.3 m (peat layer) and 0.3-0.6 m (sandy layer). For a first assessment, indicative levels of carbon content of the peat layer were determined by loss on ignition. Six sites were selected in order to achieve similar peat depths (0.25-0.3 m), differing SOC concentrations, and differing water levels. The resulting site characteristics are presented in Table 3-1. Sites with a $C_{org}$ content below 15% were classified as $C_{low}$, >15% to 35% $C_{org}$ as $C_{med}$, and >35% to 55% $C_{org}$ as $C_{high}$. Mean groundwater levels W during the study period are indicated by index in centimeters below soil surface. Resulting, sites $C_{med}$ $W_{39}$, $C_{low}$ $W_{29}$ and $C_{low}$ $W_{14}$ are located on transect 1 within 70 meters distance and sites $C_{high}$ $W_{11}$, $C_{high}$ $W_{22}$ and $C_{high}$ $W_{17}$ on transect 2 within 30 meters distance. Sites were fenced to keep off sheep and other animals.

### 2.2. Measurement of site characteristics

Photosynthetic active radiation (PAR), precipitation, and air temperature were continually measured at a local meteorological station which was located at a distance of 100 to 150 m from the sites. PAR was manually logged at each site during measurements.

Groundwater levels were continually recorded at each site every 15 minutes by groundwater data loggers (Mini-diver, Schlumberger). In order to eliminate short-term disturbances, a moving median was calculated over a 75 minute window. Subsequently, moving median values were aggregated to one hour values.

Soil temperatures in 0.1, 0.05, 0.02 m were continually logged at each site every 5 minutes from soil temperature sensors.

Mineral nitrogen ($N_{min}$) contents of the 0-0.2 m soil layer were analyzed according to VDLUFA (1997) by extraction with 0.01 M $CaCl_2$ at every $N_2O$ measurement. For each site the measured $N_{min}$ values were extrapolated to $N_{min}$ stocks per hectare. The pH values were determined with $CaCl_2$ according to DIN ISO 10390 (HBU, 2005). $C_{org}$ of each site was measured with an elemental analyzer (variomax C, Elementar). Bulk density was measured according to DIN ISO 11272 in 0–0.3 m (HBU, 1998).

**Table 3 - 1:** Site characterization.

| Site [a] | Soil class (WRB) | $C_{org}$ [%][a] | C stock [kg $m^{-2}$][b] | bulk density [g $cm^{-3}$][b] | C/N[b] | $N_{min}$ [kg $ha^{-1}$][c] | pH ($CaCl_2$) | Mean GWL [m][d] |
|---|---|---|---|---|---|---|---|---|
| $C_{med}W_{39}$ | histic Gleysol | 34.3 | 46 | 0.54 | 29 | 6 ± 3 | 3.8 | 0.39 |
| $C_{low}W_{29}$ | mollic Gleysol drainic | 11.3 | 36 | 1.06 | 27 | 17 ± 11 | 4.5 | 0.29 |
| $C_{low}W_{14}$ | mollic Gleysol drainic | 9.3 | 29 | 0.97 | 24 | 10 ± 5 | 4.5 | 0.14 |
| $C_{high}W_{11}$ | histic Gleysol drainic | 51.7 | 71 | 0.45 | 28 | 2 ± 1 | 4.1 | 0.11 |
| $C_{high}W_{22}$ | histic Gleysol drainic | 47.7 | 41 | 0.29 | 28 | 2 ± 1 | 3.8 | 0.22 |
| $C_{high}W_{17}$ | histic Gleysol drainic | 47.7 | 41 | 0.29 | 28 | 2 ± 1 | 3.8 | 0.17 |

C= carbon, W= mean annual water table

[a] Subscripts in site designations refer to low (<15%), medium (15-35%) or high (>35%) soil C content and mean annual water table depth (cm)

[b] organic carbon, C stock, C/N and bulk density in 0-30cm

[c] site mean value ± one standard deviation of mineral nitrogen in 0-20 cm in the time interval June 1, 2011 to June 1, 2012 (n=27)

[d] GWL = ground water level in the time interval June 1, 2011 to June 1, 2012

Plant species were determined according to Oberdorfer (2001) and species abundance was classified according to the Londo scale (Londo, 1976). Sedge, grass and moss cover was determined for every site.

Green biomass was manually harvested from the plots after each grazing by cutting to 5 cm above the soil surface. At all sites only the grass and sedge biomass was removed; mosses were left untouched. Fresh weight and weight after drying at 60 °C were determined. For carbon and nitrogen measurement (Leco, TruMac CN) a pooled and homogenized sample of all biomass from a plot was used. The C and N values of three replicate plots were averaged per site. C and N contents of the biomass of all cut dates were summed and defined as biomass export of each site.

### 2.3. GHG flux measurements

$CO_2$, $CH_4$, and $N_2O$ fluxes were measured with manual static chambers (Drösler, 2005) at the six sites. Rows of triplicate chamber frames (0.61 m², 0.4 m distance between frames) were installed on each site for gas flux measurements. Measurements were conducted at least fortnightly. For $CO_2$, three sites were measured per day, i.e., $C_{med}$ $W_{39}$, $C_{low}$ $W_{29}$ and $C_{low}$ $W_{14}$ on one day and $C_{high}$ $W_{11}$, $C_{high}$ $W_{22}$ and $C_{high}$ $W_{17}$ on another day.

Diurnal cycles of $CO_2$ fluxes covering the full range of PAR and soil temperature of a day were measured from sunrise till late afternoon with an infrared gas analyzer (LI-820, LI-COR, USA) connected to opaque PVC chambers (for ecosystem respiration, chamber height 0.5 m, 2 to 5 minutes chamber closure) and transparent plexiglass chambers (for net ecosystem exchange, chamber height 0.5 m, 1.5 to 3 minutes chamber closure) (PS-plastic, Eching, Germany). Exclusion criteria of $CO_2$ fluxes were PAR changes larger than 10% of the starting value and more than 1.5 °C increase in chamber temperature. However, few fluxes were removed ex post from the dataset due to these criteria, since they could be checked in the field and measurements were adjusted accordingly. For cooling of the transparent chambers thermal packs were used. During each campaign each frame was sampled by opaque chambers three to six times and by transparent chambers five to eight times depending on season and weather conditions.

Opaque PVC chambers were used for $CH_4$ and $N_2O$ flux measurements (PS-plastic, Eching, Germany). Chamber air samples were collected in headspace vials 0, 20, 40, and 60 minutes after chamber closure. Measurements were carried out with a Varian CP-3800 GC-FID/-ECD using a headspace autosampler (QUMA Elektronik & Analytik GmbH, Germany).

The period used for carbon and GHG annual balance was chosen from June 01, 2011 until June 01, 2012.

## 2.4. $CO_2$ modeling

### *2.4.1 Raw fluxes*

Fluxes were calculated by linear regression with $CO_2$-Flux Version 1.0.30 (Beetz et al., 2013, in prep.[1]). Near zero fluxes with small $R^2$ were not discarded (Alm et al., 2007). A 50 point moving window (measurement frequency 1.3 s) was applied to find fluxes with maximum $R^2$ and minimum variance, respectively. Both optimization procedures resulted often in identical flux estimates (53% of all fluxes), but differed in particular during sunrise. Therefore, the mean value of the fluxes from the two optimization procedures was used as a somewhat conservative flux estimate. 19% of all fluxes had a difference of less than 5% between the two procedures and 14% of all fluxes had a difference of more than 20%. Daily net ecosystem exchange (NEE), ecosystem respiration ($R_{eco}$), and gross primary production (GPP) were modeled according to Alm et al. (1997), Drösler (2005), and Beetz et al. (2013) with some adaptations to site conditions as described below.

### *2.4.2 Response functions*

Since the transparent chambers absorb a maximum of five percent of the incoming radiation according to the manufacturer (PS-plastic, Eching, Germany), the PAR-data from the measurement campaigns were corrected by a factor of 0.95. Diurnal cycles of PAR values differed between on-site measurements and measurements at the meteorological station. This was corrected using empirical functions ($PAR = a \times PAR_{station}^{b}$), which were derived separately for sites $C_{med}$ $W_{39}$, $C_{low}$ $W_{29}$ and $C_{low}$ $W_{14}$ and sites $C_{high}$ $W_{11}$, $C_{high}$ $W_{22}$ and $C_{high}$ $W_{17}$, respectively, using robust non-linear regression (Rousseeuw et al., 2012; Fig. S3-1 in the Supplement). The location of the sites and the meteorological station were at different distances from an adjacent tree line, which resulted in different times when direct sunlight reached the PAR sensors at dawn. Since the meteorological station logged every 0.5 h, but the radiation conditions changed at a higher frequency, additional scatter occurred in the data due to clouds and other effects.

The temperature dependent $R_{eco}$ flux model was calculated according to Lloyd-Taylor (1994):

$$R_{eco} = R_{ref} \times \exp\left[E_0 \times \left(\frac{1}{T_{ref} - T_0} - \frac{1}{T - T_0}\right)\right]. \quad (1)$$

$R_{ref}$ respiration at the reference temperature [mg $CO_2$-C $m^{-2}$ $h^{-1}$]

$E_0$ $E_0$ an activation like parameter [K]

$T_{ref}$ reference temperature: 283.15 [K]

$T_0$ temperature constant for the start of biological processes: 227.13 [K]

[1] $CO_2$-Flux Version 1.0.30 - Klima-, $CO_2$-Daten und FLUX-Berechnung. Ing.-Büro J. Hofmann, Rostock, Germany

The model was fitted to soil temperatures in 0.02 m depth, which resulted in robust fits (see Fig. S3-3 in the Supplement) and was considered to be representative both of plant and of soil respiration. On-site temperatures were used for fitting rather than temperatures from the meteorological station as they resulted in better fit quality. If fitting the temperature dependence was numerically not possible, e.g., due to the observed temperature range during a measurement campaign being too narrow, the campaign was excluded from calibration and only used for validation (Fig. S3-4 in the Supplement). This was applied to two winter campaigns (1°C temperature range in 2 cm). The temperature ranges were campaign dependent with an average range of 5 to 13 °C in 2 cm. The $R_{eco}$ models of the measurement campaigns had a median $R^2$ of 0.98 and a minimum of 0.83.

The PAR dependent NEE flux model was calculated using the Michaelis-Menten type model proposed by Falge et al. (2001) (see Fig. S3-3 in the Supplement):

$$NEE = \frac{(GP2000 \times \alpha \times PAR)}{\left(GP2000 + \alpha \times PAR - \frac{GP2000}{2000} \times PAR\right)} + R_{eco} \quad (2)$$

*GP2000* rate of carbon fixation at PAR 2000 [mg $CO_2$-C $m^{-2}$ $h^{-1}$]

*PAR* photon flux density of the photosynthetic active radiation [W $m^{-2}$]

$\alpha$ initial slope of the curve; light use efficiency [mg $CO_2$-C $m^{-2}$ $h^{-1}$ / W $m^{-2}$]

The NEE models of the measurement campaigns had an median $R^2$ of 0.97 and a minimum of 0.60. PAR values used for fitting were again on-site values.

### *2.4.3 Interpolation to annual models*

The annual model was calculated separately for each site. Values between two measurement campaigns were calculated separately using the campaign results on both sides, and then taken as the distance weighted mean of both values. To account for management events, $E_0$ and $R_{ref}$ were kept constant from the preceding measurement campaign until the cut date. After the cut parameters were taken from the subsequent measurement campaign. The annual $R_{eco}$ model was calculated on a 0.5 hourly basis using on-site temperature data. Biomass cuts were included in the NEE model by applying *α* and *GP2000* from the preceding measurement campaign until the cut date and setting α to -0.01 and *GP2000* to -4 after the cut according to observations on other grassland sites (Drösler et al., 2013). NEE values were modeled using corrected PAR values from the meteorological station. In the end GPP was calculated on a 0.5 hourly basis:

$$\mathrm{GPP} = \mathrm{NEE} - \mathrm{R_{eco}} \quad (3)$$

For error estimation of the $CO_2$ fluxes (NEE, GPP, $R_{eco}$) and to construct a confidence interval for the annual NEE, GPP and $R_{eco}$ fluxes a Monte Carlo simulation was conducted for each site as follows:

1. The robust fit of the PAR correction function was performed 1000 times with bootstrap resamples of the PAR data points (on-site/station).
2. From the $R_{eco}$ fits of all measurement campaigns bootstrap parameter samples were created using bootstrap of the residuals (Efron, 1979). Bootstrap of the residuals preserves the distribution of x values, which is particularly important for small data size. The bootstrap sample size was again 1000, but bootstrap fits were discarded if they did not successfully model a temperature dependence ($E_0 = 0$). On average 70% of the fits were successful. Using these, about 700 annual $R_{eco}$ models were calculated for each site. The medians of these models were in excellent agreement with the original models. 97.5% and 2.5% quantiles at each time point were used to construct confidence intervals of the time series. Confidence intervals of the annual sums were constructed in the same way.
3. Each $R_{eco}$ bootstrap fit was paired with a PAR correction bootstrap fit and based on these the NEE models were refitted for each site and measurement campaign. With these NEE fits, bootstrap of the residuals was conducted as described above. Again only successful fits (52 % on average) were used. The high number of failed fits results from the strong non-linearity of the NEE model and the relatively low number of data points at each measurement campaign. About 364,000 (700 × 520) annual models were calculated from the bootstrap parameter samples and confidence intervals constructed as described before.

### 2.5. $CH_4$ and $N_2O$ flux calculation

The following algorithm was used to calculate $CH_4$ and $N_2O$ fluxes:

1. Flux rates were calculated using ordinary linear regression, robust linear regression (Huber, 1981), and Hutchinson-Mosier regression (HMR; Pedersen et al., 2010).
2. For the standard case of 4 data points the flux calculated by robust linear regression was used per default. Only if the following conditions were met, the non-linear flux estimation (HMR) was used instead:
    a. the HMR function could be fitted,
    b. Akaike information criterion (AIC; Burnham and Anderson, 2004) was smaller for HMR fit than for linear fit,
    c. p-value of flux calculated using HMR was smaller than that from robust linear fit,
    d. and the flux calculated using HMR was not more than 4 times the flux from robust linear regression. This avoided severe overestimation of fluxes (see Figure S3-5 for an example).

3. Ordinary linear regression was applied for three data points. If less than three data points were available (due to loss of samples) no flux was calculated and the measurement discarded.

As a result 27 % of all $CH_4$ fluxes and 16% of all $N_2O$ fluxes were calculated non-linearly. Depicting square roots of the flux standard error (calculated from the regressions) in boxplots and histograms showed distributions relatively similar to normal distribution. Median standard errors were 12 µg $CH_4$-C $m^{-2}$ $h^{-1}$ and 3 µg $N_2O$-N $m^{-2}$ $h^{-1}$, which demonstrates a good accuracy of the flux measurements. Some extreme standard error values were detected. Associated flux values were considered carefully as potential outliers based on field and lab notes as well as the pattern of $CO_2$ concentrations. If the third or last $CO_2$ concentration was not plausible, e.g., lower than the previous one, the sample was deleted and linear regression applied. If an outlier occurred with $CH_4$ and $N_2O$ fluxes and not with $CO_2$, values were not corrected since $CH_4$ and $N_2O$ were often near ambient or near zero fluxes occurred.

Mean annual fluxes were calculated by linear interpolation between measurement campaigns.

### 2.6. Statistical analyses

R 2.15.2 (R Core R, 2012) was used for statistics and modeling. In particular, package *nlme* (package version 3.1.108; Pinheiro et al., 2013) was used for linear mixed-effects models.

## 3. Results

### 3.1. Driver variables

In the investigation period, daily mean value of the air temperature ranged from -14.8 to 23.5 °C and the 0.02 m soil temperatures were between -1.6 °C and 20.7 °C. Daily mean air temperature was below zero degrees Celsius during 27 days, while this was the case for soil temperature on 11 days (Fig. 3-1). A longer period of snow cover occurred during February 2012.

Groundwater levels (GWL) were within the peat layer at each site during different periods. At the driest sites ($C_{med}$ $W_{39}$ and $C_{low}$ $W_{29}$) GWLs were in the peat layer for 128 and 214 days, respectively. In contrast, sites $C_{low}$ $W_{14}$, $C_{high}$ $W_{22}$ and $C_{high}$ $W_{17}$ had a similar number of days with high water levels (304, 271 and 273, respectively) whereas at the wettest site ($C_{high}$ $W_{11}$) water levels were within the peat layer for the whole year. Groundwater levels above the surface occurred only on the wet sites ($C_{low}$ $W_{14}$, $C_{high}$ $W_{11}$, and $C_{high}$ $W_{17}$) during 83, 34, and 35 days, respectively. Longer periods of water saturation were observed on these sites during the winter season, whereas during the summer season few precipitation events caused short periods of flooding. Site $C_{high}$ $W_{11}$ showed the lowest

groundwater level dynamics whereas site $C_{med}$ $W_{39}$ had the highest groundwater level dynamics of all sites (Fig. S3-2 in the Supplement).

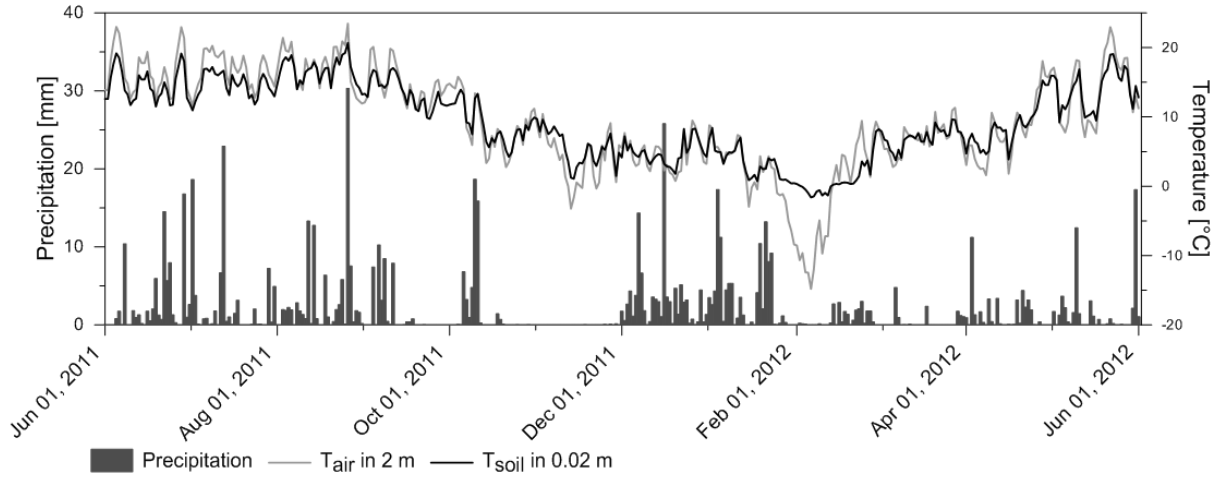


**Fig. 3 - 1**: Time series of precipitation, air, and 2cm soil temperature at meteorological station.

Mineral nitrogen stock was low on all sites (Tab. 3-1). The maximum value of 17 kg $ha^{-1}$ was found at site $C_{low}$ $W_{29}$ with the highest plant biomass, whereas the moss-dominated sites $C_{high}$ $W_{11}$, $C_{high}$ $W_{22}$ and $C_{high}$ $W_{17}$ contained the smallest $N_{min}$ stocks of 2 kg $ha^{-1}$. The $N_{min}$ differences between the sites were also reflected in vegetation composition and biomass amounts.

Plant species composition and vegetation cover were similar within one site whereas vegetation showed clear differences between the individual sites (Tab. 3-2). Sites where the histic horizon was mixed with sand, or the mean annual water table was below about 20 cm, had high abundance of grasses and moderate productivity. Sphagnum and other mosses were present on sites with high $C_{org}$ and little drainage, where productivity was low. In detail, $C_{med}$ $W_{39}$, $C_{low}$ $W_{29}$ and $C_{low}$ $W_{14}$ were dominated by sedges and grasses in different levels and without any moss occurrence, which is also reflected in the highest biomass exports (1.7 to 2.9 t $ha^{-1}$ $a^{-1}$; three grazing events and one mulching event) in comparison to the other sites. In contrast, $C_{high}$ $W_{11}$, $C_{high}$ $W_{22}$ and $C_{high}$ $W_{17}$ had high moss abundance and a lower grass and sedge biomass. The biomass export on these sites was only in the range of 0.3 to 0.6 t $ha^{-1}$ $a^{-1}$ during one grazing and one mulching event.

### 3.2. $CO_2$

Gross primary production on sites $C_{med}$ $W_{39}$, $C_{low}$ $W_{29}$ and $C_{low}$ $W_{14}$ was about 12 t C $ha^{-1}$ $a^{-1}$, whereas on sites $C_{high}$ $W_{11}$, $C_{high}$ $W_{22}$ and $C_{high}$ $W_{17}$ GPP was about 6 t C $ha^{-1}$ $a^{-1}$ (Tab. 3-3), reflecting the difference of biomass productivity and nitrogen content between the different sites (Tab. 3-2 and 3-1).

**Table 3 - 2**: Biomass export from sites (June 1, 2011 to June 1, 2012; site mean value ± one standard deviation between replicate plots) and cover of sedges, grasses and mosses.

| Site[a] | Mg C $ha^{-1}$ $a^{-1}$ | kg N $ha^{-1}$ $a^{-1}$ | sedge cover [%][b] | grass cover [%][b] | moss cover [%][b] |
|---|---|---|---|---|---|
| $C_{med}$ $W_{39}$ | 2.26 ± 0.10 | 95 ± 3 | 10 | 70 | 0 |
| $C_{low}$ $W_{29}$ | 2.92 ± 0.14 | 138 ± 7 | 0 | 90 | 0 |
| $C_{low}$ $W_{14}$ | 1.69 ± 0.28 | 68 ± 10 | 55 | 15 | 0 |
| $C_{high}$ $W_{11}$ | 0.28 ± 0.03 | 8 ± 1 | 35 | 25 | 95 |
| $C_{high}$ $W_{22}$ | 0.57 ± 0.04 | 19 ± 2 | 15 | 65 | 65 |
| $C_{high}$ $W_{17}$ | 0.39 ± 0.02 | 14 ± 1 | 50 | 20 | 75 |

[a] Subscripts in site designations refer to low (<15%), medium (15-35%) or high (>35%) soil C content and mean annual water table depth (cm).

[b] Cover values are indicated nearest to 5 %. Since the cover of grasses, sedges and mosses is observed separately and species can overlap, the total plot cover can exceed 100 %.

During the vegetation period plant growth influenced NEE budgets of all sites, which as a result became $CO_2$ sinks as well as $CO_2$ sources over the course of the year (especially right after grazing). From October until March NEE fluxes were on a low level on all sites and they were dominated by $R_{eco}$ since GPP was near zero on all sites (Fig. 3-2).

$C_{med}$ $W_{39}$, $C_{low}$ $W_{29}$ and $C_{low}$ $W_{14}$ showed a similar time series (Fig. 3-2). However, in spring and summer GPP gradually decreased from $C_{low}$ $W_{29}$ to $C_{med}$ $W_{39}$ and $C_{low}$ $W_{14}$. This is in line with the productivity differences of grass and sedge species on the respective sites. $C_{high}$ $W_{11}$, $C_{high}$ $W_{22}$ and $C_{high}$ $W_{17}$ also feature similar time series. Though in spring and summer GPP of site $C_{high}$ $W_{22}$ was larger than on sites $C_{high}$ $W_{17}$ and $C_{high}$ $W_{11}$, these three sites had nearly identical annual GPP fluxes. GPP is in line with the different productivity of grass and sedge vs. moss species (Tab. 3-2).

Ecosystem respiration of sites $C_{med}$ $W_{39}$, $C_{low}$ $W_{29}$ and $C_{low}$ $W_{14}$ (about 18 t C $ha^{-1}$ $a^{-1}$) was nearly twice as high as of sites $C_{high}$ $W_{11}$, $C_{high}$ $W_{22}$ and $C_{high}$ $W_{17}$ (10 t C $ha^{-1}$ $a^{-1}$). This again reflects the vegetation differences. The same trends were found between the sites as before for GPP. This leads to the assumption that plant respiration was dominating $R_{eco}$ differences between the sites, which is confirmed by highly significant correlations between daily mean values of GPP and $R_{eco}$ for each site ($p < 2.2 \times 10^{-16}$, mean $R^2$ 0.64 for all sites).

All of the sites in the Grosses Moor were both source and sink of $CO_2$ at different times with some clear annual NEE trends (Fig. 3-2). $C_{med}$ $W_{39}$, $C_{low}$ $W_{29}$ and $C_{low}$ $W_{14}$ exhibited NEE values of about 5 t C $ha^{-1}$ $a^{-1}$ whereas sites $C_{high}$ $W_{11}$ and $C_{high}$ $W_{17}$ had a NEE of about 3 t C $ha^{-1}$ $a^{-1}$ only (Tab. 3-3). NEE of site $C_{high}$ $W_{22}$ was between the two groups. Differences between sites in annual NEE were less prominent than for GPP and $R_{eco}$. Grass dominated sites, the sites with higher plant productivity, exhibited

higher NEE fluxes than sites containing predominantly mosses. However, low NEE fluxes occurred on all sites during the winter season because grasses were cut in autumn.

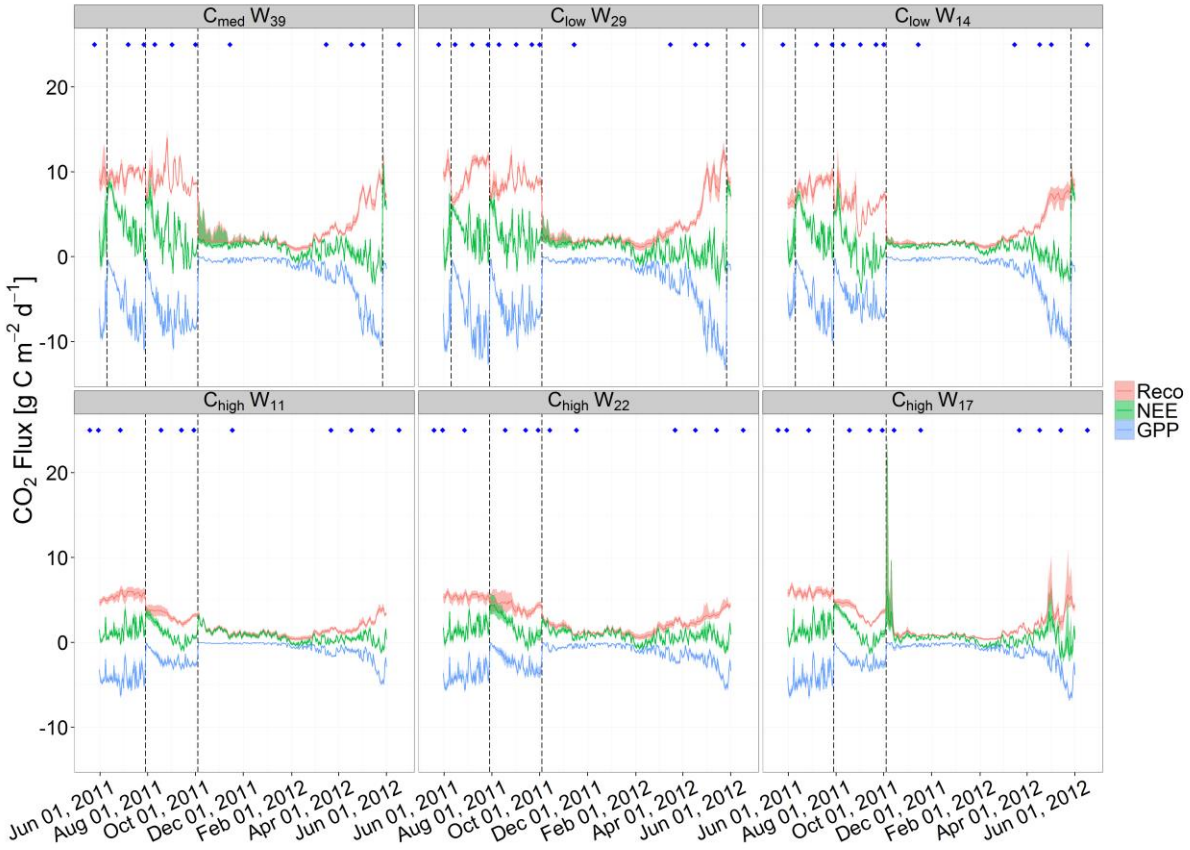


**Fig. 3 - 2**: Time series of daily $CO_2$ fluxes [g C $m^{-2}$ $d^{-1}$] at each site (June 1, 2011 - June 1, 2012). Depicted are modeled fluxes and 95% confidence band. Dashed lines indicate grazing and mulching events.

### 3.3. $CH_4$

$CH_4$ fluxes were on a low level with highest $CH_4$ emissions on site $C_{high}$ $W_{17}$ whereas site $C_{low}$ $W_{29}$ emitted the lowest amounts of $CH_4$ (Tab. 3-3) reflecting water level differences. Annual fluxes ranged from 3 to 203 kg C $ha^{-1}$ $a^{-1}$ and therefore all sites represented small sources. Strongest $CH_4$ emissions occurred during periods with high water levels and warm temperatures (Figure S3-6A in the Supplement).

**Table 3 - 3**: Annual fluxes of NEE, Reco and GPP, $CH_4$ and $N_2O$ (June 1, 2011 to June 1, 2012; annual flux ± uncertainty*).

| Site[a] | NEE [Mg C $ha^{-1}$ $a^{-1}$] | Reco [Mg C $ha^{-1}$ $a^{-1}$] | GPP [Mg C $ha^{-1}$ $a^{-1}$] | $CH_4$ [Mg C $ha^{-1}$ $a^{-1}$] | $N_2O$ [kg N $ha^{-1}$ $a^{-1}$] |
|---|---|---|---|---|---|
| $C_{med}$ $W_{39}$ | 6.3 ± 0.4 | 18.6 ± 0.4 | -12.3 ± 0.2 | 0.003 ± 0.003 | 1.09 ± 0.17 |
| $C_{low}$ $W_{29}$ | 5.7 ± 0.4 | 19.7 ± 0.4 | -14.0 ± 0.3 | -0.003 ± 0.003 | 1.40 ± 0.23 |
| $C_{low}$ $W_{14}$ | 4.9 ± 0.3 | 15.4 ± 0.3 | -10.5 ± 0.2 | 0.104 ± 0.030 | 0.98 ± 0.16 |
| $C_{high}$ $W_{11}$ | 3.0 ± 0.3 | 8.6 ± 0.3 | -5.6 ± 0.2 | 0.203 ± 0.067 | 0.51 ± 0.15 |
| $C_{high}$ $W_{22}$ | 3.9 ± 0.3 | 10.4 ± 0.3 | -6.5 ± 0.2 | 0.021 ± 0.009 | 0.50 ± 0.36 |
| $C_{high}$ $W_{17}$ | 3.2 ± 0.4 | 9.6 ± 0.3 | -6.5 ± 0.2 | 0.141 ± 0.037 | 0.66 ± 0.11 |

[a] Subscripts in site designations refer to low (<15%), medium (15-35%) or high (>35%) soil C content and mean annual water table depth (cm)

* Uncertainty values represent the accumulated measurement uncertainty and spatial heterogeneity, given for NEE, Reco and GPP as ± one standard deviation calculated by the Monte Carlo method, and for $CH_4$ and $N_2O$ as ± one standard deviation of the replicates.

### 3.4 $N_2O$

Only near zero $N_2O$ fluxes and no emission peaks occurred on any site. Annual fluxes ranged from 0.5 kg $N_2O$-N $ha^{-1}$ $a^{-1}$ to 1.4 kg $N_2O$-N $ha^{-1}$ $a^{-1}$ and were not significant ($p > 0.05$ according to a t-test with Bonferroni-adjustment for multiple testing; Figure S3-6B in the Supplement).

### 3.5 Annual C and GHG balance

Including the carbon from vegetation export (Tab. 3-2) and from $CH_4$ emissions (Tab. 3-3), the annual carbon balance of the sites was in the range of 3.5 to 8.8 t C $ha^{-1}$ $a^{-1}$ (Tab. 3-4, GWP-GHG balance).

Differences in the amount of exported carbon altered the ranking of sites according to their annual carbon and greenhouse gas balance compared to their NEE ranking. Sites $C_{low}$ $W_{29}$ and $C_{med}$ $W_{39}$ emitted more GHGs than site $C_{low}$ $W_{14}$. This indicates that higher productive sites emitted more GHGs. More distinct differences between the sites became apparent this way than if NEE was considered in isolation. The ranking of the sites according to their GHG balance did not change if $N_2O$ emissions were included (Tab. 3-4).

**Table 3 - 4**: Global warming potential for a time horizon of 100 years (GWP100) of Net C balance (NEE plus harvest), $CH_4$ and $N_2O$ and total GHG balance (annual flux ± uncertainty*; IPCC 2007).

| Site[a] | GWP100-C balance [Mg $CO_2$-C eq. $ha^{-1}$ $a^{-1}$] | GWP100-$CH_4$ [Mg $CO_2$-C eq. $ha^{-1}$ $a^{-1}$] | GWP100-$N_2O$ [Mg $CO_2$-C eq. $ha^{-1}$ $a^{-1}$] | GWP100-GHG balance [Mg $CO_2$-C eq. $ha^{-1}$ $a^{-1}$] |
|---|---|---|---|---|
| $C_{med}$ $W_{39}$ | 8.5 ± 0.4 | 0.003 ± 0.003 | 0.146 ± 0.023 | 8.7 ± 0.4 |
| $C_{low}$ $W_{29}$ | 8.6 ± 0.4 | -0.003 ± 0.003 | 0.188 ± 0.030 | 8.8 ± 0.4 |
| $C_{low}$ $W_{14}$ | 6.6 ± 0.4 | 0.104 ± 0.030 | 0.131 ± 0.021 | 6.8 ± 0.4 |
| $C_{high}$ $W_{11}$ | 3.3 ± 0.3 | 0.203 ± 0.067 | 0.068 ± 0.020 | 3.5 ± 0.3 |
| $C_{high}$ $W_{22}$ | 4.5 ± 0.3 | 0.021 ± 0.009 | 0.067 ± 0.049 | 4.6 ± 0.3 |
| $C_{high}$ $W_{17}$ | 3.5 ± 0.4 | 0.141 ± 0.037 | 0.088 ± 0.015 | 3.8 ± 0.4 |

[a] Subscripts in site designations refer to low (<15%), medium (15-35%) or high (>35%) soil C content and mean annual water table depth (cm)

* Uncertainty values represent the accumulated measurement uncertainty and spatial heterogeneity, given for GWP 100-C as ± one standard deviation calculated by the Monte Carlo method, and for $CH_4$ and $N_2O$ as ± one standard deviation of the replicates. Uncertainty values of the GHG balance were derived using Gaussian error propagation.

# 4. Discussion

## 4.1. Magnitude of GHG fluxes

The $CO_2$ fluxes of the Grosses Moor are within the range of other studies in comparable German peatlands (e.g. Drösler, 2005) as well as in peatlands of northern latitudes (e.g. Alm et al., 1997; Bellisario et al., 1998). Similar NEE fluxes and biomass export were observed on drained permanent grassland in Denmark (Elsgaard et al., 2012). In comparison to further German grassland sites on organic soils, emissions of the Grosses Moor are in the upper range of all considered GHG balances (Fig. 3-3; Drösler et al., 2013).

Low $CH_4$ emissions similar to those from the dry sites ($C_{med}$ $W_{39}$ and $C_{low}$ $W_{29}$) were reported by Drösler (2005) for a dry, peat cut heath. The two sites with the highest fluxes ($C_{high}$ $W_{11}$ and $C_{high}$ $W_{17}$) are in the lower third of average emission rates of 5-80 mg $CH_4$-C $m^{-2}$ $d^{-1}$ given by Blodau (2002) for natural peatlands. Comparable low $CH_4$ fluxes were found in three drained Danish peatlands, increasing with higher cover of plants with aerenchymatic tissues (Schäfer et al., 2012). Also in the Grosses Moor, sites with a higher cover of sedges (Tab. 3-3) emitted more $CH_4$. Because of their aerenchymatic tissue, which channels $CH_4$ fluxes from soil, sedges prevent $CH_4$ from further oxidation by soil microbes (Thomas et al., 1996). Low water levels during warm periods can result in oxidation of $CH_4$ by methanothrophic bacteria to $CO_2$ in the aerated soil zone, thereby increasing respiration

(Lai, 2009). According to Blodau (2002) large root density can increase $CH_4$ oxidation which results in low $CH_4$ emission rates at the soil surface. The $CH_4$ emission patterns observed at the Grosses Moor are in accordance with these mechanisms.

Low $N_2O$ values as in the Grosses Moor were reported for a dry peat cutting area by Drösler (2005). In soils with C/N ratios above 25 (Tab. 3-1), low $N_2O$ emissions can be expected (Klemedtsson et al., 2005). Other drained peatlands with permanent grass cover but deeper peat layer emitted even lower amounts of $N_2O$ (Petersen et al., 2012). The Grosses Moor reacts like nutrient-poor bogs with regard to $N_2O$.

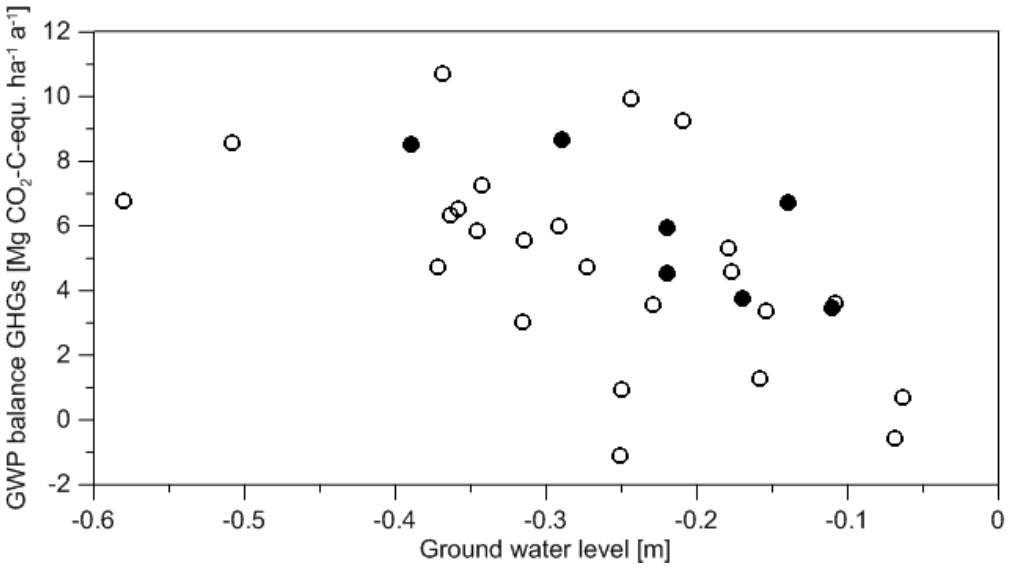


**Fig. 3 - 3**: Annual GHG balances vs. water table level of shallow peat sites in the Grosses Moor (filled circles) and several deep peat grassland sites (open circles) in Germany (Drösler et al. 2013).

### 4.2. Precision of the annual $CO_2$ budget

Our error analysis is based in principle on the bootstrap approach and error propagation using Monte-Carlo simulation. Resulting confidence intervals, which include measurement error as well as on-site heterogeneity, were overall relatively narrow (Fig. 3-2). However, the interpolation between the measurement campaigns could constitute a significant additional source of error. The calibration of temperature and PAR models by frequent campaigns captures effects of changing water table and biomass. But for interpolation between campaigns we assume a linear change from one calibration to the next one. With the available data it was not possible to quantify the interpolation error in the error analysis. The interpolation error could be quantified by very frequent measurement campaigns with automated chambers. We used measurement campaigns, which did not result in adequate model fits, for validating the interpolation. The $CO_2$ fluxes of the validation campaigns were well

described by the models so that we can conclude that the interpolation is relatively robust (Fig. S3-4 in the Supplement).

Most of the $CO_2$ measurement campaigns covered the full range of temperature and radiation for the interpolation so that the model error remained low for most of the time and the method was robustly applied. There were few periods (< 5 days in summer and < 47 days in winter) for which temperature was continuously outside the temperature range of at least one of the adjacent campaign days. These periods are characterized by higher model uncertainty due to extrapolation of the $R_{eco}$ fits (Fig. 3-2).

Our NEE error estimates (about ± 0.4 Mg C $ha^{-1}$ $yr^{-1}$) without interpolation error were at the low end of error estimates for eddy covariance measurements, for which errors in the range of ± 0.3 to ± 1.8 Mg C $ha^{-1}$ $yr^{-1}$ (Woodward and Lomas, 2004) or higher (Kruijt et al., 2004) have been reported. We expect that the error of the chamber based approach with interpolation error is likely to be comparable with eddy covariance. Thus, the chamber technique with model-based $CO_2$ flux interpolation is a reliable method for studying small-scale heterogeneity and sites where eddy covariance is not applicable.

### 4.3. $C_{org}$ effects

The GHG fluxes of the histic grasslands of the Grosses Moor are in the upper range of German managed grassland sites on organic soils with deep peat layers (Fig.3-3; Drösler et al., 2013). This is opposite to our expectation of lower GHG emissions from soil with shallow histic layers, in which less soil organic carbon is exposed to mineralization by drainage than in soils with deep peat layers. Obviously, the substrate quality and decomposition level of the peat play a larger role on emission rates (Berglund and Berglund, 2011) than peat depth. Our results are in accordance with Reiche et al. (2010) who did not find a clear relationship for the prediction of $CO_2$ and $CH_4$ production rates under anoxic conditions in dependence of the degree of humification.

We defined the effective C stock as the fraction of aerated carbon in the soil profile. Effective C stock showed no effect on GHG emissions. Moreover no significant correlation was found between $C_{org}$ concentration in the topsoil and GHG emissions (Fig. 3-4A).

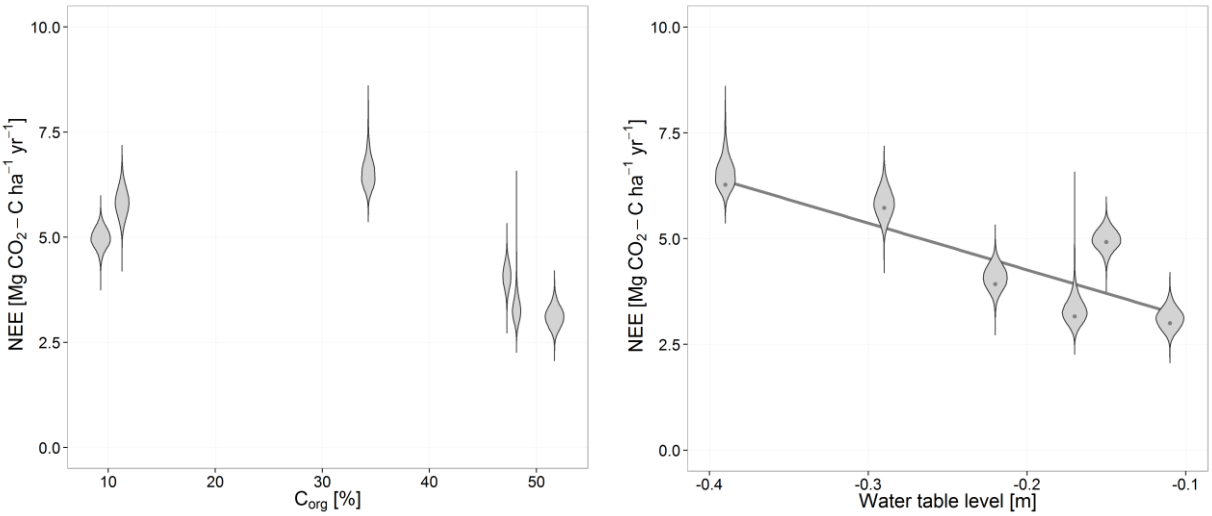


**Fig. 3 - 4**: Violin plots of NEE emissions vs. $C_{org}$ (A; $R^2$=0.49, p= 0.121) and NEE emissions vs. water table level (B; $R^2$=0.71, p= 0.035). Violins (A, B): distribution of all simulated aggregated annual NEE sums of each site; points (B): modeled annual NEE of each site, used as basis for linear regression.

All sites exhibited highly degraded (H10 on the Van-Post scale; AG Boden, 2005), amorphous organic material in the peat layer (0 to 0.3 m). The sand intermixture ($C_{med}$ $W_{39}$, $C_{low}$ $W_{29}$ and $C_{low}$ $W_{14}$) resulted in yield increase via harvested biomass (Tab. 3-2) instead of $C_{org}$ stabilization on the mineral phase. We therefore reject our hypothesis that peat mixed with mineral subsoil and resulting lower $C_{org}$ concentration emits lower amounts of GHG than unmixed peat soil with a high $C_{org}$ concentration.

Mixing peat with sand has been a widespread soil management practice to improve the suitability of peat soils for agriculture (Göttlich, 1990) and is still practiced today. Our findings suggest that peat mixing does not mitigate GHG emissions from high organic carbon soils.

This finding has serious consequences for regional to national GHG balances because histic Gleysols are relatively widespread. Due to a lack of data, shallow or mixed organic soils such as histic Gleysols, which do not fall under the definition of Histosols but do fall under the definition of organic soils of IPCC (IPCC, 2006), tended to be neglected as source of GHGs in national GHG inventories under the UNFCCC or estimated to emit half of the annual $CO_2$ emissions of real Histosols (Nielsen et al., 2012). Adding histic Gleysols to the Histosol area, the land area with GHG emission hotspots due to drainage is likely to be much larger than anticipated.

### 4.4. Water level effects

The variation between measurement campaigns showed that GPP was not significantly influenced by water levels but mainly by radiation. This was also reported by Lindroth et al. (2007).
Water levels had a strong influence on $R_{eco}$ fluxes (p=0.0004, correlation between both: $R^2$=0.91; Fig. 3-5) as analyzed by a linear mixed-effect model (Table S3-1 in the Supplement). A strong correlation between water table and $CO_2$ emissions was also observed by Silvola et al. (1996) and Berglund and Berglund (2011).

Annual NEE budgets were positively correlated to mean annual water table levels (Fig. 3-4B). Peat mineralization generally increases linearly when the water table lowers (Dinsmore et al., 2009). Our study confirms this linear relationship between ecosystem respiration and water table level on a daily time scale (Fig. 3-5) and it could even be observed in net ecosystem exchange on an annual time scale (Fig. 3-4B). The increase in heterotrophic respiration may level off in dry conditions when the water table falls below the peat layer, and little extra SOC from deeper soil is exposed to aerobic conditions. On our sites, however, there was no significant difference in the relation between $R_{eco}$ and water table when water levels were in the peat or the in subjacent sand layer. Only the water table level and the depth of the aerated soil zone affected $R_{eco}$ but not the effective aerobic SOC stock although water table sometimes dropped to -30 cm below the peat layer. Consequently, peat mineralization seems to be driven by soil moisture in the topsoil rather than by peat layer depth. Deeper water levels result in drier topsoil, which is hence faster mineralized.

We confirm our hypothesis that GHG emissions of histic Gleysols (mainly $CO_2$) increase linearly with drainage depth but reject our hypothesis that $CO_2$ emissions level off when the water table falls below the peat layer.

Histic Gleysols are frequently subject to deep drainage for agriculture. Moreover, histic Gleysols tend to be more intensively used for agriculture than Histosols due to more suitable soil physical and chemical properties. Our study suggests that deeply drained histic Gleysols could be much stronger sources of GHGs than expected.

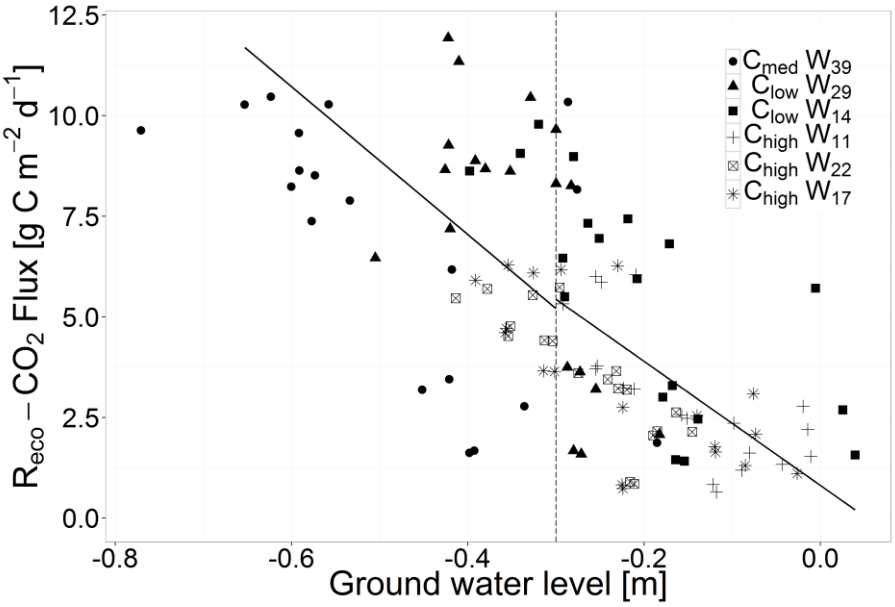


**Fig. 3 - 5**: Ground water levels [m] vs. $R_{eco}$-$CO_2$ Flux [g C $m^{-2}$ $d^{-1}$] on the campaign dates for all six sites. Dotted vertical line: border of peat horizon; continuous line: population mean prediction from the linear mixed effects model for all sites; a fixed effect was used to distinguish water levels below the peat horizon (-0.8 to -0.3 m) and within the peat horizon (-0.3 to +0.1 m).

### 4.5. Vegetation effects

Differences in vegetation composition and biomass amounts were reflected in GPP amounts (Fig. 3-2). $R_{eco}$ is not only affected by temperature, which is very similar for all sites, but also by plant biomass, which differs between sites. The assumption that plant respiration was dominating $R_{eco}$ differences between the sites is confirmed by highly significant correlations between daily mean values of GPP and $R_{eco}$ for each site ($p < 2.2 \times 10^{-16}$, mean $R^2 = 0.64$ for all sites). However, since the ratio of the annual $R_{eco}$ to GPP was almost the same on all sites (mean value of 1.5 ± 0.07; Tab. 3-3), the influence of the vegetation on NEE of the different sites can be ruled out. Therefore, differences in NEE can be attributed to varying microbial activity as well as carbon degradation differences between the individual sites.

The C balance of all sites was clearly affected by harvest / grazing. Carbon export was as important as NEE for the annual C balance, especially on sites with high grass biomass (up to 30 percent of the C balance for site $C_{low}$ $W_{29}$). In Danish permanent grassland sites, yield export had a similar contribution to the C balance as in the Grosses Moor (Elsgaard et al., 2012).

## 5. Conclusions

We showed that GHG emissions of histic Gleysols (mainly $CO_2$) increase linearly with drainage depth and do not level off when the water table falls below the peat level. Drained histic Gleysols are GHG hotspots, which have so far been neglected or underestimated.

Grasslands on histic Gleysols emit as many GHGs as grasslands on Histosols. This confirms the wide definition of organic soils for use in GHG emission inventories by IPCC (IPCC, 2006). Since shallow histic Gleysols emit as much $CO_2$ as deep peat soils, they should be integrated in the national and international definitions of Histosols in terms of climate relevant carbon sources.

Peat mixed with mineral subsoil and Corg concentration around 10% emits as much GHG as unmixed peat soil (>30% $C_{org}$). This implies that peat mixing with underlying sand is not a GHG mitigation option.

**Acknowledgments**

- The joint research project “Organic soils” funded by the Thünen Institute and its twelve participating research institutes aims at closing the data gap by monitoring emissions from eleven catchments in Germany. Various peatlands, differing in preservation and utilization, are investigated in order to derive specific emission factors.
- HU Berlin, especially N. Rosskopf, for soil identification and soil properties
- M. Hunziger and D. Olbrich for help during the measurement campaigns and in the lab
- K. Gilke, R. Lausch, A Oehns-Rittgerodt for laboratory assistance
- S. Belting for plant species knowledge
- DWD for climate data of stations Braunschweig, Uelzen, Wittingen-Vorhop and Wolfsburg (Südwest).
- Schäferei Paulus and Herr Horny for research permission
- the peat group of the Thünen Institute of Climate-Smart Agriculture (B. Tiemeyer, E. Frahm, U. Dettmann, S. Frank, M. Bechtold, T. Leppelt) for discussion

## 6. References

AG Boden, 2005. Bodenkundliche Kartieranleitung (German soil mapping guide) - KA5. Bundesanstalt für Geowissenschaften und Rohstoffe in Zusammenarbeit mit den Staatlichen Geologischen Diensten, Hannover. 438 pp.

Alm, J., Shurpali, N. J., Tuittila, E.-S., Laurila, T., Maljanen, M., Saarnio, S., Minkkinen, K., 2007. Methods for determining emission factors for the use of peat and peatlands - flux measurements and modelling. Boreal Environment Research 12, 85-100.

Alm, J., Talanov, A., Saarnio, S., Silvola, J., Ikkonen, E., Aaltonen, H., Nykanen, H., Martikainen, P. J., 1997. Reconstruction of the carbon balance for microsites in a boreal oligotrophic pine fen, Finland. Oecologia 110, 423-431.

Beetz, S., Liebersbach, H., Glatzel, S., Jurasinski, G., Buczko, U., Hoeper, H., 2013. Effects of land use intensity on the full greenhouse gas balance in an Atlantic peat bog. Biogeosciences 10, 1067-1082.

Bellisario, L.M., Moore, T.R., Bubier, J.L., 1998. Net ecosystem $CO_2$ exchange in a boreal peatland, northern Manitoba. Ecoscience 5, 534-541.

Berglund, O., Berglund, K., 2011. Influence of water table level and soil properties on emissions of greenhouse gases from cultivated peat soil. Soil Biology & Biochemistry 43, 923-931.

Blodau, Christian, 2002. Carbon cycling in peatlands: A review of processes and controls. Environmental Reviews 10, 111-134.

Burnham, K. P., Anderson, D. R., 2004. Multimodel Inference: Understanding AIC and BIC in Model Selection. Sociological Methods & Research 33, 261-304.

Dinsmore, K. J., Skiba, U. M., Billett, M. F., Rees, R. M., 2009. Effect of water table on greenhouse gas emissions from peatland mesocosms. Plant and Soil 318, 229-242.

Don, A., Rödenbeck, C., Gleixner, G., 2013. Unexpected control of soil carbon turnover by soil carbon concentration. Environmental Chemistry Letters 11, 407-413.

Drösler, M., 2005. Trace gas exchange and climatic relevance of bog ecosystems, Southern Germany. Dissertation, TUM München.

Drösler, M., Adelmann, W., Augustin, J., Bergmann, L., Beyer, C., Chojnicki, B., Förster, C., Freibauer, A., Giebels, M., Görlitz, S., Höper, H., Kantelhardt, J., Liebersbach, H., Hahn-Schöfl, M., Minke, M., Petschow, U., Pfadenhauer, J., Schaller, L., Schägner, P., Sommer, M., Thuille, A., Wehrhan, M. , 2013. Klimaschutz durch Moorschutz. Schlussbericht des Vorhabens "Klimaschutz - Moorschutzstrategien" 2006-2010. 201 pp.

Drösler, M., Freibauer, A., Christensen, T. R., Friborg, T. , 2008. Observations and status of peatland greenhouse gas emissions in Europe, In: Dolman, A.J., Freibauer, A., Valentini, R. (Ed.), The continental-scale greenhouse gas balance of Europe. Springer, New York, 243-261.

Efron, B., 1979. Bootstrap methods: Another look at the jackknife. Ann. Statist. 7, 1-26.

Elsgaard, L., Gorres, C.-M., Hoffmann, C. C., Blicher-Mathiesen, G., Schelde, K., Petersen, S. O., 2012. Net ecosystem exchange of $CO_2$ and carbon balance for eight temperate organic soils under agricultural management. Agriculture Ecosystems & Environment 162, 52-67.

Falge, E., Baldocchi, D., Olson, R., Anthoni, P., Aubinet, M., Bernhofer, C., Burba, G., Ceulemans, R., Clement, R., Dolman, H., Granier, A., Gross, P., Grunwald, T., Hollinger, D., Jensen, N. O., Katul, G., Keronen, P., Kowalski, A., Lai, C. T., Law, B. E., Meyers, T., Moncrieff, H., Moors, E., Munger, J. W., Pilegaard, K., Rannik, U., Rebmann, C., Suyker, A., Tenhunen, J., Tu, K., Verma, S., Vesala, T., Wilson, K., Wofsy, S., 2001. Gap filling strategies for defensible annual sums of net ecosystem exchange. Agricultural and Forest Meteorology 107, 43-69.

Göttlich, K., 1990. Moor- und Torfkunde. E. Schweizerbart'sche Verlagsbuchhandlung (Nägele und Obermiller), Stuttgart, 529 pp.

HBU, 1998. Handbook of soil analyses (HBU), Soil quality - Determination of dry bulk density Beuth Verlag GmbH, Berlin, p. 10.

HBU, 2005. Handbook of soil analyses (HBU), Soil quality - Determination of pH. Beuth Verlag GmbH, Berlin, p. 9.

Huber, P. J., 1981. Robust Statistics. J. Wiley, New York.

IPCC, 2006. Guidelines for National Greenhouse Gas Inventories.Chapter 3: Consistent Representation of Lands. 42 pp.

Klemedtsson, L., von Arnold, K., Weslien, P., Gundersen, P., 2005. Soil CN ratio as a scalar parameter to predict nitrous oxide emissions. Global Change Biology 11, 1142-1147.

Kottek, M., Grieser, J., Beck, C., Rudolf, B., Rubel, F., 2006. World Map of the Köppen-Geiger climate classification updated. Meteorologische Zeitschrift 15, 259-263.

Kruijt, B., Elbers, J. A., von Randow, C., Araujo, A. C., Oliveira, P. J., Culf, A., Manzi, A. O., Nobre, A. D., Kabat, P., Moors, E. J., 2004. The robustness of eddy correlation fluxes for Amazon rain forest conditions. Ecological Applications 14, S101-S113.

Lai, D. Y. F., 2009. Methane dynamics in northern peatlands: a review. Pedosphere 19, 409-421.

Limpens, J., Berendse, F., Blodau, C., Canadell, J. G., Freeman, C., Holden, J., Roulet, N., Rydin, H., Schaepman-Strub, G., 2008. Peatlands and the carbon cycle: from local processes to global implications - a synthesis. Biogeosciences 5, 1475-1491.

Lindroth, A., Lund, M., Nilsson, M., Aurela, M., Christensen, T. R., Laurila, T., Rinne, J., Riutta, T., Sagerfors, J., Stroem, L., Tuovinen, J.-P., Vesala, T., 2007. Environmental controls on the $CO_2$ exchange in north European mires. Tellus Series B-Chemical and Physical Meteorology 59, 812-825.

Lloyd, J., Taylor, J. A., 1994. On the temperature dependence of soil respiration. Functional Ecology 8, 315-323.

Londo, G., 1976. Decimal scale for releves of permanent quadrats. Vegetatio 33, 61-64.

Marschner, B., Brodowski, S., Dreves, A., Gleixner, G., Gude, A., Grootes, P. M., Hamer, U., Heim, A., Jandl, G., Ji, R., Kaiser, K., Kalbitz, K., Kramer, C., Leinweber, P., Rethemeyer, J., Schaeffer, A., Schmidt, M. W. I., Schwark, L., Wiesenberg, G. L. B., 2008. How relevant is recalcitrance for the stabilization of organic matter in soils? Journal of Plant Nutrition and Soil Science-Zeitschrift Fur Pflanzenernahrung Und Bodenkunde 171, 91-110.

Mikutta, R., Kleber, M., Torn, M.S., Jahn, R., 2006. Stabilization of Soil Organic Matter: Association with Minerals or Chemical Recalcitrance? Biogeochemistry 77, 25-56.

Montanarella, L., Jones, R. J. A., Hiederer, R., 2006. The distribution of peatland in Europe. Mires and Peat 1, 1-11.

Nielsen, O.-K., Mikkelsen, M.H., Hoffmann, L., Gyldenkærne, S., Winther,, M., Nielsen, M., Fauser, P., Thomsen, M., Plejdrup, M.S., Albrektsen, R., Hjelgaard,, K., Bruun, H.G., Johannsen, V.K., Nord-Larsen, T., Bastrup-Birk, A., Vesterdal, L.,, Møller, I.S., Rasmussen, E., Arfaoui, K., Baunbæk, L. & Hansen, M.G., 2012. Denmark's National Inventory Report 2012. Emission Inventories 1990-2010 - Submitted under the United Nations Framework Convention on Climate Change and the Kyoto Protocol. 1168 pp.

Oberdorfer, E., 2001. Pflanzensoziologische Exkursionsflora für Deutschland und angrenzende Gebiete, 8. Aufl ed. Verlag Eugen Ulmer, Stuttgart, 1051 pp.

Overbeck, Fritz, 1952. Das Große Moor bei Gifhorn im Wechsel hygrokliner und xerokliner Phasen der nordwestdeutschen Hochmoorentwicklung. [The "Großes Moor" near Gifhorn during the alternation of hygrocline and xerocline periods of the northwestern German peat bog development]. Walter Dorn Verlag, Bremen.

Pedersen, A. R., Petersen, S. O., Schelde, K., 2010. A comprehensive approach to soil-atmosphere trace-gas flux estimation with static chambers. European Journal of Soil Science 61, 888-902.

Petersen, S. O., Hoffmann, C. C., Schafer, C. M., Blicher-Mathiesen, G., Elsgaard, L., Kristensen, K., Larsen, S. E., Torp, S. B., Greve, M. H., 2012. Annual emissions of CH4 and N2O, and ecosystem respiration, from eight organic soils in Western Denmark managed by agriculture. Biogeosciences 9, 403-422.

Pinheiro, J., Bates, D., DebRoy, S., Sarkar, D., Team, R Development Core, 2013. Linear and nonlinear mixed effect models, R package version 3.1-108. ed.

R Core Team 2012. R: A language and environment for statistical computing. R Foundation for Statistical Computing, Vienna, Austria. http://www.R-project.org/

Reiche, M., Gleixner, G., Küsel, K., 2010. Effect of peat quality on microbial greenhouse gas formation in an acidic fen. Biogeosciences 7, 187-198.

Richter, A., 1998. Bodenübersichtskarte der Bundesrepublik Deutschland - BÜK 1000 (Soil survey map), Bundesanstalt für Geowissenschaften und Rohstoffe (BGR), 2. Aufl. ed.

Rousseeuw, P., Croux, C., Todorov, V., Ruckstuhl, A., Salibian-Barrera, M., Verbeke, T., Koller, M., Maechler, M., 2012. robustbase: Basic Robust Statistics, R package version 0.9-4. ed.

Schäfer, C. M., Elsgaard, L., Hoffmann, C. C., Petersen, S. O., 2012. Seasonal methane dynamics in three temperate grasslands on peat. Plant and Soil 357, 339-353.

Schrier-Uijl, A. P., Kroon, P. S., Hensen, A., Leffelaar, P. A., Berendse, F., Veenendaal, E. M., 2010. Comparison of chamber and eddy covariance-based $CO_2$ and $CH_4$ emission estimates in a heterogeneous grass ecosystem on peat. Agricultural and Forest Meteorology 150, 825-831.

Silvola, J., Alm, J., Ahlholm, U., Nykanen, H., Martikainen, P. J., 1996. CO2 fluxes from peat in boreal mires under varying temperature and moisture conditions. Journal of Ecology 84, 219-228.

Smith, K. A., Conen, F., 2004. Impacts of land management on fluxes of trace greenhouse gases. Soil Use and Management 20, 255-263.

Thomas, K. L., Benstead, J., Davies, K. L., Lloyd, D., 1996. Role of wetland plants in the diurnal control of $CH_4$ and $CO_2$ fluxes in peat. Soil Biology & Biochemistry 28, 17-23.

UBA, 2012. National Inventory Report for the German Greenhouse Gas Inventory 1990 – 2010. Submission under the United Nations Framework Convention on Climate Change and the Kyoto Protocol 2012. Dessau, Germany, 827 pp.

VDLUFA, 1997. Bestimmung von mineralischem (Nitrat-)Stickstoff in Bodenprofilen (Nmin-Labormethode), In: VDLUFA (Ed.), Methodenbuch Teil 2, Speyer, Germany.

Woodward, F. I., Lomas, M. R., 2004. Vegetation dynamics - simulating responses to climatic change. Biological Reviews 79, 643-670.

WRB, 2008. World Reference Base for Soil Resources 2006. Ein Rahmen für internationale Klassifikation, Korrelation und Kommunikation., Deutsche Ausgabe ed. Bundesanstalt für Geowissenschaften und Rohstoffe, Hannover, 148 pp.

# 7. Supplement

**Table S3 - 1**: Linear mixed-effects model of $R_{eco}$ vs. Water table.

```
Linear mixed-effects model fit by REML
 Data: Dat
      AIC      BIC    logLik
  475.256 496.8599 -229.628

Random effects:
 Formula: ~WTpeat | site
 Structure: General positive-definite, Log-Cholesky parametrization
            StdDev    Corr
(Intercept) 2.256385 (Intr)
WTpeatTRUE  2.409026 -0.896
Residual    1.748395

Fixed effects: Reco ~ WT * WTpeat
                    Value Std.Error  DF   t-value p-value
(Intercept)     -0.307262  1.705472 105 -0.180163  0.8574
WT             -18.378873  3.385580 105 -5.428574  0.0000
WTpeatTRUE       1.119596  1.826929 105  0.612829  0.5413
WT:WTpeatTRUE    2.969354  4.246360 105  0.699270  0.4859
 Correlation:
               (Intr) WT     WTTRUE
WT              0.787
WTpeatTRUE     -0.922 -0.733
WT:WTpeatTRUE -0.628 -0.796  0.752

Standardized Within-Group Residuals:
         Min           Q1          Med           Q3          Max
-2.571112023 -0.514414249 -0.005306694  0.612438896  2.697319770

Number of Observations: 114
Number of Groups: 6
```

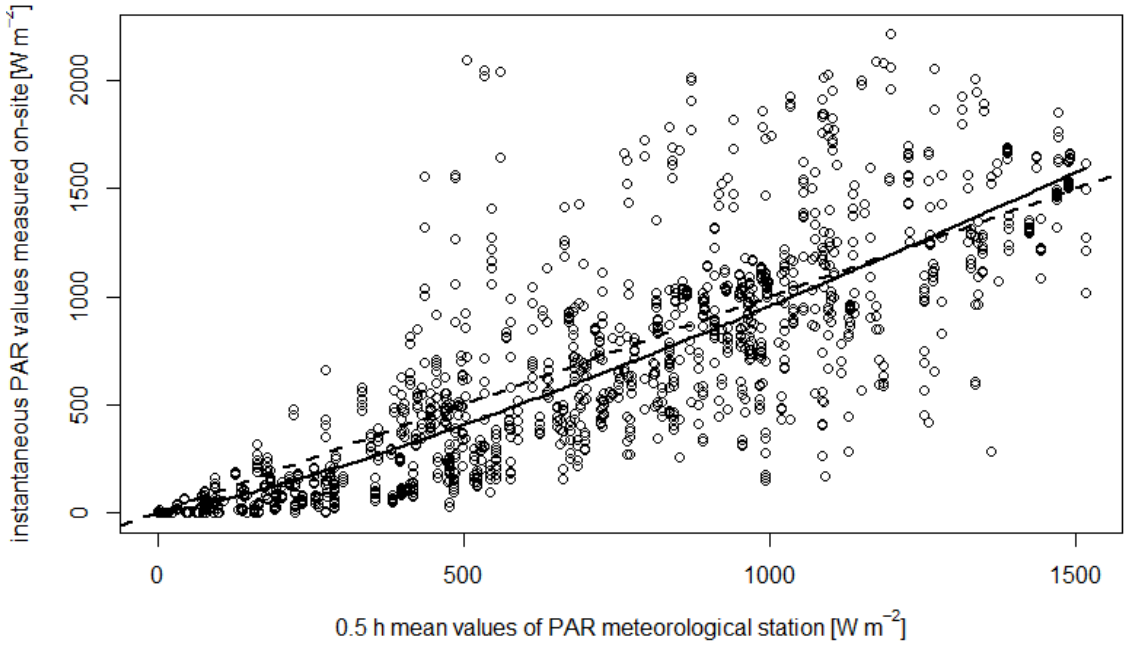


**Fig. S3 - 1**: PAR correction for site $C_{med}$ $W_{low}$, $C_{low}$ $W_{low}$ and $C_{low}$ $W_{high}$ at a distance of 50 metres from the tree line. Dashed line = 1:1 line, continuous line = correction function $PAR = \alpha * PAR_{station}^{\beta}$.

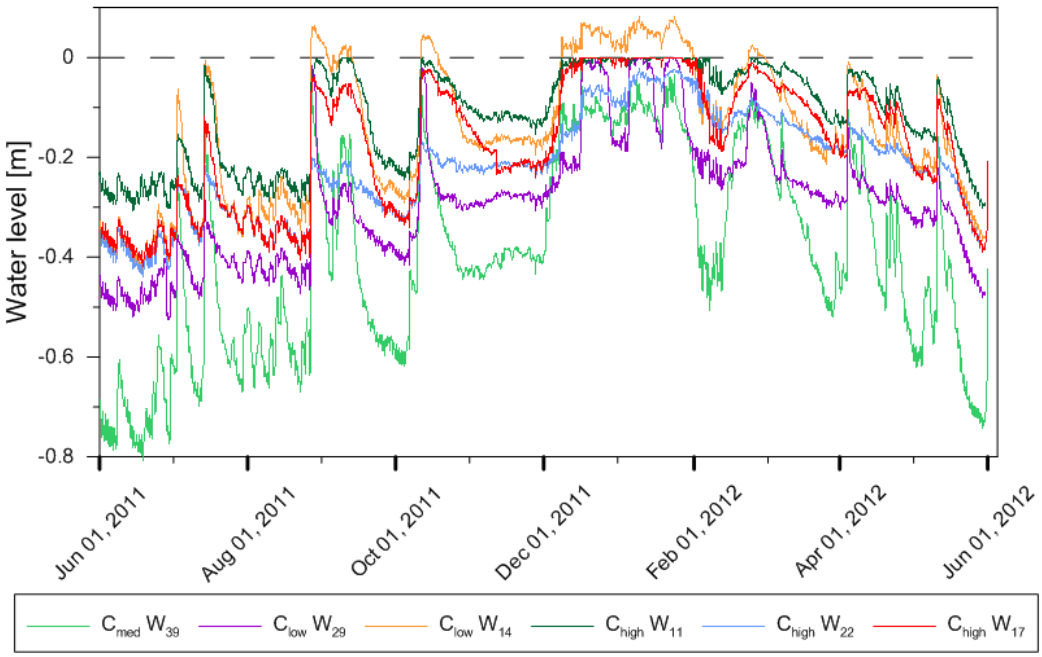


**Fig. S3 - 2**: Time series of water table levels at each site (June 1, 2011 to June 1, 2012).

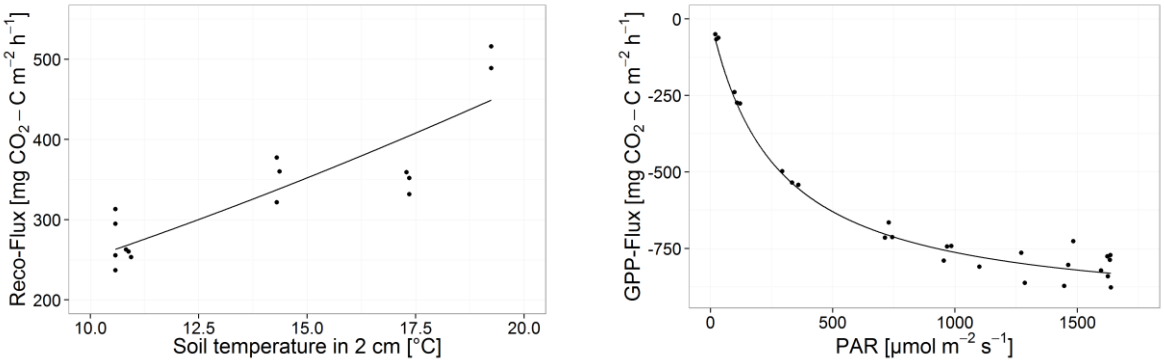


**Fig. S3 - 3**: $R_{eco}$ flux model (A) and GPP flux model (B) of an exemplary measurement campaign (02 May 2012) showing measured data as dots and fits as lines.

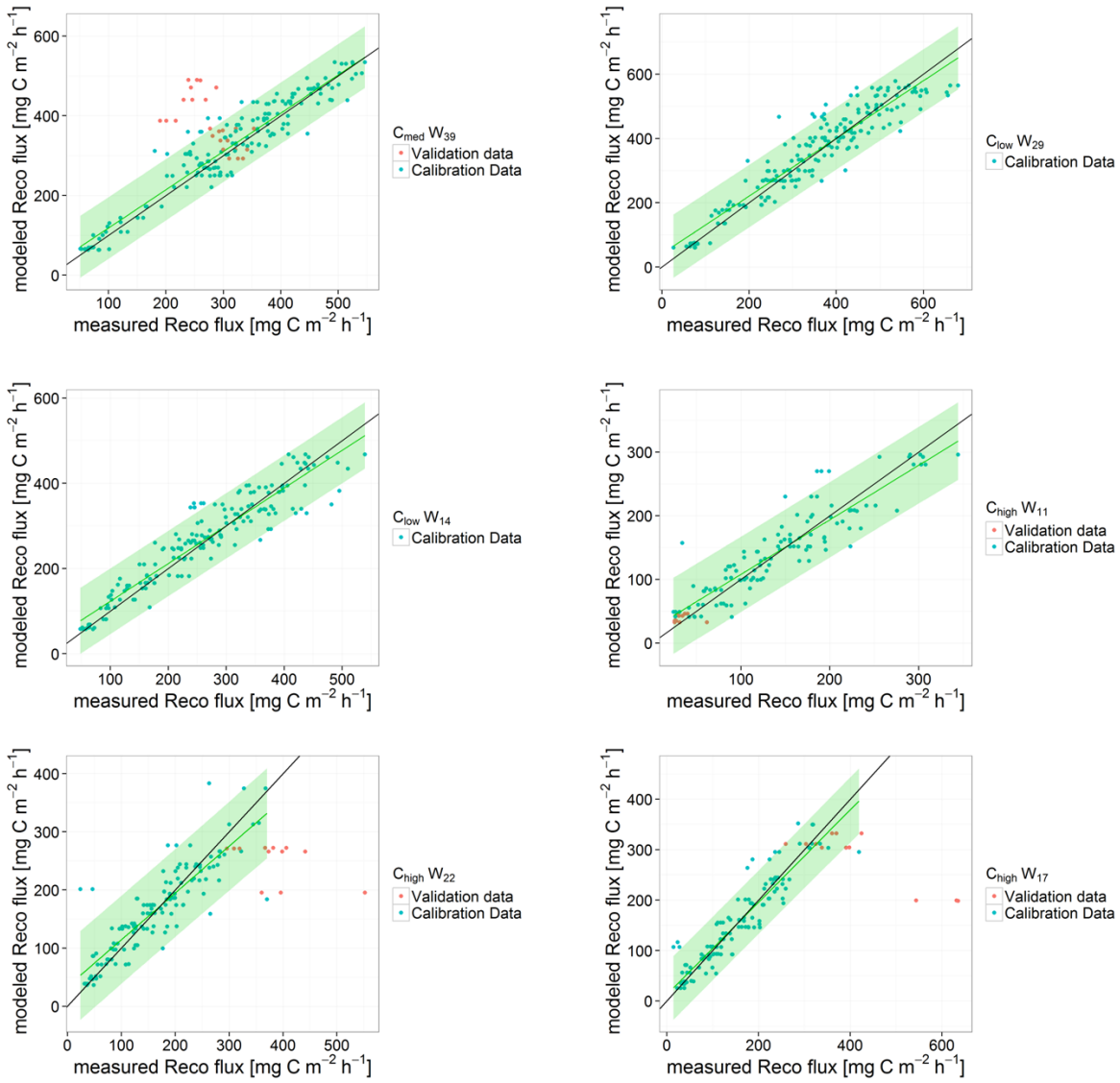
modeled Reco flux [mg C m$^{-2}$ h$^{-1}$]
measured Reco flux [mg C m$^{-2}$ h$^{-1}$]
$C_{med}$ $W_{39}$
Validation data
Calibration Data
$C_{low}$ $W_{29}$
Calibration Data
$C_{low}$ $W_{14}$
Calibration Data
$C_{high}$ $W_{11}$
Validation data
Calibration Data
$C_{high}$ $W_{22}$
Validation data
Calibration Data
$C_{high}$ $W_{17}$
Validation data
Calibration Data

**S 3-4A**

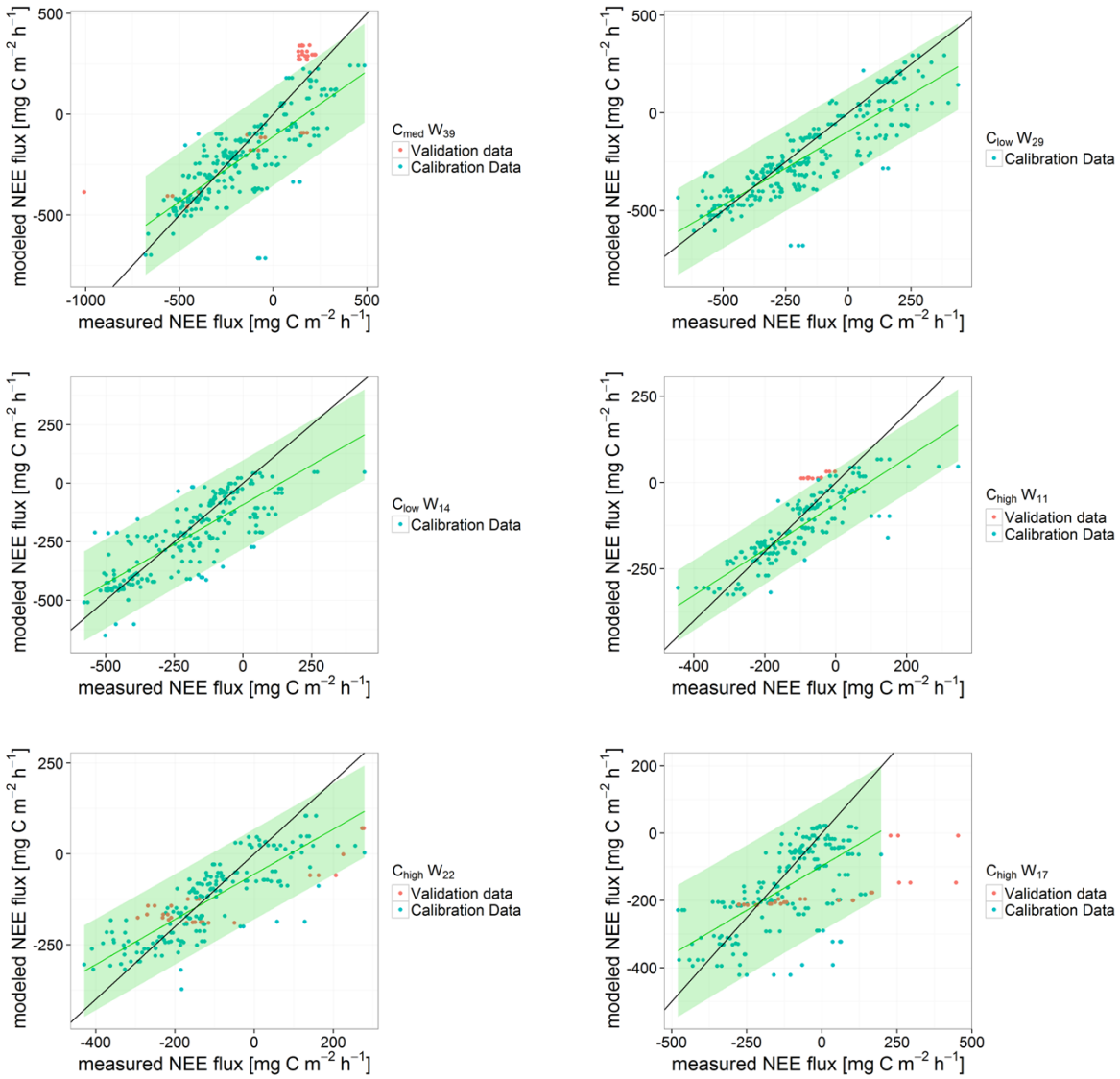


**S 3-4B**

**Fig. S3 - 4: A:** Plots of measured $R_{eco}$ fluxes vs. modeled $R_{eco}$ fluxes of all measurement campaigns seperated by site (1 June 2011 to 1 June 2012). **B**: Plots of measured NEE fluxes vs. modeled NEE fluxes of all measurement campaigns seperated by site (1 June 2011 to 1 June 2012).

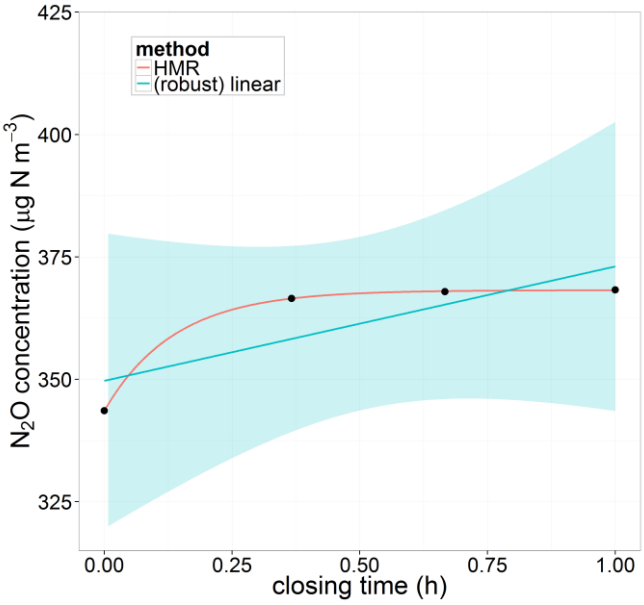


**Fig. S3 - 5**: Example of a flux measurement where the non-linear fit severely overestimates the flux. $N_2O$ concentrations were close to ambient and (by chance) the second to fourth concentration were almost identical and the first concentration was lower by 20 ppb (which is within typical measurement error). Robust linear fit equaled linear fit with flux = 13 µg N $m^{-2}$ $h^{-1}$, p = 0.2, AIC=-24. Shaded area depicts confidence band of the linear fit. HMR fit resulted in flux = 96 µg N $m^{-2}$ $h^{-1}$, p = 2E-5, AIC=-59. Since the HMR flux estimate is more than four times the robust linear flux estimate, we used the latter.

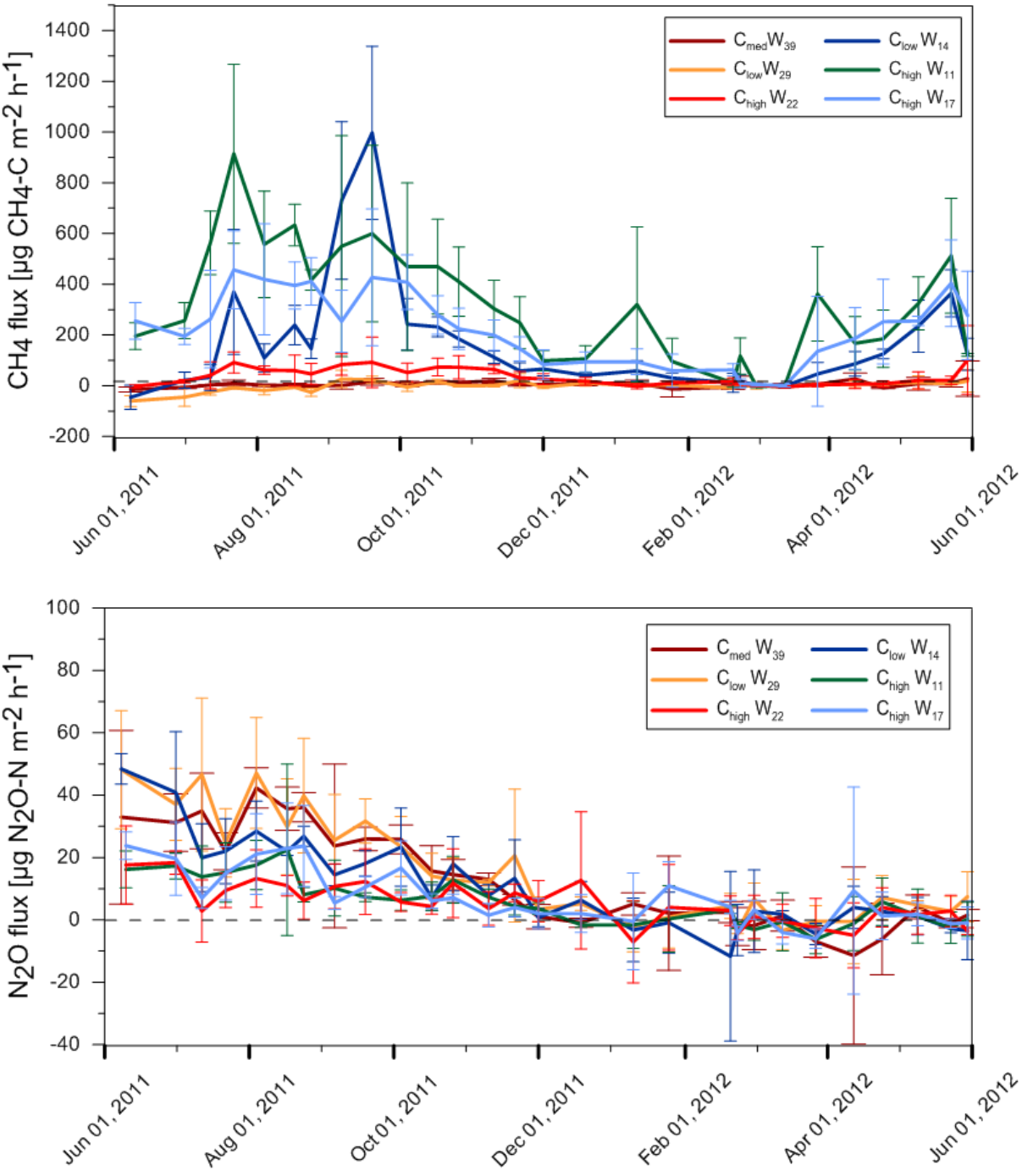


**Fig. S3 - 6:** Annual time lines of $CH_4$ (A) and $N_2O$ (B) (mean ± standard error of the replicates; June 1, 2011 to June 1, 2012).

# Chapter 4: Publication no.3

## Sheep excreta cause no positive priming of peat-derived $CO_2$ and $N_2O$ emissions

**Authors:**

K. Leiber-Sauheitl[1*], R. Fuß[1], St. Burkart[1], F. Buegger[2], S. Dänicke[3], U. Meyer[3], K. J. Petzke[4], A. Freibauer[1]

[1] Thuenen Institute of Climate-Smart Agriculture, Bundesallee 50, 38116 Braunschweig

[2] Helmholtz Zentrum Muenchen, Institute of Biochemical Plant Pathology, Ingolstaedter Landstr. 1, 85764 Neuherberg

[3] Friedrich Loeffler Institute, Institute of Animal Nutrition, Bundesallee 50, 38116 Braunschweig

[4] German Institute of Human Nutrition, Potsdam-Rehbruecke, Arthur-Scheunert-Allee 155, 14558 Nuthetal

**Status of publication:**

published in Soil Biology & Biochemistry 88 (2015), 282-293; incl. Corrigendum to be published 2016

**Own contributions:**

- experimental design
- sheep labeling
- accomplishment of microcosm experiment
- soil analyses
- data analyses
- preparation of the manuscript

**Contributions by coauthors:**

- R. Fuß: discussion on experimental design, contribution to the manuscript
- St. Burkart: $^{13}C$-$CO_2$ measurements, comments to improve the manuscript
- F. Buegger: $^{15}N$-$N_2O$ analyses, comments to improve the manuscript
- S. Dänicke, U. Meyer & K. J. Petzke: provided facilities, tracer and sheep metabolism cages, comments to improve the manuscript
- A. Freibauer: discussion on experimental design, contribution to the manuscript

## Abstract

Large areas of peatlands in Germany and the Netherlands are affected by drainage and high nitrogen deposition. Sheep grazing is a common extensive management activity on drained peatlands, in particular on nature protection areas. However, input of easily mineralisable material such as sheep excrements could enhance degradation of soil organic carbon ($C_{org}$), thereby increasing the effect of these ecosystems on national GHG budgets.

Thus, a microcosm experiment on the influence of sheep excreta on GHG emissions from a histic Gleysol with strongly degraded peat was set up. The $^{15}N$ and $^{13}C$ stable isotope tracer technique was used to partition sources of $CO_2$ and $N_2O$. Labeled sheep faeces and urine were obtained by feeding enriched material. Undisturbed soil columns were treated with surface application of urine, faeces or mixtures of both in different label combinations to distinguish between direct effects and possible priming effects. Incubation was done under stable temperature and precipitation conditions. Fluxes as well as $^{15}N$ and $^{13}C$ enrichment of $N_2O$ and $CO_2$, respectively, were measured for three weeks.

Addition of sheep excreta increased emission of total $CO_2$ in proportion to the added carbon amounts. There was no $CO_2$ priming in the peat. No effect on $CH_4$ and $N_2O$ was observed under the aerobic experimental conditions. The $N_2O$-N source shifted from peat to excreta, which indicates negative priming, but priming was not significant.

The results indicate that sheep excreta do not significantly increase GHG emissions from degraded peat soils. Considering the degraded peatland preserving benefits, sheep grazing on peatlands affected by drainage and high nitrogen deposition should be further promoted.


## 1. Introduction

Sheep grazing on peatlands is a common practice (Germer, 2006), which aims at maintaining grass and heath and preventing growth of birch and shrubbery, in particular when soils are drained. Sheep grazing preserves an open landscape, which offers habitats and ecological niches for rare species. Moreover, it directly affects the greenhouse gas (GHG) balance of a peatland by plant biomass export, $CH_4$ emissions from enteric fermentation and GHG released from faeces or urine patches. Excreta are hotspots of biological activity. In a Mongolian grassland GHG emissions ($CO_2$, $N_2O$, $CH_4$) were 20% higher from urine and fresh faeces patches than from unaffected soil (Ma et al., 2006).

$N_2O$ emissions on peat soils from artificial urine patches emitted maximal 50 mg $N_2O$-N $m^{-2}$ $d^{-1}$ mainly via nitrification in a study by Koops et al. (1997). In the Netherlands 1.5 - 9.9% of the nitrogen in faeces and urine N input was emitted as $N_2O$ from a peat grassland (Velthof et al., 1996). It is

unknown whether the reported $N_2O$ fluxes originated entirely from the excreta or whether additional nitrogen was mobilized from the peat soil by priming. Priming occurs if easily degradable substances added to soils activate or hamper microbial activity. Positive priming increases carbon and / or nitrogen mineralization from soil organic matter compared to a control treatment. Negative priming reduces emissions and soil organic matter decomposition (Kuzyakov et al., 2000).

Drainage induces peat decomposition which results in high $CO_2$ emissions (Smith and Conen, 2004). Decomposition of pure peat is slow, but in previous incubation studies (Reiche et al., 2010; Hahn-Schoefl et al., 2011) $CO_2$ emissions drastically increased when labile, energy-rich substrates were present. Again it is unknown whether the reported fluxes originated entirely from the labile plant-derived material mixed with the peat in the laboratory (Reiche et al., 2010; Hahn-Schoefl et al., 2011) or whether additional carbon was mobilized from the peat soil by priming. Positive or no priming effects have been observed in peat soil after the addition of substrates typical for plant debris (e.g. glucose, oxalic acid, etc.; Hamer and Marschner, 2002).

Stable isotopes ($^{13}C$ and / or $^{15}N$) are commonly used to study priming effects in soil. Bol et al. (2000) traced cattle dung-derived carbon in a temperate grassland using $^{13}C$ natural abundance measurements. After 150 days only around 10% of cattle dung C remained in the upper 5 cm of soil. Angers et al. (2007) observed significant $CO_2$ emissions from pig slurry but no priming effect in mineral soil. In general, very few studies have investigated priming effects or the fate of excreta C or N and studies have exclusively been performed in mineral soils (Monaghan and Barraclough, 1993; Bol et al., 2000). So far, priming effects of excreta have not been studied in organic soils.

Sheep excreta contain active microbes, labile substances and a C/N ratio narrower than the peat. Consequently, they have a strong potential for positive priming in peat soil. We hypothesize that

1. Sheep excreta increase emissions of $CO_2$, $CH_4$ and $N_2O$ from peat soil.
2. Sheep excreta induce a positive carbon and nitrogen priming in peat soil and trigger $CO_2$ and $N_2O$ release from the peat.

Therefore, we studied the influence of sheep excreta on GHG emissions from a degraded peat soil using stable isotope tracers to partition sources and determine possible priming effects.

## 2. Materials and methods

### 2.1 Experimental design

A microcosm study under constant temperature and moisture conditions was performed with pure peat and sheep excreta amendments to test the hypotheses. Sheep excreta were applied on the surface of undisturbed peat columns from a nutrient-poor peat grassland. One excretion event by

one sheep was simulated by surface application of faeces, urine, or faeces plus urine. Priming effects and source attribution of $CO_2$ and $N_2O$ to peat soil versus excreta were studied by tracing $^{13}C$ and $^{15}N$ signals in isotopically double labeled ($^{13}C$ and $^{15}N$) excreta. GHG emissions were measured for 21 days.

Seven different treatments were used in the microcosm experiment (Table 4-1). For all treatments C4 labeled excreta were applied with or without $^{15}N$ enrichment. Pure peat columns (= *pure peat*) were used as control columns for the background levels of $CO_2$, $N_2O$ and $CH_4$ fluxes. A second control containing C4 faeces with natural abundance $^{15}N$ signature on annealed sand (= *$^{14}$N faeces plus sand*) was used for plausibility checks. Peat was amended with faeces or urine or both faeces and urine as combined signal using $^{15}N$ faeces or $^{15}N$ urine (= *$^{15}$N faeces, $^{15}$N urine*, *$^{15}$N faeces plus $^{15}$N urine*, respectively). To distinguish between faeces and urine unlabeled faeces were combined with labeled urine (= *$^{14}$N faeces plus $^{15}$N urine*). Peat amended with unlabeled $^{14}N$ faeces and $^{14}N$ urine (= *$^{14}$N faeces plus $^{14}$N urine*) served as a control treatment to check for eventual isotopic effects on the priming effect.

**Table 4 - 1**: Overview on experimental treatments

| **Treatments*** | **Denomination in the text** |
|---|---|
| control 1: peat | *pure peat* |
| control 2: $^{14}N$ faeces + sand | *$^{14}$N faeces plus sand* |
| Peat + $^{15}N$ faeces | *$^{15}$N faeces* |
| Peat + $^{15}N$ urine | *$^{15}$N urine* |
| Peat + $^{15}N$ faeces + $^{15}N$ urine | *$^{15}$N faeces plus $^{15}$N urine* |
| Peat + $^{14}N$ faeces + $^{15}N$ urine | *$^{14}$N faeces plus $^{15}$N urine* |
| Peat + $^{14}N$ faeces + $^{14}N$ urine | *$^{14}$N faeces plus $^{14}$N urine* |

*For C: C3 signal of peat, C4 signal of faeces and urine.

## 2.2 Sheep excreta labeling

For the production of double labeled excreta a male sheep was housed in a metabolism cage and fed with highly enriched $^{15}N$ tracer substance and corn silage. Corn is a C4 plant (corn silage $\delta^{13}C$ -12.5 ± 0.12‰), which results in a natural abundance $^{13}C$ label of the corn silage compared to the peat material with its $\delta^{13}C$ signal of C3 vegetation (peat $\delta^{13}C$ -28.1 ± 0.15‰). The daily diet contained 2.8 kg corn silage (54.7% dry matter content), 18 g $NH_4Cl$ and 10 g urea where $NH_4Cl$ was enriched to 95% $^{15}N$. Diet enrichment was about 15 atom% $^{15}N$. After two weeks of adaptation to the fodder combination, labeled excreta were collected for 10 days. Faeces and urine were collected separately two to three times a day, bulked and frozen at -19°C until use. At the start of the labeling period, N-

unlabeled faeces and urine were collected from the same sheep fed with C4 corn silage and unlabeled $NH_4Cl$.

For C and N measurement, faeces were dried at 105°C and measured on an elemental analyzer LECO TruMac CN. C and N of urine were measured in the liquid phase on an elemental analyzer LECO TruSpec CN to avoid $NH_3$ volatilization. $^{15}N$ and $^{13}C$ abundance were measured in dried faeces and acidified urine on a Thermo Fisher Scientific Delta plus with a coupled elemental analyzer (CE Instruments FLASH EA 1112) and a Conflo II interface.

The C/N ratio of faeces was 22 in accordance with previously reported values (Floate and Torrance, 1970). More of the excreted N was found in faeces than in urine, which reflects the N-adapted diet. Sheep faeces and urine were enriched by up to 13.2 atom% $^{15}N$ and 9.6 atom% $^{15}N$, respectively. $\delta^{13}C$ of faeces and urine showed a clear C4 signal of -13.1 ± 0.1‰ (1.09 atom% $^{13}C$) and -13.3 ± 0.2‰ (1.09 atom% $^{13}C$), respectively. Further parameters are shown in Table 4-2. Enrichment of $^{15}N$ was sufficient in both excreta to enable the detection of priming effects during incubation.

### 2.3 Microcosm experiment

For the microcosm experiment intact soil cores were extracted from a histic Gleysol in Lower Saxony, Germany (for detailed site description see Leiber-Sauheitl et al., 2014). The upper 5 cm of the soil surface including vegetation and roots were removed to avoid experimental artifacts due to decaying plant material. Subsequently, 20 cm deep soil cores were extracted by hammering a stainless steel sampling device enclosing a plexiglass cylinder (30 cm high, 15 cm diameter) into the soil.

In the laboratory, these undisturbed peat columns were installed in a microcosm system (Hantschel, 1993). The headspace was flushed throughout the experiment with 10 mL $min^{-1}$ of synthetic air (20% $O_2$, 80% $N_2$, 400 ppb $N_2O$). For measurement of flow rates, a flowmeter was switched automatically from one column to the next at regular intervals so that each column was measured every 12 h. $N_2O$ was included in the synthetic air to allow for measuring possible $N_2O$ uptake into the peat column.

Suction plates with -130 hPa pressure were installed at the lower end of the columns to adjust the water content to 63 vol.% (equivalent to 80% water filled pore space (WFPS) according to a pre-experiment). Irrigation of 50 mL $d^{-1}$ (= 2.8 mm $d^{-1}$) with 0.001 M $CaCl_2$ started two weeks before the incubation to equilibrate water contents in the columns and to avoid drying of the soil surface. Incubation temperature was 15°C.

After this equilibration period, tracer was added to the top of the microcosms corresponding to hot spot conditions of faeces and urine input in natural systems. Excreta were added moist and

unconsolidated in order to have maximal decomposition rates during the experiment (Floate, 1970). To simulate C and N input representative for field conditions, C or N amounts were applied representative of one excretion event of sheep. This led to different application rates per treatment. Following the procedure in Ma et al. (2006) 33 g coarsely shredded fresh faeces and 40 mL urine were applied onto the peat columns as single treatments or in combination. This is equivalent to 6.79 g C $m^{-2}$ and 7.92 g N $m^{-2}$ for urine and 335.01 g C $m^{-2}$ and 15.20 g N $m^{-2}$ for faeces additions (Table 4-2). Properties of faeces and urine and isotopic signatures are given in Table 4-2. The difference in C input between faeces and urine treatments was large (faeces C : urine C = 49 : 1), while the N application was relatively similar with a ratio of faeces N : urine N = 2 : 1. The quality of the carbon and nitrogen substrates also differed considerably between faeces and urine treatments.

A pre-test indicated that the peat had a high turnover during the first few days after application. A field experiment of excreta or slurry application used an observation period of 16 days (Eickenscheidt et al., 2014). Accordingly, the duration of the experiment was set to 21 days.

**Table 4 - 2**: C and N content, $^{15}N$ and $^{13}C$ signature of faeces, urine and peat soil. Average C and N content per column.

| | **urine** | **faeces** | **urine + faeces** | **peat soil** |
|---|---|---|---|---|
| **Total C (%)** | 0.30 ± 0.15 * | 39.0 ± 0.13 * | - | 27.0 ± 1.6 * |
| **Total N (%)** | 0.35 ± 0.03 * | 1.77 ± 0.03 * | - | 0.90 ± 0.04 * |
| **atom % $^{15}N$** | | | | |
| $^{15}N$ labeled | 9.64 ± 0.19 * | 13.17 ± 0.19 * | - | - |
| $^{15}N$ unlabeled | 0.381 ± 0.005 * | 0.3689 ± 0.0002 # | - | 0.3677 ± 0.0004 * |
| **atom % $^{13}C$** | 1.09106 ± 0.00009 * | 1.0911 ± 0.0002 + | - | 1.0749 ± 0.0002 * |
| **Average C content (g)** | - | - | - | 508 |
| **Average N content (g)** | - | - | - | 17 |
| **C/N** | 0.85 | 22.0 | 14.8 | 29.9 |

* n=3; # n=11; + n=12

## 2.4 Analyses

The headspace of each soil column was sampled for the concentration of $N_2O$, $CO_2$, $CH_4$ and the isotopic signature of $N_2O$ via headspace vials (20 mL and 120 mL, respectively), which were interconnected to the outgoing air tubes. $N_2O$, $CO_2$ and $CH_4$ concentrations were also measured in empty control columns to check and correct for concentrations present in the stream of artificial air before passing the column. After excreta application the gas phase was sampled with diminishing

frequency, daily to weekly, as the experiment progressed. Gas measurements were carried out on a Shimadzu GC-2014 gas chromatograph with a FID and an ECD (Loftfield et al., 1997). $N_2O$ isotopic signature was measured on an isotopic ratio mass spectrometer (*Delta Plus*, Thermo Scientific, Germany) coupled with a PreCon Interface with double needle.

Carbon isotope ratio $\delta^{13}C$ of sample gas was measured with a cavity ringdown analyzer (Picarro G1101-i Analyzer, Picarro Inc. Sunnyvale Ca. USA). For this, sample gas was taken from the vent of the flowmeter of the microcosm facility. The sample gas was diluted with 20 mL $min^{-1}$ $N_2$ to keep $CO_2$ concentration inside the measurement range of the instrument. Diluted sample gas entered the instrument via a T-piece to allow the instrument to draw sample gas with its immanent flow rate (ca. 20 mL $min^{-1}$). The analyzer takes a measurement every 13 s. After switching from one soil column to the next, constant $CO_2$ concentration and $\delta^{13}C$ values were achieved after approx. 5 min. $\delta^{13}C$ value was calculated as average of the last 10 measurements before switching to the next column. Thus, the switching interval was set to ca. 8 min. For further calculation 30 s running averages of $\delta^{13}C$ were used.

Ammonia ($NH_3$) emissions from urea degradation were measured daily in urine treatments in the first week after application and afterward once at the end of the experiment. Urine treatments were equipped with two vials containing 50 mL 0.05 M $H_2SO_4$ each to trap $NH_3$. $NH_3$ was determined as N content in the acid on a Skalar Continuous-Flow Analyzer, consisting of San++ analysis system with a SA 1050 Random Access Auto Sampler. It should be noted that the air flow rate was optimized for $N_2O$ and $CO_2$ flux measurement and not for $NH_3$ flux measurement.

The mass flow of dissolved organic carbon (DOC), dissolved organic nitrogen (DON) and mineral nitrogen ($N_{min}$) from each column was sampled every four days in the suction flasks. Cumulative C and N losses by leaching were calculated according to Bol et al. (2000).

After the experiment each peat column was divided into a 0-5 cm and a 5-20 cm depth increment. For each depth increment, gravimetric water content, mineral nitrogen content ($NH_4^+$ and $NO_3^-$) according to VDLUFA (1997), bulk soil C, $^{15}N$ and C/N ratios were determined. Microbial biomass was determined in the depth increments by chloroform fumigation extraction (CFE) with 0.05 M $K_2SO_4$ (modified after Brookes et al., 1985; Joergensen, 1995). The chloroform obviously also reacted with the peat so that microbial biomass could not be determined via carbon analysis but only by nitrogen analysis. An aliquot of the extract was used for N content determination on a Mitsubishi Total Nitrogen Analyzer TN-100 with Auto Liquid Sampler and Auto Sample Injector ASI-100. 10 mL of each sample were freeze dried and $^{15}N$ was determined on a Thermo Fisher Scientific Delta plus with a coupled elemental analyzer (CE Instruments FLASH EA 1112) and a Conflo II interface.

## 2.5 Calculations

The fractions of excreta and soil derived $N_2O$-N and $CO_2$-C were calculated with the following equations. For two sources (urine + soil, faeces + soil), the measured amount of $N_2O$ or $CO_2$ ($M_a$) consisted of excreta derived ($M_{excreta}$) $N_2O$ or $CO_2$ fraction and a soil derived ($M_{soil}$) fraction by Equ. (1).

$$M_a = M_{excreta} + M_{soil} \quad \text{Equ. (1)}$$

$M_a$ - measured amount of $N_2O$ [µmol] or $CO_2$ [mmol]

$M_{excreta}$ - excreta (faeces or urine) derived $N_2O$ [µmol] or $CO_2$ fraction [mmol]

$M_{soil}$ - soil derived $N_2O$ [µmol] or $CO_2$ fraction [mmol]

Isotope signals of the background air ($at\%_{gas,back}$), of the column headspace ($at\%_{gas,lab}$) and of the added excreta ($at\%_{excreta}$) were used to calculate the faeces and urine derived fractions of the $N_2O$ or $CO_2$ emissions (Amelung et al., 1999) by Equ. (2).

$$M_{excreta} = \frac{\mathrm{at\%_{gas,lab} - at\%_{gas,back}}}{\mathrm{at\%_{excreta} - at\%_{gas,back}}} \times \mathrm{M_a} \quad \text{Equ. (2)}$$

$at\%_{gas,back}$ - at% $^{15}N$-$N_2O$ or at% $^{13}C$-$CO_2$ of background air

$at\%_{gas,lab}$ - at% $^{15}N$-$N_2O$ or at% $^{13}C$- $CO_2$ of column headspace

$at\%_{excreta}$ - at% $^{15}N$ or at% $^{13}C$- $CO_2$ of excreta (faeces or urine)

For three sources (urine + faeces + soil), the measured amount of $N_2O$ ($M_a$) consisted of a faeces derived ($M_{faeces}$), a urine derived ($M_{urine}$) and a soil derived ($M_{soil}$) $N_2O$ fraction. The urine derived fraction ($M_{urine'}$) was calculated via the *$^{14}N$ faeces plus $^{15}N$ urine* treatment evaluated with Equ. (3).

$$M_{soil} = \frac{\mathrm{M_a \times (at\%_{gas,lab} - at\%_{faeces}) - M_{urine'} \times (at\%_{urine} - at\%_{faeces})}}{\mathrm{at\%_{gas,back} - at\%_{faeces}}} \quad \text{Equ. (3)}$$

$M_{urine'}$ - urine derived $N_2O$ fraction [µmol] determined via *$^{14}N$ faeces plus $^{15}N$ urine* treatment

$at\%_{faeces}$ - at% $^{15}N$ of added faeces tracer

$at\%_{urine}$ - at% $^{15}N$ of added urine tracer

Priming effects for C and N were calculated as priming factors (PF; Bol et al., 2003) by Equ. (4).

$$PF = \frac{\mathrm{M_{soil,treat}}}{\mathrm{M_{soil,control}}} \quad \text{Equ. (4)}$$

$M_{soil,\ treat}$ - soil derived $CO_2$-C or $N_2O$-N in treatment with excreta application

$M_{soil,\ control}$ - soil derived $CO_2$-C or $N_2O$-N in pure peat control

### 2.6 Statistical analyses

All statistics were performed using R (Version 3.1.2; R Core R, 2014). If not indicated differently, mean values are always given with ± 1 standard deviation. The significance limit was set to 0.05. ANOVA tables were calculated for cumulated total, source specific gas fluxes, extractable microbial N and $N_{min}$. Subsequently, TukeyHSD was used to test for the treatment wise significance of differences. Linear models were applied in order to determine the significance of the $^{13}C$ enrichment of the different treatments in comparison to *pure peat*. Two sided t-tests of soil derived C or N fluxes of the different treatments versus the control (=*pure peat*) were performed in order to determine the significance of priming.

## 3. Results

### 3.1 Total $CO_2$ and $CH_4$ fluxes

All treatments were identified as significant sources of $CO_2$ throughout the experiment (Fig. 4-1). Cumulative $CO_2$-C emissions were in the range of 20 - 60 g within 21 days. In accordance with the different amounts of C added, cumulative $CO_2$-C fluxes of *$^{15}N$ faeces* and *$^{15}N$ faeces plus $^{15}N$ urine* were significantly higher than from *pure peat*, *$^{15}N$ urine* and *$^{14}N$ faeces plus sand*.

$CO_2$ fluxes from the *pure peat* treatment were stable over the course of the experiment at about 1.15 g $CO_2$-C $m^{-2}$ $d^{-1}$ and variance between replicate columns was small (Fig. 4-1a). This suggests that environmental conditions were stable during incubation and that differences in fluxes can be attributed to the excreta amendment. Levels of $CO_2$ fluxes varied between treatments but variance between replicates was also large in some of the excreta treatments, in particular in urine treatments. The lowest fluxes were found in the *faeces on sand* and *pure peat* treatments ranging from 0.48 to 1.44 g $CO_2$-C $m^{-2}$ $d^{-1}$ (Fig. 4-1g and a). In total, *urine* exhibited fluxes of a similar magnitude to *pure peat* but its fluxes were higher on the first day after the application (Fig. 4-1d). The *faeces* treatment nearly doubled fluxes from *pure peat* and *urine* treatments (1.68 - 3.6 g $CO_2$-C $m^{-2}$ $d^{-1}$; Fig. 4-1c) over the course of the experiment. Treatments with *faeces plus urine* showed highest fluxes (2.4 - 5.28 g $CO_2$-C $m^{-2}$ $d^{-1}$; Fig. 4-1b, e and f) with pronounced variability in time and between replicates.

$CH_4$ emissions ranged from $4.1 \times 10^{-8}$ to $9.4 \times 10^{-4}$ g $m^{-2}$ $d^{-1}$ with a mean flux of $3.3 \times 10^{-5}$ g $m^{-2}$ $d^{-1}$ over the course of the experiment and all treatments. $CH_4$ fluxes were hence negligible in all treatments and no treatment effects were observed (data not shown).

### 3.2 Excreta derived $CO_2$-C emissions

Excreta derived $CO_2$ fluxes were significantly different from *pure peat* except for the *$^{15}$N urine* treatment ($p < 0.001$). 26.7% (± 7.8%) of urine C, 9.3% (± 1.5%) of faeces C and 12.9% (± 2.3%) / 13.2% (± 1.9%) / 15.4% (± 3.5%) of faeces plus urine C (three treatments with different label combinations) were mineralized to $CO_2$ after 21 days (Fig. 4-2a). $^{13}$C enrichment in $CO_2$ was small but significant for all treatments as compared to background, at least for the first sampling dates.

Excreta $CO_2$-C emissions from treatments with combined application of urine and faeces were slightly higher than the prediction by a mixing model (9.7% of applied C) based on the results from separate application. Urine induced a small positive priming of faeces carbon. Urine derived $CO_2$ emissions followed an exponential decay function (Fig. 4-3) with a half-life of 0.7 days. Consequently, no significant contribution of urine carbon to $CO_2$ emissions was detected after four days. The dynamics is consistent with fast hydrolysis of urea in urine. The expected cumulative emission from complete hydrolysis would be 0.12 g C and the measured value was 0.11 ± 0.02 g urine C. In contrast, the contribution of faeces C to total $CO_2$ fluxes lasted over the three weeks of the experiment as indicated by significant $^{13}$C enrichment in $CO_2$ ($\delta^{13}C$ – 15.8‰) at the end of the experiment where *pure peat* showed a $\delta^{13}C$ of – 26.2‰. Thus, faeces decomposition was not completed at the end of the incubation.

Flux rates of excreta derived $CO_2$-C followed linear or exponential trends with small fluctuations during the sampling period depending on treatment. Variations among columns of the same treatment were small (see Appendix Fig. S4-1 a-c).

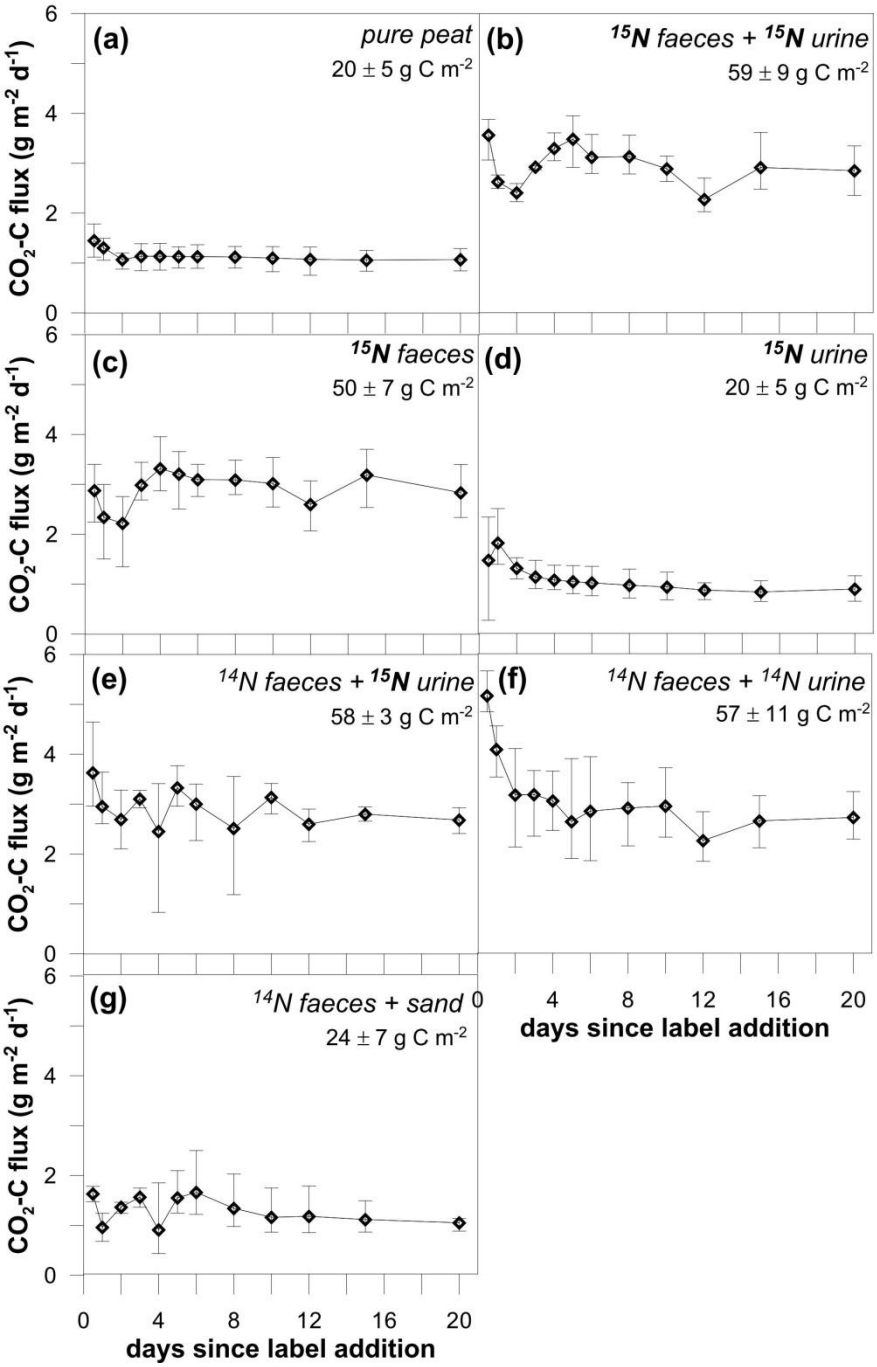


**Fig. 4 - 1**: Time series of $CO_2$ fluxes since labeling of pure peat (=background; a) and different $^{15}N$ labeled treatments (b-g). Bars represent minimum and maximum values of replicates. Cumulated C fluxes of each treatment over 21 days are indicated in g C $m^{-2}$ ± standard deviation of the replicates.

### 3.3 Soil derived $CO_2$-C emissions

During the incubation 0.01% (± 0.00%) to 0.07% (± 0.03%) of the soil C was mineralized (Fig. 4-2b). Soil $CO_2$ contributed more than 85% to the total fluxes in the *$^{15}N$ urine* treatment and 38% in the *$^{15}N$*

*faeces* treatment. This difference is primarily a consequence of the different amounts of C added (Fig. 4-6).

Priming factors indicate mostly non-significant negative priming effects for all treatments (Table 4-3). Significantly less soil C was converted to $CO_2$ if urine and faeces were present: Two of the three urine plus faeces treatments (*$^{14}$N faeces plus $^{14}$N urine, $^{14}$N faeces plus $^{15}$N urine*) exhibited significantly lower soil C derived respiration than *pure peat* ($p < 0.05$ and $p < 0.01$, respectively) and the other treatment (*$^{15}$N faeces plus $^{15}$N urine)* exhibited the same trend ($p = 0.05$). *$^{15}$N urine* as well as *$^{15}$N faeces* exhibited no significant difference to *pure peat*, although there was also a trend towards lower soil C derived respiration.

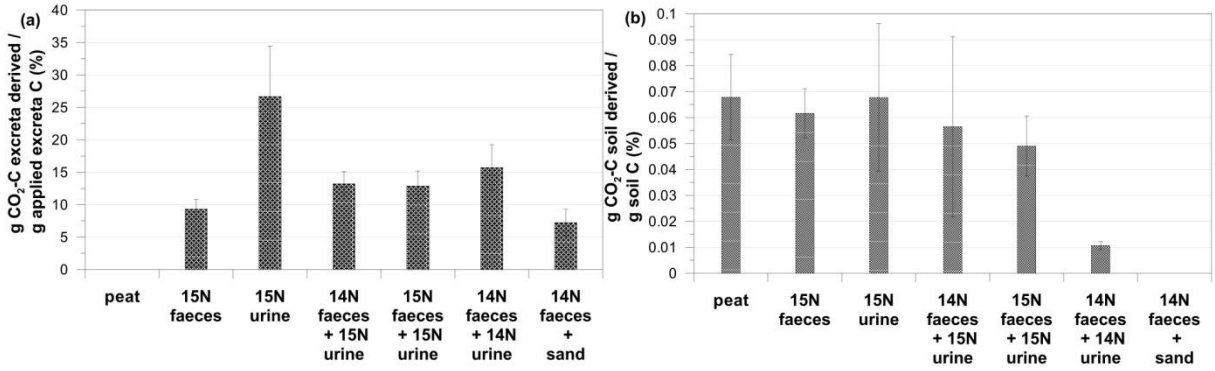


**Fig. 4 - 2**: Proportion of excreta C (a) and of soil C (b) mineralized to $CO_2$ during 3 weeks (mean ± standard deviation of the replicates; n=4).

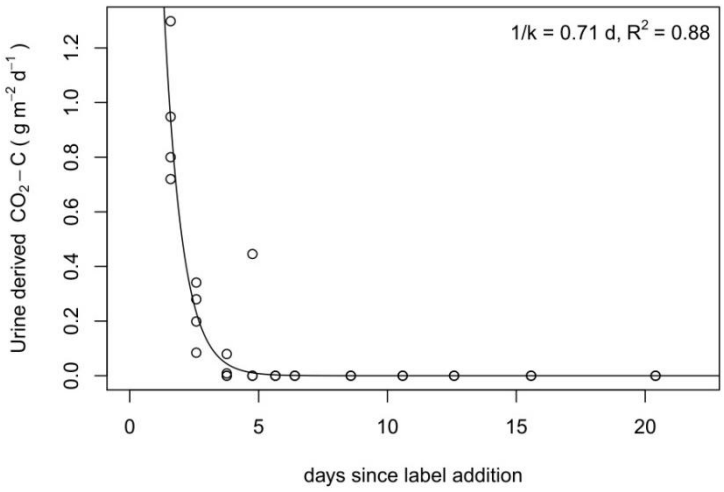


**Fig. 4 - 3**: Mineralization kinetics for urine carbon (flux ~ c1 × exp (-k × time) with c1 = 8.73 ± 2.99 g $m^{-2}$ $d^{-1}$ and k = 1.41 ± 0.21 $d^{-1}$) derived from the $^{15}$N urine treatment (n=4).

### 3.4 DOC export

Cumulative DOC export ranged from 10.5 ± 1.3 to 15.6 ± 1.7 g C $m^{-2}$ (21 days)$^{-1}$. DOC export was generally high and similar in magnitude and dynamics among the treatments. Peat was apparently the most important source of DOC. DOC loss was equivalent to 0.04% - 0.06% of the total C stock in the columns (peat plus excreta). Hence, DOC contributed to total C export equivalent to 17% - 25% of the gaseous C emissions.

### 3.5 Total $N_2O$ and $NH_3$ fluxes

Cumulative $N_2O$-N emissions ranged from 0.01 to 0.14 g N $m^{-2}$ (21 days)$^{-1}$ and did not differ significantly between treatments. $N_2O$ emissions from treatments with peat were between $7.2 \times 10^{-3}$ and $9.6 \times 10^{-3}$ g $m^{-2}$ $d^{-1}$ (Fig. 4-4a-f). Lower emissions were observed in the *$^{14}N$ faeces plus sand* treatment ($3.6 \times 10^{-4}$ to $7.2 \times 10^{-4}$ g $m^{-2}$ $d^{-1}$; Fig. 4-4g). Similar to the respiration results, $N_2O$ emissions from *pure peat* exhibited a low standard deviation (SD) of up to $3.7 \times 10^{-3}$ g $m^{-2}$ $d^{-1}$ (Fig. 4-4a). Treatments with excreta varied more among the replicates (SD increasing in the order *$^{14}N$ faeces plus sand* < *pure peat* < *$^{15}N$ faeces* < *$^{15}N$ urine*; SD of up to $1.0 \times 10^{-2}$ g $m^{-2}$ $d^{-1}$). Towards the end of the experiment, $N_2O$ emissions tended to increase except for the *$^{15}N$ faeces* treatment where $N_2O$ remained constant (Fig. 4-4c). In the *$^{14}N$ faeces plus $^{14}N$ urine* treatment $N_2O$ emissions were comparable to the *pure peat* treatment and variance between replicates was low (up to $2.4 \times 10^{-3}$ g $m^{-2}$ $d^{-1}$; Fig. 4-4f).

Low $NH_3$ emissions were observed in all urine treatments (< $1.2 \times 10^{-7}$ g $m^{-2}$ $d^{-1}$). This is consistent with fast infiltration of urine, the daily irrigation and the low soil pH (3.9), which all suppress $NH_3$-N losses (Black et al., 1987; Clough et al., 1996).

### 3.6 Excreta derived $N_2O$ emissions

$N_2O$-N of the column headspace was highly enriched in all treatments with $^{15}N$ excreta addition (up to 8 atom% $^{15}N$) which reflects the high turnover of excreta nitrogen. Large variability among the replicates (Fig. 4-4) in total as well as source-specific $N_2O$-N fluxes masked treatment effects so that no significant differences could be detected. Except for urine derived $N_2O$-N in the *$^{14}N$ faeces plus $^{15}N$ urine* treatment, excreta derived $N_2O$-N differed non-significantly, but tended to decrease in the order *$^{15}N$ urine* > *$^{15}N$ faeces plus $^{15}N$ urine* > *$^{14}N$ faeces plus $^{15}N$ urine* > *$^{15}N$ faeces*. Soil derived $N_2O$-N was highest in the *pure peat* and *$^{15}N$ faeces* treatment.

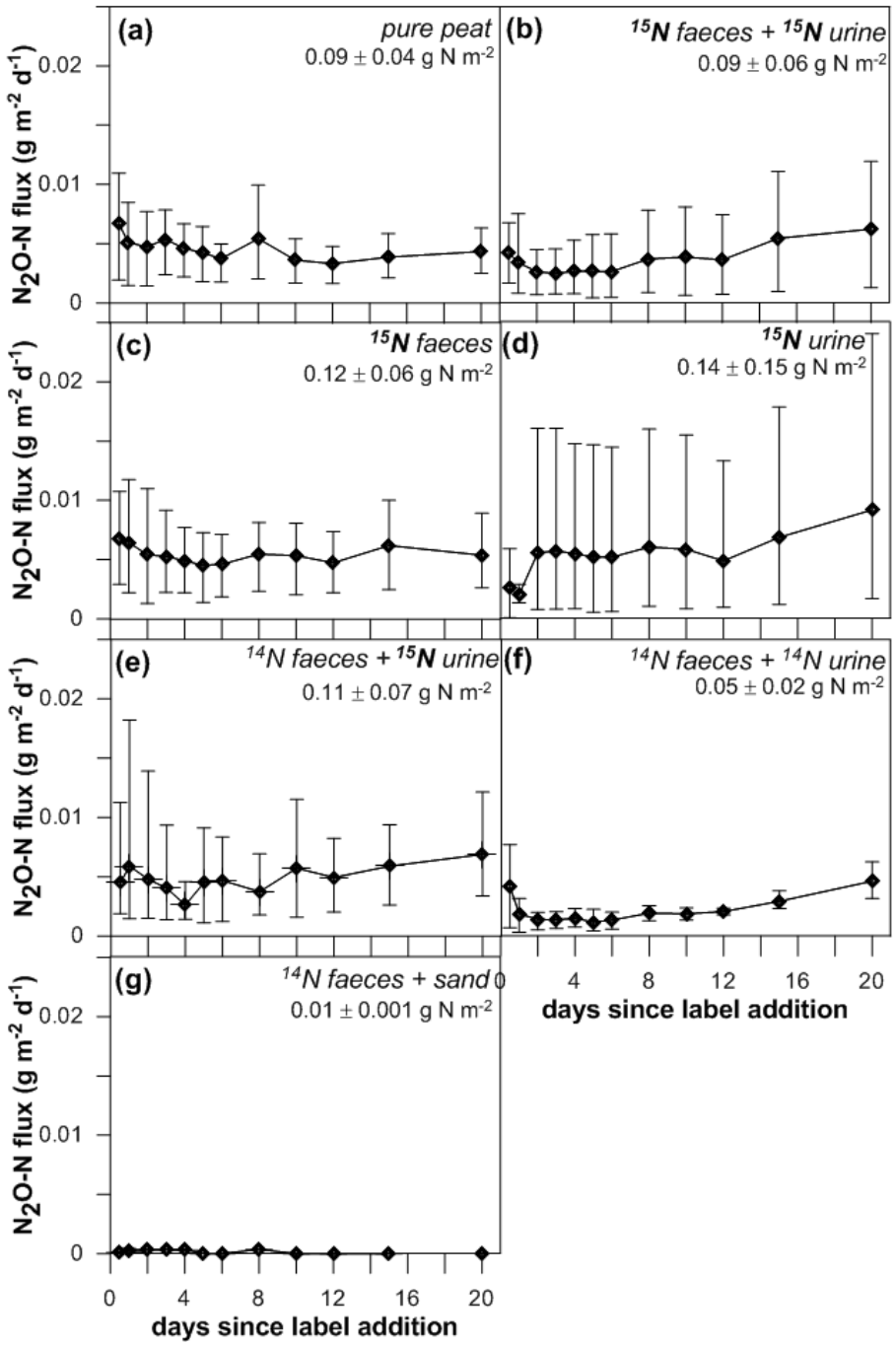


**Fig. 4 - 4**: Time series of $N_2O$ fluxes since labeling of pure peat (=background; a) and different $^{15}N$ labeled treatments (b-g). Bars represent minimum and maximum values of replicates. Cumulated N fluxes of each treatment over 21 days are indicated in g N $m^{-2}$ $d^{-1}$ ± standard deviation of the replicates.

The proportion of excreta N mineralized to $N_2O$ during 21 days was highest in the *$^{15}N$ urine* treatment (1.17% ± 0.60%) and lowest in the *$^{15}N$ faeces* treatment (0.12% ± 0.12%; Fig. 4-5a). In *urine plus faeces* treatments 0.66% (± 0.25%; *$^{14}N$ faeces plus $^{15}N$ urine*) and 0.63% (± 0.46%; *$^{15}N$ faeces plus $^{15}N$ urine*) of the added $^{15}N$ was emitted as $N_2O$ which was in the range expected from a mixing model based on the results from separate application (0.81%).

Flux rates of excreta derived $N_2O$-N followed linear or exponential trends during sampling period depending on treatment and the respective column. For *$^{15}$N faeces*, trends between single columns varied strongly. In contrast, for *$^{15}$N urine* trends of all columns were very similar (See Appendix Fig. S4-1 d-g).

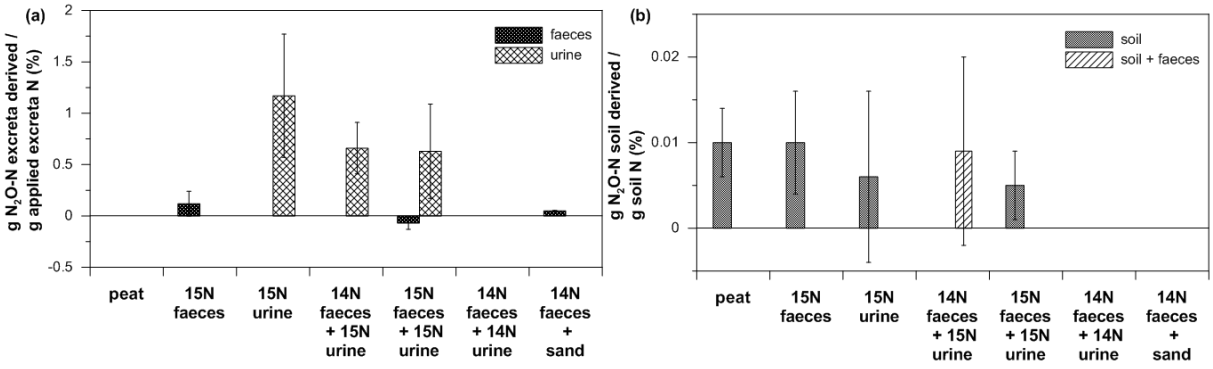


**Fig. 4 - 5**: Proportion of excreta N (a) and soil N (b) mineralized to $N_2O$ during 3 weeks (mean ± standard deviation of the replicates; n=4).

### 3.7 Soil derived $N_2O$ emissions

The amount of soil N mineralized to $N_2O$ ranged from 0.005% ± 0.004% - 0.010% ± 0.006% (Fig. 4-5b). Priming factors (Table 4-3) of *$^{15}$N faeces* were slightly above one, indicating a small positive priming effect, which was not significant. There was a tendency towards a negative priming effect as indicated by results from the *$^{15}$N faeces plus $^{15}$N urine* and the *$^{15}$N urine* treatments in comparison to *pure peat* treatment.

**Table 4 - 3**: Priming factors (PF) of soil $CO_2$ and $N_2O$ calculated according to Bol et al. (2003). Values >1 indicated positive priming, values <1 indicate negative priming. Standard deviations were calculated using Gaussian error propagation. p values were derived from two sided t-tests treatment vs. control ( = pure peat).

| Treatment | PF ($CO_2$) | | PF ($N_2O$) | |
|---|---|---|---|---|
| $^{15}$N *faeces* | 0.79 ± 0.21 | (p = 0.18) | 1.08 ± 0.11 | (p = 0.84) |
| $^{15}$N *urine* | 0.83 ± 0.27 | (p = 0.30) | 0.46 ± 0.09 | (p = 0.26) |
| $^{15}$N *faeces* + $^{15}$N *urine* | 0.66 ± 0.19 | (p = 0.05) | 0.52 ± 0.07 | (p = 0.13) |
| $^{14}$N *faeces* + $^{15}$N *urine* | 0.58 ± 0.23 | (p < 0.05) | n. d. | n. d. |
| $^{14}$N *faeces* + $^{14}$N *urine* | 0.21 ± 0.05 | (p < 0.01) | n. d. | n. d. |

### 3.8 Extractable microbial N

Extractable microbial N did not differ significantly between treatments. Considering the complete columns, the amount of extractable microbial N per g dry soil ranged from 35 ± 30 µg N / g dry soil (*pure peat*) to 48 ± 18 µg N / g dry soil (*$^{15}$N faeces plus $^{15}$N urine*) with large scatter among replicates (Table 4-4). Extractable microbial biomass was higher in the top layer (0-5 cm: 42-60 µg N / g dry soil) than in the bottom layer (5-20 cm: 11-36 µg N / g dry soil; data not shown). More extractable microbial N was observed in *$^{15}$N faeces plus $^{15}$N urine* than in *$^{15}$N urine*, *$^{15}$N faeces* or *pure peat* in 0-5 cm. In the 5-20 cm layer higher extractable microbial N was found in *$^{15}$N faeces plus $^{15}$N urine* than in *$^{15}$N urine* or in *pure peat*.

Unfumigated samples (=exchangeable N) indicated a higher enrichment than fumigated ones (= exchangeable N plus microbial N) with 6 atom% $^{15}$N versus 4 atom% $^{15}$N (data not shown). During chloroform fumigation not only microbial cells can be lysed, but ammonium or old cell wall fragments of the peat substrate could also have been released (Miltner et al., 2012), causing dilution of the $^{15}$N label due to their low $^{15}$N content. Apparently, chloroform fumigation does not allow a robust quantification of microbial biomass in peat soil.

**Table 4 - 4**: Extractable microbial N and $NO_3^-$, $NH_4^+$, mineral N and DON contents after 21 days.

| Treatment | extractable microbial N (mg N / g dry soil) | $NO_3^-$ (mg N per column) | $NH_4^+$ (mg N per column) | $N_{min}$ (mg N per column) | DON (g N $m^{-2}$ in 21 days) |
|---|---|---|---|---|---|
| *pure peat* | 0.04 ± 0.03 | 2.49 ± 0.64 | 18.13 ± 6.83 | 20.63 ± 3.30 | 0.47 ± 0.04 |
| $^{15}$N *faeces* | 0.04 ± 0.02 | 2.28 ± 2.64 | 34.19 ± 7.41 | 36.47 ± 10.40 | 0.56 ± 0.06 |
| $^{15}$N *urine* | 0.04 ± 0.03 | 5.41 ± 8.19 | 102.66 ± 56.96 | 108.07 ± 36.29 | 0.44 ± 0.03 |
| $^{15}$N *faeces plus* $^{15}$N *urine* | 0.05 ± 0.02 | 2.48 ± 2.17 | 71.63 ± 24.98 | 74.11 ± 11.67 | 0.57 ± 0.07 |
| $^{14}$N *faeces plus* $^{15}$N *urine* | n. d. | 0.69 ± 1.23 | 72.93 ± 29.65 | 73.59 ± 14.90 | 0.46 ± 0.11 |
| $^{14}$N *faeces plus* $^{14}$N *urine* | n. d. | 6.39 ± 10.04 | 165.38 ± 33.68 | 171.77 ± 36.54 | 0.52 ± 0.09 |

### 3.9 Mineral nitrogen

There were significant differences in mineral N ($N_{min}$) contents of soil between treatments ($p < 0.0001$). $N_{min}$ was dominated by ammonium, which contributed about 96% and 83% to $N_{min}$ in the top and bottom layer, respectively (Table 4-4). As expected, $N_{min}$ was higher in the top than in the bottom layer. Lowest $N_{min}$ contents were found in the *pure peat* and *$^{15}$N faeces* treatment.

### 3.10 DON

Cumulative DON export was similar in magnitude and dynamics among all treatments and ranged from 0.4 ± 0.03 up to 0.6 ± 0.07 g N $m^{-2}$ over 21 days (Table 4-4). Among 0.04% - 0.08% of the total N content of the columns (peat plus added excreta N) was lost by DON export. DON export was three to six times higher than the gaseous nitrogen loss as $N_2O$.

Figure 4-6 gives an overview of the observed cumulative carbon and nitrogen export during the experiment.

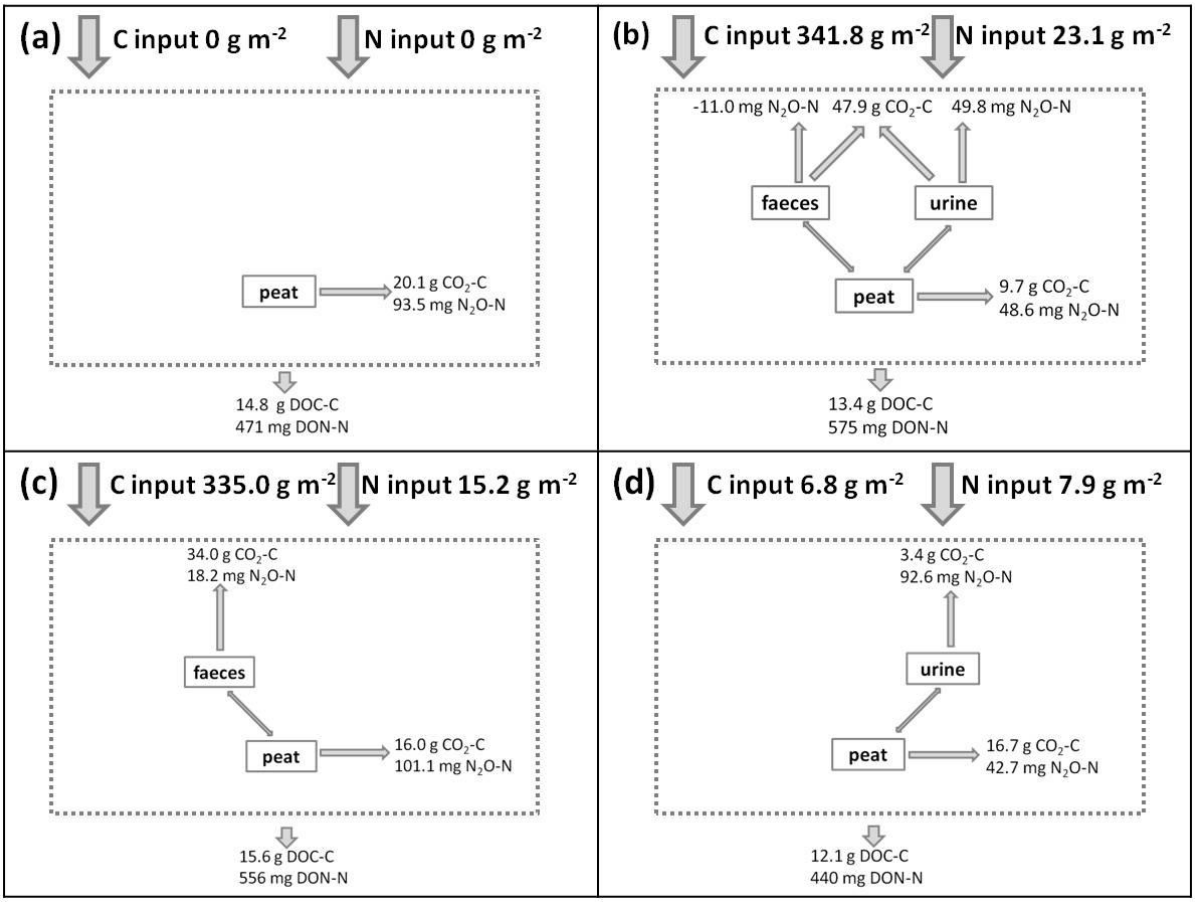


**Fig. 4 - 6**: Source specific carbon and nitrogen release (g C or mg N $m^{-2}$) of different treatments over 21 days: (a) pure peat, (b) $^{15}N$ faeces and $^{15}N$ urine (for $CO_2$-C emissions mean value of all faeces plus urine treatments), (c) $^{15}N$ faeces and (d) $^{15}N$ urine. DOC-C and DON-N refer to emissions from total column. On top of each figure (a-d) amounts of C and N input per column are indicated. The dotted boxes represent one microcosm system.

# 4. Discussion

## 4.1 Carbon losses after excreta application on peat soil

We confirmed our first hypothesis that sheep excreta increase emissions of $CO_2$ from peat soil, but found no effect on $CH_4$ under aerobic conditions. Indeed, $CO_2$ emissions increased proportionally to the amount of carbon added as excreta. We rejected, however, our second hypothesis and found no stimulation of peat mineralization by excreta application.

The magnitude and dynamics of $CO_2$ emissions from excreta applied to peat soil in the microcosm experiment agree with previous findings. In a field experiment on Mongolian mineral soils, Ma et al. (2006) also observed no significant difference in $CO_2$ fluxes between plots with urine amendment and control plots, but between plots with faeces and control plots.

Mineralization of urine C to $CO_2$ was completed within a day whereas mineralization of faeces C would have continued for longer than the 21 days of our experiment. The 10% of faecal C mineralized within 21 days in the peat soil of our experiment is similar to that in mineral soils (Kristiansen et al., 2004), which seems to indicate that mineralization of faeces on the soil surface is not influenced strongly by the soil and its microbial community.

The $CO_2$ release from urea may have been entirely due to the physical process of hydrolysis or by a combination of physical and microbial processes. Around 80% of total N in sheep urine is present in the form of urea (Bristow et al., 1992), which dissociates in water into $CO_2$ and $NH_3$. After excreta application, easily available C compounds are preferentially degraded by microorganisms. Subsequently more complex compounds are used according to their utilizability (urine derived > faeces derived > soil derived) (Kuzyakov and Bol, 2006). As soon as the easily available substances are consumed, $CO_2$ fluxes decline to background level (*pure peat*) as observed in the $^{15}$*N urine* treatment (Fig. 4-1d). As proposed by Blagodatskaya et al. (2009), the input of easily available substrate - here sheep urine - could have stimulated fast growing r-strategists whereas slowly available substrate - here sheep faeces – might have shifted the microbial community to slow growing K-strategists. This could explain the different release patterns for total $CO_2$-C in urine and faeces treatments (Fig. 4-1).

The incubated peat was a significant $CO_2$ source of about 1.15 g C $m^{-2}$ $d^{-1}$. Although the most intensively rooted surface peat had been removed before extracting the soil cores the peat still contained the deeper roots of grasses and herbs. The $CO_2$ release from the incubated peat tended to be lower than from the same soil during field measurements (Leiber-Sauheitl et al., 2014). Ecosystem respiration measured at around 15°C in the grassland site ranged from 6 to 11 g C $m^{-2}$ $d^{-1}$. About half of ecosystem respiration can be attributed to autotrophic respiration from the vegetation and the other half is soil respiration (Schulze et al., 2009). Plant roots, in turn, roughly contribute 35 - 50% to

soil respiration (Silvola et al., 1996; von Arnold et al., 2005). Using these rough assumptions we can estimate a soil derived $CO_2$ source of 20 - 30% of measured ecosystem respiration, equivalent to 1.2 - 3.3 g C $m^{-2}$ $d^{-1}$. The field site included the intensively rooted surface peat and may have been drier than the incubated peat, which likely explains its slightly higher soil derived $CO_2$ emission.

Peat mineralization is a much stronger $CO_2$ forming process than SOC mineralization in mineral soils. Adding relatively small amounts of extra carbon on the surface of the peat column as excreta may have little effect on microbial activity unless there are strong energy or nutrient limitations. The incubated peat (*pure peat*) emitted 39 mg C kg $C^{-1}$ $d^{-1}$ in aerobic conditions. The $CO_2$ release is higher than in anaerobically incubated peat, where topsoil layer peat and peat with roots emitted $CO_2$ of up to 28 mg C kg $C^{-1}$ $d^{-1}$ (Hahn-Schoefl et al., 2011). Decomposition is much faster in aerobic than in anaerobic conditions. The peat in our incubation seems relatively inert and thus could be expected to have the potential for positive priming by fresh carbon sources. Nevertheless, we found no mechanism that would suggest a risk of increased peat mineralization by sheep excreta. In contrast to studies on mineral soils (Shand et al., 2002; Shand and Coutts, 2006), DOC loss was not enhanced by excreta application on peat (Fig. 4-6). Obviously, the degraded peat was the prevailing source of the massive DOC loss in our experiment.

## 4.2 Nitrogen losses after excreta application on peat soil

We must reject our hypothesis that sheep excreta increase emissions of $N_2O$ from peat soil, at least for the degraded peat soil in our study, but cannot rule out a risk of elevated $N_2O$ emissions. In contrast, we found a source shift of $N_2O$ from peat to excreta derived nitrogen.

$N_2O$ emission levels in our incubation exceeded emissions observed in the field after urine (Clough et al., 1996) and slurry application (Eickenscheidt et al., 2014). We observed high background $N_2O$ emissions from the peat (Fig. 4-6). This contrasts with these two field studies and with the field observations at the grassland site from which the incubated soil originated. At this site mean and maximum field $N_2O$ emissions were $3.4 \times 10^{-4}$ g N $m^{-2}$ $d^{-1}$ and $2.2 \times 10^{-3}$ g N $m^{-2}$ $d^{-1}$, respectively (Leiber-Sauheitl et al., 2014). $N_2O$ emission levels in our incubation are in the upper range observed in field studies of peat grassland soils (Leppelt et al., 2014).

Acid soils like our peat soil have high $N_2O/N_2$ production ratios and thus high potential $N_2O$ emissions (Mørkved et al., 2007; Liu et al., 2010). The peat substrate in our incubation, however, had a C/N ratio of 29, which is close to the threshold of 30-35 for very low $N_2O$ formation (Leppelt et al., 2014). Thus, soil properties are inconclusive for explaining the relatively high $N_2O$ emission levels in the incubation.

$N_{min}$ content in the incubation experiment exceeded the values found in the field, which were almost exclusively present as ammonium as well (Leiber-Sauheitl et al., 2014). Absence of plants, and consequently no plant N-uptake, might have resulted in a stronger $N_{min}$ accumulation. The laboratory results highlight that a peat soil can quickly switch from low to high $N_2O$ emissions when $N_{min}$ contents rise and environmental conditions are favorable for $N_2O$ producing processes of the N cycle, such as denitrification or nitrifier denitrification.

Urine application indicated a risk of elevated $N_2O$ emissions, but the variability in the treatments was too high for a robust statement. The source partitioning, however, clearly indicated a source shift from peat to urine in $N_2O$ formation. A similar, but less pronounced shift in N substrate was induced by faeces.

The fraction of $N_2O$-N emitted per unit of applied N is defined as the emission factor (IPCC, 2006). The source partitioning traced by isotopic label resulted in emission factors, which were in the range of the default emission factor of IPCC (2006) of 2% of N as $N_2O$ from grazing animal excreta by an order of magnitude. Field studies on mineral soils estimated an emission factor of 0.4% of N from cattle dung patches and of <0.1 - 3.8%, with 1.5% as overall mean for urine (Oenema et al., 1997). After the application of cattle excreta to a Scottish grassland on mineral soil, Bell et al. (2015) reported N emission factors of urine (1.1%) and dung (0.2%) in summer which were in all experiments lower than the IPCC default of 2%. N emission factors smaller than 1% were also found for cattle slurry application on organic soils (Eickenscheidt et al., 2014). The field studies and the IPCC emission factors refer to apparent N application effects by comparing total emissions from sites with excreta with emissions from control sites. This approach ignores the substrate shift from soil N to excreta N, which was the main effect in our experiment. Calculating apparent emission factors in line with IPCC (2006) results in near zero emission factors in our experiment as well.

### 4.3 Priming effects for C and N

We reject our priming hypothesis and found instead no or negative carbon and nitrogen priming in peat soil by sheep excreta.

$CO_2$ from excreta was additive to $CO_2$ from the peat with no obvious interaction. We found, however, a clear source shift from soil to sheep excreta. This finding contrasts with results for a mineral soil. Ma et al. (2013) found a positive priming effect on soil C decomposition by sheep faeces application on two Mongolian grassland soils. The contrasting effects could be a consequence of dryer conditions in the Mongolian study, carbon limitation of decomposition or a different microbial community in the mineral soil as opposed to the degraded peat soil in our study.

The C addition to peat soil was a mixture of pulse inputs (easily degradable substances in faeces and urine such as urea or amino acids) and continuous inputs (more recalcitrant substances in faeces such as lignin) as defined by Kuzyakov (2010). In a first step bacteria decompose easily degradable substances whereas afterward fungi produce extracellular enzymes to degrade more stable soil organic matter (Kuzyakov, 2010). Fungi would stimulate positive priming effects while bacteria would induce no or negative priming by preferential feeding on energy-rich substrate. Given the methodological difficulty of extracting microbes from peat soil we could not distinguish bacteria from fungi. Nevertheless our findings suggest that the excreta have stimulated bacterial activity, which preferentially fed on easily degradable substances, and bacterial nitrification and denitrification. Of course, a non-negligible number of microorganisms were also added with the excreta, in particular with the faeces (Kristiansen et al., 2004; Ritz et al., 2004).

## 4.4 Field application of lab results

Sheep grazing is often conducted on peatlands protected for nature conservation with a low stocking density.

The surface area of a sheep faeces patch is roughly below 0.005 $m^2$ and that of a sheep urine patch (wetted area) about 0.03 $m^2$ (= one excretion event; Oenema et al., 1997). A typical stocking density of 0.5 livestock units per hectare, equivalent to 5 ewes would result in about 50 kg $ha^{-1}$ $a^{-1}$ of N and 750 kg $ha^{-1}$ $a^{-1}$ of C input by excreta (Haenel et al., 2014). During one sheep excreta application event in our experiment, 34% of N as urine and 66% as faeces were added (Table 4-2 and Fig. 4-6). Jones et al. (1979) found 70% of the total excreted N in urine and 30% in faeces. With a recommended maximal herd size of 1100 sheep (Germer, 2006), an area of 33 $m^2$ and 5.5 $m^2$ is covered with urine and faeces patches, respectively. Urine and faeces would affect 3.3% and 0.5% per grazed hectare, respectively. Possible, but according to our results negligible priming effects would be constrained to a small area.

Compaction by sheep trampling may help conserve the peat. In a laboratory study the presence of sheep trampling led to smaller $CO_2$ fluxes independent of the trampling intensity (Clay and Worrall, 2013). This came from the damaged vegetation and from an increase in surface bulk density which affected the connectivity of the pore space. It is to be expected that soil conditions become more anaerobic and therefore peat is less degraded. Soil compaction by trampling could, however, cause increased wetness, which in turn may increase $N_2O$ or $CH_4$ emissions. This was not tested in the microcosms. Compaction mainly occurs when stocking density is high and long periods of grazing are conducted on a grassland on wet peat soil. However, this risk is minimized by grazing

recommendations on grasslands in nature conservation areas where low stocking density and short periods of grazing are mandatory.

As we already indicated for priming effects low stocking densities minimize impact of sheep excreta to a small area. Therefore, the risk of increased $N_2O$ and $CH_4$ emissions due to water logging should also be constrained to a small area. Consequently, wetness induced by compaction should not alter our conclusions.

Worrall and Clay (2012) have developed a model, which uses submodels of the physical impact of grazing, biomass production, energy usage in sheep, and peat accumulation in combination with IPCC emission factors (IPCC, 2006) to estimate the greenhouse balance in a near-natural peatland in dependence of grazing intensity. They estimated an average GHG emission from the peat soil of about 166 kg $CO_2$-eq. $yr^{-1}$ $ewe^{-1}$. Their results indicate that, depending on the GHG sink of the peat soil, grazing intensities between 0.2 and 1.7 ewes $ha^{-1}$ can result in a neutral greenhouse balance. In Germany and the Netherlands, however, peat soils are usually drained for forage production and grazing. In such a situation where peat is constantly lost by aerobic decomposition, the greenhouse gas balance of sheep grazing on drained peat is always a net $CO_2$ source.

So far, there are no comparable field experiments that would allow immediate conclusions for practice. Nevertheless, the mechanisms and trends we observed agree with field observations on peat soils in other studies and their interpretation, but disagree with findings in mineral soils. We therefore suggest that our laboratory results can be generalized for grazed peat soils.

In total, sheep grazing will slow down peat soil degradation by small negative carbon priming and compaction by trampling.

## 5. Conclusions

In the microcosm experiment, sheep excreta did enhance $CO_2$ emissions proportionally to the amount and type of C added. In contrast, $N_2O$ and $CH_4$ emissions were not affected by excreta addition. Methane emissions were very small and so not relevant during excreta decomposition. Sheep excreta caused no or small negative priming on peat decomposition and led to a source shift of the nitrogen released as $N_2O$ from peat to labile N forms in excreta. We found no mechanism that would suggest a risk of increased peat mineralization by sheep excreta. Sheep excreta cover a small fraction of the grazed area and exert no or slightly negative carbon priming. Sheep also compact the soil by trampling. Overall, sheep grazing can be expected to slow down the degradation of drained peat soil.

**Acknowledgments**

The “Organic soils” joint research project funded by the Thuenen Institute.

We thank B. Klauke, M. Hunziger and D. Olbricht for their help in the lab as well as A. Junghans and D. Wolters for support during sheep labeling. Furthermore, we acknowledge the support of J. Ehe, A. Giesemann and M. Zerbian; and two anonymous reviewers for their instructive comments.

## 6. References


Amelung, W., Bol, R., Friedrich, C., 1999. Natural $^{13}C$ abundance: a tool to trace the incorporation of dung-derived carbon into soil particle-size fractions. Rapid Communications in Mass Spectrometry 13, 1291-1294.

Angers, D. A., Rochette, P., Chantigny, M. H., Lapierre, H., 2007. Use of $^{13}C$ abundance to study short-term pig slurry decomposition in the field. Soil Biology & Biochemistry 39, 1234-1237.

Bell, M. J., Rees, R. M., Cloy, J. M., Topp, C. F. E., Bagnall, A., Chadwick, D. R., 2015. Nitrous oxide emissions from cattle excreta applied to a Scottish grassland: Effects of soil and climatic conditions and a nitrification inhibitor. Science of the Total Environment 508, 343-353.

Black, A. S., Sherlock, R. R., Smith, N. P., 1987. Effect of timing of simulated rainfall on ammonia volatilization from urea, applied to soil of varying moisture-content. Journal of Soil Science 38, 679-687.

Blagodatskaya, E. V., Blagodatsky, S. A., Anderson, T. H., Kuzyakov, Y., 2009. Contrasting effects of glucose, living roots and maize straw on microbial growth kinetics and substrate availability in soil. European Journal of Soil Science 60, 186-197.

Bol, R., Amelung, W., Friedrich, C., Ostle, N., 2000. Tracing dung-derived carbon in temperate grassland using $^{13}C$ natural abundance measurements. Soil Biology & Biochemistry 32, 1337-1343.

Bol, R., Moering, J., Kuzyakov, Y., Amelung, W., 2003. Quantification of priming and $CO_2$ respiration sources following slurry-C incorporation into two grassland soils with different C content. Rapid Communications in Mass Spectrometry 17, 2585-2590.

Bristow, A. W., Whitehead, D. C., Cockburn, J. E., 1992. Nitrogenous constituents in the urine of cattle, sheep and goats. Journal of the Science of Food and Agriculture 59, 387-394.

Brookes, P. C., Landman, A., Pruden, G., Jenkinson, D. S., 1985. Chloroform fumigation and the release of soil-nitrogen - a rapid direct extraction method to measure microbial biomass nitrogen in soil. Soil Biology & Biochemistry 17, 837-842.

Clay, G. D., Worrall, F., 2013. The response of $CO_2$ fluxes from a peat soil to variation in simulated sheep trampling. Geoderma 197, 59-66.

Clough, T. J., Sherlock, R. R., Cameron, K. C., Ledgard, S. F., 1996. Fate of urine nitrogen on mineral and peat soils in New Zealand. Plant and Soil 178, 141-152.

Eickenscheidt, T., Heinichen, J., Augustin, J., Freibauer, A., Drosler, M., 2014. Nitrogen mineralization and gaseous nitrogen losses from waterlogged and drained organic soils in a black alder (Alnus glutinosa (L.) Gaertn.) forest. Biogeosciences 11, 2961-2976.

Floate, M. J. S., 1970. Decomposition of organic materials from hill soils and pastures part 4: the effects of moisture content on the mineralization of carbon nitrogen and phosphorus from plant materials and sheep faeces. Soil Biology and Biochemistry 2, 275-283.

Floate, M. J. S., Torrance, C. J., 1970. Decomposition of organic materials from hill soils and pastures part1: incubation method for studying mineralisation of carbon, nitrogen and phosphorus. Journal of the Science of Food and Agriculture 21, 116-120.

Germer, P., 2006. Regeneration des Großes Torfmoores - LIFE-Natur-Projekt (Regeneration of the Großes Torfmoor - LIFE-Nature-Project). NUA-Heft 23, 80-84.

Haenel, H.-D., Rösemann, C., Dämmgen, U., Poddey, E., Freibauer, A., Wulf, S., Eurich-Menden, B., Döhler, H., Schreiner, C., Bauer, B., Osterburg, B. , 2014. Calculations of gaseous and particulate emissions from German agriculture 1990 - 2012. Thünen Report 17 Braunschweig, 348 pp.

Hahn-Schoefl, M., Zak, D., Minke, M., Gelbrecht, J., Augustin, J., Freibauer, A., 2011. Organic sediment formed during inundation of a degraded fen grassland emits large fluxes of $CH_4$ and $CO_2$. Biogeosciences 8, 1539-1550.

Hamer, U., Marschner, B., 2002. Priming effects of sugars, amino acids, organic acids and catechol on the mineralization of lignin and peat. Journal of Plant Nutrition and Soil Science 165, 261-268.

Hantschel, R. E., Flessa, H., Beese, F., 1993. An automated microcosm system for studying soil ecological processes. Soil Science Society of America Journal 58, 401-404.

IPCC, 2006. Guidelines for National Greenhouse Gas Inventories.Chapter 3: Consistent Representation of Lands. 42 pp.

Joergensen, R. G., 1995. Die quantitative Bestimmung der mikrobiellen Biomasse in Böden mit der Chloroform-Fumigations-Extraktions-Methode (The quantitative determination of the microbial biomass in soil by the chloroform fumigation extraction method), 104 ed. Göttinger Bodenkundliche Berichte, Göttingen, 229 pp.

Jones, M. B., Woodmansee, R. G., 1979. Biogeochemical cycling in annual grassland ecosystems. Botanical Review 45, 111-144.

Koops, J. G., vanBeusichem, M. L., Oenema, O., 1997. Nitrous oxide production, its source and distribution in urine patches on grassland on peat soil. Plant and Soil 191, 57-65.

Kristiansen, S. M., Brandt, M., Hansen, E. M., Magid, J., Christensen, B. T., 2004. $^{13}C$ signature of $CO_2$ evolved from incubated maize residues and maize-derived sheep faeces. Soil Biology & Biochemistry 36, 99-105.

Kuzyakov, Y., 2010. Priming effects: Interactions between living and dead organic matter. Soil Biology & Biochemistry 42, 1363-1371.

Kuzyakov, Y., Bol, R., 2006. Sources and mechanisms of priming effect induced in two grassland soils amended with slurry and sugar. Soil Biology & Biochemistry 38, 747-758.

Kuzyakov, Y., Friedel, J. K., Stahr, K., 2000. Review of mechanisms and quantification of priming effects. Soil Biology & Biochemistry 32, 1485-1498.

Leiber-Sauheitl, K., Fuß, R., Voigt, C., Freibauer, A., 2014. High $CO_2$ fluxes from grassland on histic Gleysol along soil carbon and drainage gradients. Biogeosciences 11, 749-761.

Leppelt, T., Dechow, R., Gebbert, S., Freibauer, A., Lohila, A., Augustin, J., Drösler, M., Fiedler, S., Glatzel, S., Höper, H., Järveoja, J., Lærke, P. E., Maljanen, M., Mander, Ü, Mäkiranta, P., Minkkinen, K., Ojanen, P., Regina, K., Strömgren, M., 2014. Nitrous oxide emission budgets and land-use-driven hotspots for organic soils in Europe. Biogeosciences 11, 6595-6612.

Liu, B., Mørkved, P. T., Frostegård, Å., Bakken, L. R., 2010. Denitrification gene pools, transcription and kinetics of NO, $N_2O$ and $N_2$ production as affected by soil pH. Fems Microbiology Ecology 72, 407-417.

Loftfield, N., Flessa, H., Augustin, J., Beese, F., 1997. Automated gas chromatographic system for rapid analysis of atmospheric trace gases methane, carbon dioxide, and nitrous oxide. Journal of Environmental Quality 6, 560-564.

Ma, X., Ambus, P., Wang, S., Wang, Y., Wang, C., 2013. Priming of Soil Carbon Decomposition in Two Inner Mongolia Grassland Soils following Sheep Dung Addition: A Study Using $^{13}C$ Natural Abundance Approach. Plos One 8, 1-9.

Ma, X., Wang, S., Wang, Y., Jiang, G., Nyren, P., 2006. Short-term effects of sheep excrement on carbon dioxide, nitrous oxide and methane fluxes in typical grassland of Inner Mongolia. New Zealand Journal of Agricultural Research 49, 285-297.

Miltner, A., Bombach, P., Schmidt-Bruecken, B., Kaestner, M., 2012. SOM genesis: microbial biomass as a significant source. Biogeochemistry 111, 41-55.

Monaghan, R. M., Barraclough, D., 1993. Nitrous-oxide and dinitrogen emissions from urine-affected soil under controlled conditions. Plant and Soil 151, 127-138.

Mørkved, P. T., Dörsch, P., Bakken, L. R., 2007. The $N_2O$ product ratio of nitrification and its dependence on long-term changes in soil pH. Soil Biology and Biochemistry 39, 2048-2057.

Oenema, O., Velthof, G. L., Yamulki, S., Jarvis, S. C., 1997. Nitrous oxide emissions from grazed grassland. Soil Use and Management 13, 288-295.

R Core Team, 2014. R: A language and environment for statistical computing. R Foundation for Statistical Computing., Vienna, Austria. Version 3.1.2, available at: http://www.R-project.org/

Reiche, M., Gleixner, G., Kuesel, K., 2010. Effect of peat quality on microbial greenhouse gas formation in an acidic fen. Biogeosciences 7, 187-198.

Ritz, K., McNicol, W., Nunan, N., Grayston, S., Millard, P., Atkinson, D., Gollotte, A., Habeshaw, D., Boag, B., Clegg, C. D., Griffiths, B. S., Wheatley, R. E., Glover, L. A., McCaig, A. E., Prosser, J. I.,

2004. Spatial structure in soil chemical and microbiological properties in an upland grassland. Fems Microbiology Ecology 49, 191-205.

Schulze, E. D., Luyssaert, S., Ciais, P., Freibauer, A., Janssens, I. A., Soussana, J. F., Smith, P., Grace, J., Levin, I., Thiruchittampalam, B., Heimann, M., Dolman, A. J., Valentini, R., Bousquet, P., Peylin, P., Peters, W., Roedenbeck, C., Etiope, G., Vuichard, N., Wattenbach, M., Nabuurs, G. J., Poussi, Z., Nieschulze, J., Gash, J. H., CarboEurope, Team, 2009. Importance of methane and nitrous oxide for Europe's terrestrial greenhouse-gas balance. Nature Geoscience 2, 842-850.

Shand, C. A., Coutts, G., 2006. The effects of sheep faeces on soil solution composition. Plant and Soil 285, 135-148.

Shand, C. A., Williams, B. L., Dawson, L. A., Smith, S., Young, M. E., 2002. Sheep urine affects soil solution nutrient composition and roots: differences between field and sward box soils and the effects of synthetic and natural sheep urine. Soil Biology & Biochemistry 34, 163-171.

Silvola, J., Alm, J., Ahlholm, U., Nykanen, H., Martikainen, P. J., 1996. The contribution of plant roots to $CO_2$ fluxes from organic soils. Biology and Fertility of Soils 23, 126-131.

Smith, K. A., Conen, F., 2004. Impacts of land management on fluxes of trace greenhouse gases. Soil Use and Management 20, 255-263.

VDLUFA, 1997. Bestimmung von mineralischem (Nitrat-)Stickstoff in Bodenprofilen (Nmin-Labormethode), In: VDLUFA (Ed.), Methodenbuch Teil 2, Speyer, Germany.

Velthof, G. L., Brader, A. B., Oenema, O., 1996. Seasonal variations in nitrous oxide losses from managed grasslands in The Netherlands. Plant and Soil 181, 263-274.

von Arnold, K., Nilsson, M., Hanell, B., Weslien, P., Klemedtsson, L., 2005. Fluxes of $CO_2$, $CH_4$ and $N_2O$ from drained organic soils in deciduous forests. Soil Biology & Biochemistry 37, 1059-1071.

Worrall, F., Clay, G. D., 2012. The impact of sheep grazing on the carbon balance of a peatland. Science of the Total Environment 438, 426-434.

## 7. Supplement

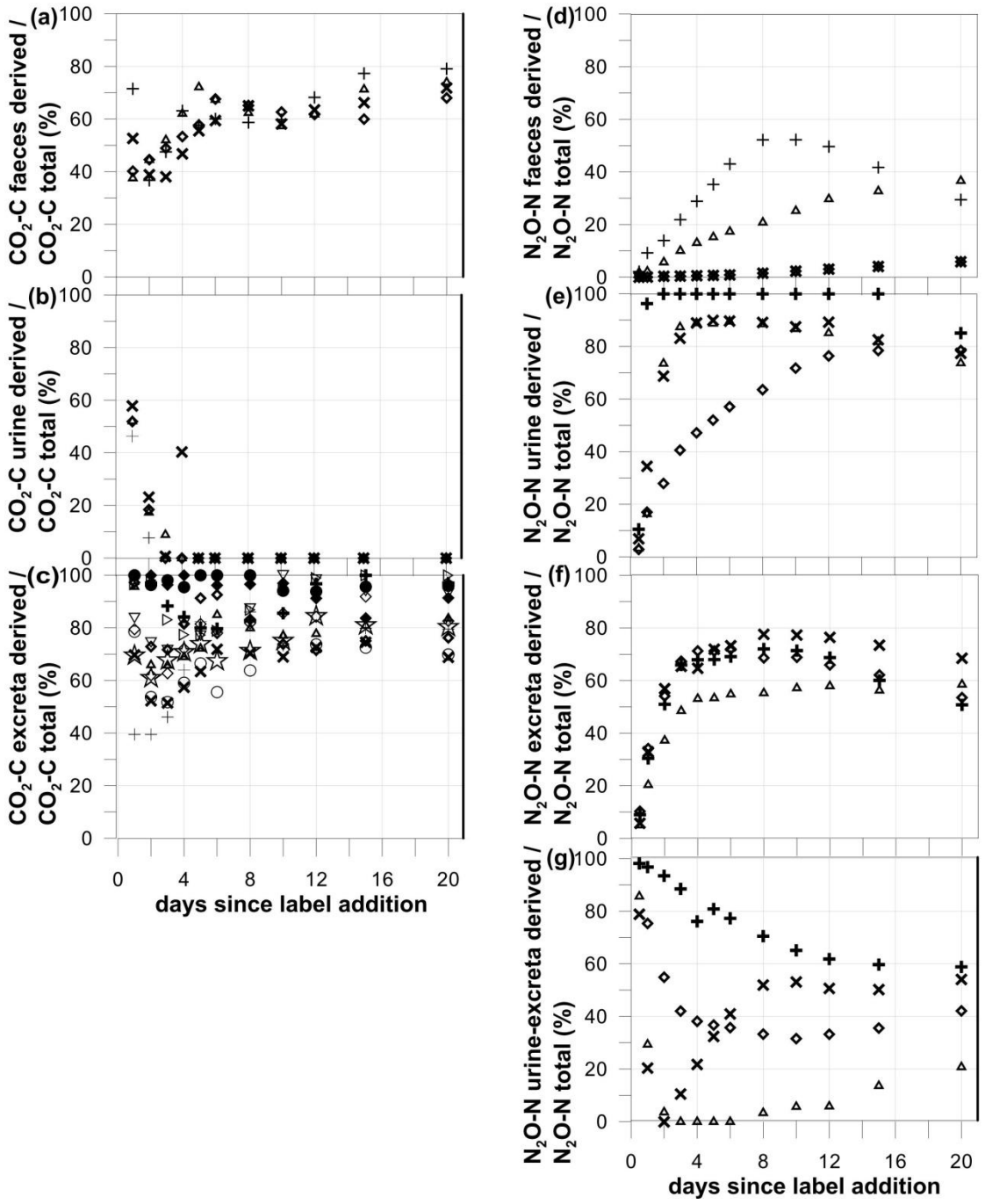


**Fig. S4 - 1**: Time series of excreta derived $CO_2$ fluxes (a-c) and excreta derived $N_2O$ fluxes (d-g) since labeling. In the figures the replicates of the same treatment are displayed. For C $^{15}N$ faeces (a, n=4), $^{15}N$ urine (b, n=4), faeces plus urine treatments (c, n=12); for N $^{15}N$ faeces (d, n=4), $^{15}N$ urine (e, n=4), $^{15}N$ faeces plus $^{15}N$ urine (f, n=4), $^{14}N$ faeces plus $^{15}N$ urine (g, n=4).

# Chapter 5: Comprehensive discussion and conclusions

In the individual sections of this chapter, the main results of the three publications are finally summarized (part 1.) followed by a comprehensive discussion of the findings with respect to the overall hypotheses (part 2.-5.).

First, the robustness of the GHG flux measurements is elucidated in detail. Second, it is shown that the strong vulnerability of peat derived carbon extends to soils with relatively low C content. Third, recommendations of a climate-smart management of grasslands on organic soils are proposed. At the end, further implications and general conclusions are given.

## 1. Summary of results

### 1.1 Minimum measurement frequency for robust annual budgets of ecosystem respiration

A continuous seasonal $R_{eco}$ data set (June to October) was measured by an automatic chamber system. This was used to create synthetic subsample data sets in order to test if manual campaign-wise measurements of $R_{eco}$ are robust when minimum standards are met.

*Main results:*

- $R_{eco}$ measurements based on campaigns of diurnal $CO_2$ fluxes are suitable for determining robust annual $R_{eco}$ sums.
- $R_{eco}$ models based on pure daytime or nighttime measurements are substantially biased. Therefore, $R_{eco}$ measurements should be distributed from early in the morning (before sunrise) until the late afternoon.
- Models based on $CO_2$ campaigns during sunny, dry weather conditions generate more accurate and precise $R_{eco}$ sums and should be preferred to a strict interval based measurement pattern.
- A measurement frequency of three weeks is sufficient for histic Gleysols under grassland.

### 1.2 High $CO_2$ fluxes from histic Gleysols under grassland management

The annual carbon and GHG balance of grassland was determined via manual chambers for six sites. The sites were located on nutrient-poor histic Gleysols with a shallow (0.3 m) histic horizon partly mixed with mineral soil and differed in their $C_{org}$ content (9 to 52 %) and mean annual groundwater level (0.11 m – 0.39 m).

*Main results:*

- The net GHG balance, corrected for carbon export by harvest, was around 4 t $CO_2$-C-eq $ha^{-1}$ $yr^{-1}$ on soils with peat layer and little drainage (mean annual water table < 0.20 m below surface). The net GHG balance reached 7-9 t $CO_2$-C-eq $ha^{-1}$ $yr^{-1}$ on soils with sand mixed into the peat layer and water tables between 0.14 m and 0.39 m below surface.
- GHG emissions (mainly $CO_2$) of histic Gleysols increased linearly with drainage depth and did not level off when the water table fell below the peat level.
- GHG emissions from grasslands on histic Gleysols were found to be as high as those from grasslands on Histosols.
- Peat mixed with mineral subsoil and $C_{org}$ concentration around 10% emitted as much GHG as unmixed peat soil (> 30 %$C_{org}$).

## 1.3 Sheep excreta cause no positive priming effects on $CO_2$ and $N_2O$ emissions from peat soil

The effect of sheep excreta on GHG emissions from a histic Gleysol with strongly degraded peat was investigated in a microcosm experiment. The $^{15}N$ and $^{13}C$ stable isotope tracer technique was used to partition soil organic matter and sheep excreta as sources of $CO_2$ and $N_2O$. Undisturbed soil columns were treated with surface application of urine, faeces or mixtures of both in different label combinations to distinguish between direct effects and possible priming effects. Incubation was done under stable temperature and precipitation conditions for three weeks.

*Main results:*

- Sheep excreta enhanced $CO_2$ emissions proportionally to the amount and type of C added.
- In contrast, $N_2O$ and $CH_4$ emissions were not affected by the addition of excreta. Methane emissions were very small and thus not relevant during excreta decomposition.
- Sheep excreta caused either no or only a small negative priming on peat decomposition but led to a source shift of the nitrogen released as $N_2O$ from peat to labile N forms in excreta.
- No mechanism was found that would suggest a risk of increased peat mineralization in the presence of sheep excreta.

## 2. The robustness of methods for GHG flux measurements

The first challenge in the quantification of robust GHG balances is the choice of the appropriate measurement technique. The applicability of eddy covariance techniques, automated or manual chambers under the existing conditions has to be evaluated in the beginning. Since drained peatlands often exhibit a small-scale heterogeneity, eddy covariance cannot be used at these sites (Foken, 2006). Many treatments on heterogeneous landscapes require manual chamber measurements, since automatic ones with the ability to include vegetation are too expensive for deployment in many different treatments and replicates (Subke et al., 2009).

In studies on soil respiration measurements not including plants, automated measurements with relatively small chambers and several replicates capturing the spatial heterogeneity in soil conditions can be established with high cost efficiency (Savage and Davidson, 2003). On the contrary, recording of ecosystem respiration, which includes vegetation, requires larger chambers suitable for high vegetation in order to represent both, heterogeneity in vegetation as well as spatial heterogeneity in soil conditions. Several replicates covering spatial heterogeneity are often too expensive to purchase. As an alternative, a number of replicates can be measured by manual chambers coupled to an infrared gas analyzer system, which is more cost efficient and covers spatial heterogeneity (e.g. Beetz et al., 2013; Eickenscheidt et al., 2015). Manual chamber measurements are associated with a lower measurement frequency due to a campaign based approach. This implies a measurement frequency of three to four weeks, depending on vegetation growth of e.g. grassland or crops and on management events (soil cultivation activities, harvest, fertilization), which requires a measurement shortly before and after such an event.

In this PhD thesis an approach was tested to assess the impact of measurement frequency on accuracy (bias) and precision (random uncertainty) of seasonal $R_{eco}$ sums. We used high resolution automatic chamber $R_{eco}$ data to evaluate the measurement frequency of theoretical manual chamber campaigns. The applied Lloyd-Taylor response function to calculate $R_{eco}$ sums showed to be very robust. None of the other tested response functions using temperature, temperature and soil moisture, and temperature and groundwater table performed significantly better. In contrast to studies on mineral soils (e.g. Savage and Davidson, 2003), we did not detect any direct influence of soil moisture on $R_{eco}$. Only a small loss of accuracy (by < 6%) and a certain loss of precision (by 5-20%) was observed when moving from continuous to campaign-based calculated $R_{eco}$ sums.

Therefore, the evaluation of automatic chamber data proved that the manual campaign-wise measurements of $R_{eco}$ and also NEE are robust if minimum standards are met. Using only daytime or nighttime based measurement campaigns induce over- or underestimation of $R_{eco}$ fluxes and consequently also of NEE fluxes. Thus, measurement campaigns based on shading of transparent

chambers during daytime (e.g. Elsgaard et al., 2012; Goerres et al., 2014), which result in a strong bias in $R_{eco}$ and NEE fluxes, cannot be recommended. Good weather campaigns covering the diurnal cycle, in particular the day-night pattern, are suitable to set up a robust $R_{eco}$ model and calculate cumulated $R_{eco}$ sums with high accuracy and adequate precision. These measurement conditions are also needed for obtaining robust NEE data sets, since the full daily range of PAR (corresponding to the season) can be covered.

From these results, guidelines of the good practice for manual chamber measurements on managed organic soils can be derived: A minimum measurement frequency of every three weeks can be recommended for extensive grasslands on organic soils in order to receive robust results on $CO_2$ emissions. A measurement campaign should start before sunrise and continue until the late afternoon to cover the complete range of temperature and PAR values. In the case of intensively managed organic soils, e.g. intensive grassland with multiple cuts and fertilization or intensive cropping with several soil cultivation events, this measurement frequency can be adjusted by additional measurements directly before and after events. Therefore, recommendations are valid beyond this study and confirm the campaign-wise measurement standard applied in the joint research project “Organic soils” (coordinated by the Thünen Institute 2009-2012).

A second challenge in the quantification of robust GHG balances poses the partitioning of the total $CO_2$ fluxes into soil derived and plant derived contributions. For a better understanding of peat degradation, the fraction of carbon emitted from the peat pool is of great importance.

The C balance method widely used in the field (e.g. Beetz et al., 2013; Schrier-Uijl et al., 2014) was successfully applied at our site. Since an accurate determination of harvest (= C export) is critical, quality criteria for good practice were applied and met. Bi- to three-weekly measurements of biomass height and measurements of wet and dry biomass weight as well as plant $C_{org}$ content at each cutting event were sufficient for the adequate recording of plant phenology. $C_{org}$ content of the biomass was equivalent to 9-51% of NEE emissions on the investigated field site. Thus, over- or underestimated biomass values would result in large errors of the total carbon or GHG balance of a site if not or incorrectly considered. Although biomass weights within a chamber frame might not necessarily be representative for the whole plant composition of a field site, a biomass weight measured within a chamber frame is the accurate value to correct $CO_2$ fluxes derived from this particular plot.

The peat derived carbon amounts calculated for our study site showed a small limitation since we had to fence the field measurement plots to avoid destruction of the instruments by grazing sheep. Therefore, grazing (excreta application plus trampling) could not be tested in the field during this PhD thesis, but an estimation of the biomass removed by sheep was made via cutting. However, results of

the laboratory study confirmed that the addition of sheep excreta did not cause significant priming effects on peat derived carbon and nitrogen.

So far, priming effects of excreta have not been studied in organic soils. Stable isotopes were successfully used in the laboratory study to separate soil and excreta derived fluxes (in a closed system for isotope recovery and under stable temperature and moisture conditions). Isotopic partitioning directly showed the contribution of excreta and peat derived carbon to the total fluxes, e.g. the abiotic dissociation of urea could be shown by the application of $^{13}C$ labeled urine to peat columns. Future research may concentrate on the verification by field measurements (with vegetation and varying temperature and moisture levels).

## 3. Strong vulnerability of peat derived carbon extends to relatively low C containing soils

In previous studies high emissions of peat derived carbon were detected mainly on deep peat soils (Drösler et al., 2013). In this PhD thesis it was shown that shallow peat soils released as much GHGs as deep peat soils. Peat mixed with sand and $C_{org}$ contents of less than 10% emitted as much GHGs as peat with a $C_{org}$ content of more than 30%. Therefore, peat remains vulnerable and highly labile under oxic conditions, regardless of its concentration in soil. It should be kept in mind that the differences in C stocks (0-30 cm) between sand mixed and unmixed sites were not as pronounced as differences in C concentrations. This is because sand mixing increased bulk density, which filled the pore space of the peat with material, rather than reducing the C stock in the aerated zone of the soil profile. Therefore, the aerated C stock plays a more decisive role for the magnitude of C fluxes, as also found by Pohl et al. (2015), and a dilution of carbon should not be overrated.

The position of the groundwater table was the main driver for $CO_2$ emissions from shallow organic soils in this study. The depth of the groundwater table is a proxy for peat aeration and peat moisture content. With decreasing groundwater table more peat carbon is aerated and mineralized (Dinsmore et al., 2009). In our study this relationship was linear, even when the groundwater table fell below the carbon rich soil horizon. This can be attributed to increased amounts of aerated carbon due to lowered soil moisture in the peat horizon as not only the groundwater table but also the capillary fringe is descending. This indicates that under warm and dry weather conditions during summertime, carbon emissions were not limited due to drought since soil conditions were optimal for mineralization. With respect to more frequent and longer drought events in the future, soil moisture in the topsoil could reach low levels, so that peat mineralization is affected and reduced depending on the hydraulic conductivity of the respective soil type.

In contrast to former laboratory studies (Reiche et al., 2010; Hahn-Schoefl et al., 2011), peat soil in our study could be excluded as a source of large amounts of GHGs when easily available C and N is added. Increased total emissions in the laboratory study could definitely be attributed to be derived from sheep excreta. Additionally, no C or N priming was observed on the peat soil in this study which is in opposition to positive priming of sheep excreta on mineral soils (Ma et al., 2013). Therefore, grazing does not seem to increase vulnerability of peat and can be performed in an extensive way on organic soils. Management of organic soils should be promoted in a climate-smart way which is elucidated in detail in the following section.

## 4. Towards climate-smart management of grasslands on organic soils

Productivity, resilience and mitigation are the three main components of climate smart agriculture (FAO, 2013). Results of this PhD thesis showed that GHG emissions (mainly $CO_2$) from shallow organic soils were of the same magnitude as for deep peat soils. Therefore, raising the groundwater table for peat carbon conservation is a desirable GHG mitigation option. Increasing the groundwater table should still allow sufficient grass growth (= productivity) for further grassland utilization. Sowing of plant species (grasses) adapted to wetter conditions should be promoted and attention should be paid to the suitability of these species as sheep fodder or as an alternative application. Since sheep grazing was found to be positive (or at least not negative) for peat carbon conservation, one to three times short term sheep grazing events per year should be an objective. If the load bearing capacity of the peat soil is high enough, even larger livestock could be used for grazing. Additionally, a raised groundwater table would also support the resilience of the grassland vegetation to drought spells which will occur more often in future (Turral et al., 2011).

However, at sites with organic soils which are not sealed off to the mineral subsoil, dry spells during summer months cannot be avoided without some periods of the year being too wet for grassland utilization. Controlled water management would be a solution, which requires the construction of weirs and dams and subsequent subsurface drainage (Van den Akker et al., 2012).

Extensification has already been used successfully for GHG mitigation in the Netherlands. Schrier-Uijl et al. (2014) observed a mitigation of GHG emissions from drained, intensively used, agricultural peatlands, achieved by the reduction of the intensity of land management, combined with rewetting. The authors argued that managed peatlands could be transferred from a GHG source to a GHG sink within 15 years of abandonment and rewetting. In their case a shift from an intensively managed grass-on-peat area to an extensively managed one reduced the GHG emissions. This was mainly due to decreased $N_2O$ emissions and lower farm-based $CH_4$ emissions.

Even if organic soils are managed in a climate-smart way, emissions of these sites are huge compared to sites on mineral soils in the same region which are managed in a relative intensive way (Dechow and Freibauer, 2011). In Germany, intensive grassland management on mineral soils released between 0.5 and 0.9 t $CO_2$-C equ. $ha^{-1}$ $yr^{-1}$ (1990-2003; Dechow and Freibauer, 2011). Compared to these values the extensive grassland in this study yielded up to 15 times more GHGs.

These results clearly show that a significant reduction of GHG emissions of organic soils can only effectively be reached by rewetting following good practice procedures. Due to a rising $CH_4$ emission potential and a reduced productivity, flooding of organic soils should be avoided. In a recently published PhD thesis on the influence of water table and organic substrate on GHG emissions from rewetted peatlands (Hahn-Schoefl, 2015), an elevated groundwater table close to the soil surface at least during some periods of the year minimized carbon release and even restored the GHG sink function.

## 5. Implications and general conclusions

The results of this PhD thesis emphasize that the importance of drained organic soils as most important GHG source of the agricultural sector is not restricted to deep peat soils, but also valid for shallow organic soils. Generally, raising of groundwater tables in organic soils will result in lower GHG emissions and, according to the results of this PhD thesis, this is equally important on shallow organic soils and deep organic soils. Controlled water management of shallow organic soils can contribute to a wet, climate-smart management of these soils. Grazing of shallow organic soils can be recommended. Additionally, rewetting can also be an effective measure for GHG mitigation on shallow organic soils.

Our results indicate that mitigation options should not be restricted to deep peat soils, since mitigation measures also provide considerable reduction of GHG emissions on shallow peat soils. It is often proposed to limit measures like rewetting or the increase of the ground water level to areas with deep peat in order to concentrate small funds on sites with large carbon stocks. Since shallow sites show emissions of the same magnitude, it is desirable to realize measures also on these sites in order to preserve the remaining carbon. On the one hand rewetting measures are positive due to their positive climatic impact, if good practice is applied, and on the other hand in order to preserve the organic soil per se and to prevent degradation to a mineral soil in the long term. This study shows that rewetting of organic soils including histic Gleysols has a higher relevance for GHG mitigation strategies than currently assumed.

In this PhD thesis a high vulnerability of peat material with low carbon concentrations was found. Due to this further studies are needed to find the maximum C concentration for peats below which GHG emissions decrease or to find out if this level exists at all. Mixing peat and sand with a $C_{org}$ content of 9% obviously does not result in a reduction of GHG emissions. Mineral soils under grassland, which were formed under aerobic conditions, with 2-4% $C_{org}$ release significantly less GHGs. Thus, the quality of organic carbon and probably the missing interaction with a reactive mineral phase might induce continuing peat mineralization and not stabilization such as aerobic soil organic matter of mineral soils. Peat material seems to remain vulnerable or is even mobilized if mixed with sand. Therefore, sand mixing culture cannot be rated as climate protection activity as the aerated $C_{org}$ stock is not reduced by this technique.

As opposed to most national and international soil classifications of Histosols, the IPCC definition of organic soils also includes shallow histic topsoils. This study confirms that the wider definition is reasonable, since it considers the anthropogenic GHG emissions of drained organic soils. Currently, countries apply soil maps for the national GHG inventories which often do not include these histic Gleysols, i.e. shallow drained organic soils. Thus, the land surface area with hot spots of GHG emissions may be strongly underestimated.

Due to the same emission potential of shallow and deep peat soils, GHG inventories should report both with the same emission factors. These results have already been included in the German national inventory report, but e.g. Denmark still underestimates the emissions of shallow drained organic soils. In the second commitment period (2013-2020) $CO_2$ emissions of drained organic soils under forestry are a mandatory activity under the Kyoto Protocol, but under cropland and grassland they are an optional eligible activity of the Kyoto Protocol. Besides Germany, also other European countries such as Denmark, Ireland and Great Britain consider these emissions under the Kyoto Protocol, in contrast to other countries with large areas of peatlands such as Sweden, Finland and the Netherlands. Only by reporting grassland and cropland under the Kyoto Protocol, important GHG mitigation potentials can be considered and reporting should thus be mandatory for all countries that have ratified the Kyoto Protocol.

# 6. References


Beetz, S., Liebersbach, H., Glatzel, S., Jurasinski, G., Buczko, U., Hoeper, H., 2013. Effects of land use intensity on the full greenhouse gas balance in an Atlantic peat bog. Biogeosciences 10, 1067-1082.

Dechow, R., Freibauer, A., 2011. Assessment of German nitrous oxide emissions using empirical modelling approaches. Nutrient Cycling in Agroecosystems 91, 235-254.

Dinsmore, K. J., Skiba, U. M., Billett, M. F., Rees, R. M., 2009. Effect of water table on greenhouse gas emissions from peatland mesocosms. Plant and Soil 318, 229-242.

Drösler, M., Adelmann, W., Augustin, J., Bergmann, L., Beyer, C., Chojnicki, B., Förster, C., Freibauer, A., Giebels, M., Görlitz, S., Höper, H., Kantelhardt, J., Liebersbach, H., Hahn-Schöfl, M., Minke, M., Petschow, U., Pfadenhauer, J., Schaller, L., Schägner, P., Sommer, M., Thuille, A., Wehrhan, M. , 2013. Klimaschutz durch Moorschutz. Schlussbericht des Vorhabens "Klimaschutz - Moorschutzstrategien" 2006-2010. 201 pp.

Eickenscheidt, T., Heinichen, J., Drösler, M., 2015. The greenhouse gas balance of a drained fen peatland is mainly controlled by land-use rather than soil organic carbon content. Biogeosciences 12, 5161-5184.

Elsgaard, L., Gorres, C.-M., Hoffmann, C. C., Blicher-Mathiesen, G., Schelde, K., Petersen, S. O., 2012. Net ecosystem exchange of $CO_2$ and carbon balance for eight temperate organic soils under agricultural management. Agriculture Ecosystems & Environment 162, 52-67.

FAO, 2013. Climate-smart agriculture - Sourcebook. Rome, Italy, 570 pp.

Foken, T., 2006. Angewandte Meteorolgie - Mikrometeorologische Methoden. Springer-Verlag, Berlin, Heidelberg, New York, 336 pp.

Goerres, C. M., Kutzbach, L., Elsgaard, L., 2014. Comparative modeling of annual $CO_2$ flux of temperate peat soils under permanent grassland management. Agriculture Ecosystems & Environment 186, 64-76.

Hahn-Schoefl, M., 2015. Water table and organic substrate as triggers of greenhouse gas emissions from rewetted peatlands. PhD thesis, Gottfried Wilhelm Leibniz Universität Hannover.

Hahn-Schoefl, M., Zak, D., Minke, M., Gelbrecht, J., Augustin, J., Freibauer, A., 2011. Organic sediment formed during inundation of a degraded fen grassland emits large fluxes of $CH_4$ and $CO_2$. Biogeosciences 8, 1539-1550.

Ma, X., Ambus, P., Wang, S., Wang, Y., Wang, C., 2013. Priming of Soil Carbon Decomposition in Two Inner Mongolia Grassland Soils following Sheep Dung Addition: A Study Using $^{13}C$ Natural Abundance Approach. Plos One 8, 1-9.

Pohl, M., Hoffmann, M., Hagemann, U., Giebels, M., Albiac Borraz, E., Sommer, M., Augustin, J., 2015. Dynamic C and N stocks – key factors controlling the C gas exchange of maize in heterogenous peatland. Biogeosciences 12, 2737-2752.

Reiche, M., Gleixner, G., Kuesel, K., 2010. Effect of peat quality on microbial greenhouse gas formation in an acidic fen. Biogeosciences 7, 187-198.

Savage, K. E., Davidson, E. A., 2003. A comparison of manual and automated systems for soil $CO_2$ flux measurements: trade-offs between spatial and temporal resolution. Journal of Experimental Botany 54, 891-899.

Schrier-Uijl, A. P., Kroon, P. S., Hendriks, D. M. D., Hensen, A., Van Huissteden, J., Berendse, F., Veenendaal, E. M., 2014. Agricultural peatlands: towards a greenhouse gas sink - a synthesis of a Dutch landscape study. Biogeosciences 11, 4559-4576.

Subke, J.-A., Heinemeyer, A., Reichstein, M., 2009. Experimental design: scaling up in time and space, and its statistical considerations., In: Kutsch, W., Bahn, M., Heinemeyer, A. (Eds.), Soil carbon dynamics: an integrated methodology. Cambridge University Press, Cambridge, UK, 34-48.

Turral, H., Burke, J., Faurès, J. M., 2011. Climate change, water and food security. FAO Water Report No. 36, Rome, 18 pp.

Van den Akker, J.J.H., Hendriks, R.F.A., Pleijter, M., 2012. $CO_2$ emissions of peat soils in agricultural use: calculation and prevention. Agrociencia 16, 43-50.

## Acknowledgements

For the support during this PhD thesis I would like to thank several people:

**Prof. Dr. J. Böttcher** who generously supervised this work at the Leibniz University Hannover.

**Prof. Dr. H. Flessa** who supervised this work at the Thünen Institute of Climate-Smart Agriculture and who supported this work by providing support by technical assistants in the lab and field whenever needed.

**Dr. A. Freibauer** who inspired this work, gave scientific support and supervision as well as motivation whenever possible and needed.

**Dr. R. Fuß** who supported this work by sharing his statistical knowledge and expertise as well as his R programming skills.

**Prof Dr. W. Zech** whose fascination and devotion to soil science was handed on to me.

The whole **Moorteam**, especially **Dr. B. Tiemeyer** and **Dr. M. Bechtold**, for weekly constructive discussions and more than scientific support.

**D. Lempio**, **M. Hunziger** and **D. Olbricht** for their enormous support an inventive talent during lab and long days of field work.

**My friends** Katrin, Caro, Britta and Michi who supported me in all circumstances of life and with all things needed (companionship, coffee, chocolate, cake, ...).

**My family**, especially my parents, who encouraged me to do what interested me most.

**My husband** Poldi, for his patience, encouragement and being there whenever I needed it.

# Curriculum vitae

## *Persönliche Angaben:*

| | |
|---|---|
| Name: | **Katharina** Dominica **Leiber-Sauheitl** |
| Geburtstag: | 3. Februar 1982 |
| Geburtsort: | Bad Neustadt a. d. Saale |
| Staatsangehörigkeit: | deutsch |

## *Ausbildung und beruflicher Werdegang:*

| | |
|---|---|
| 10/2002 bis 07/2008 | Studium der Geoökologie an der Universität Bayreuth |
| 29.07.2008 | Diplom im Fach Geoökolgie an der Universität Bayreuth mit dem Thema „Rekonstruktion der Boden-, Klima- und Vegetationsentwicklung entlang einer Catena auf der Nordseite des Kilimanjaro“ |
| 03/2009 bis 02/2010 | wissenschaftliche Mitarbeiterin in der Abteilung Bodenphysik, Universität Bayreuth |
| 03-04/2010 | wissenschaftliche Mitarbeiterin an der Brown University, Providence, RI, USA |
| 11/2010 bis 02/2014 | wissenschaftliche Mitarbeiterin am Thünen Institut für Agrarklimaschutz in Braunschweig (Promotionsstelle) |
| 05/2014 bis 08/2014 | wissenschaftliche Mitarbeiterin am Thünen Institut für Agrarklimaschutz in Braunschweig (Projektstelle zum wissenschaftlichen Methodenvergleich und zur Qualitäts-sicherung von manuellen $CO_2$-Messdaten in deutschen Mooren) |
| 10/2014 bis 03/2015 | wissenschaftliche Mitarbeiterin am Thünen Institut für Agrarklimaschutz in Braunschweig (Drittmittelstelle zur Methodenentwicklung und Berechnung von $CO_2$-Flüssen in Mooren Baden-Württembergs für die Universität Ulm) |
| 05/2015 bis 02/2016 | wissenschaftliche Mitarbeiterin am Thünen Institut für Agrarklimaschutz in Braunschweig |